



Strål  
säkerhets  
myndigheten

Swedish Radiation Safety Authority

Author: Tobias Backers  
Ove Stephansson

Research

# 2011:26

The influence of temperature and fluid pressure on the fracture network evolution around deposition holes of a KBS-3V concept at Forsmark, Sweden



## **SSM perspective**

### **Background**

In preparation for the review of SKB's license application for disposal of spent nuclear fuel, SSM is conducting studies to evaluate the performance of the multi-barrier principle on which the KBS-3 concept is based. Copper canisters containing the spent nuclear fuel are placed into granitic bedrock at about 500 m depth and embedded in clay. Thus, the rock, the clay and the copper canister are acting as barriers in order to retard the possibility of spent fuel to escape the repository and reach the biosphere. During a very long time period (e.g. millions of years), the rock will be subjected to thermal, mechanical and hydraulic changes that can induce failure and propagation of the existing fractures providing new pathways for the spent fuel to escape the repository.

### **Objectives**

For SSM, the goal of this study is to improve the scientific basis for the evaluation of the performance of the bedrock as a barrier in the KBS-3 repository concept and enhance the knowledge about the thermal-mechanical-hydraulic processes affecting the bedrock. These simulation series focus on the natural and/or induced fractures in the bedrock surrounding the canister and their possibility to initiate or propagate due to the changes of stress and water pressure in the bedrock. These changes will be caused by the construction of the repository for spent nuclear fuel, its thermal phase and, in particular, by a glacial period affecting the bedrock at the repository site.

### **Results**

According to the modeling results, during construction and thermal phase of the repository, no major alterations of the fracture network are expected. However, a large increase of fluid pressure due to a glaciation period has a pronounced impact on the fracture network. In a high magnitude stress field, fractures tend to close and mobilize their frictional resistance. However, in a low magnitude stress field, existing fractures tend to propagate with consequent major changes the fracture network. In conclusion, the understanding of the magnitude of the in-situ stress field at Forsmark appears to be critical for the evolution of the fracture network.

### **Need for further research**

More effort should be made in modeling the changes of the fracture network considering the effect of large fluid pressure onto the tunnel system at repository scale. Also the effect on the fracture network of large earthquakes and surface rebound after glaciation should be studied by explicitly taking into account fracture propagation. Several different realization of the discrete fracture network should be preferably considered.

### **Project information**

Contact person SSM: Lena Sonnerfelt

Reference: SSM 2010/1144





Strål  
säkerhets  
myndigheten

Swedish Radiation Safety Authority

**Authors:** Tobias Backers and Ove Stephansson  
Geomecon GmbH, Potsdam, Germany

# 2011:26

The influence of temperature and fluid pressure on the fracture network evolution around deposition holes of a KBS-3V concept at Forsmark, Sweden

Date: march 2011

Report number: 2011:26 ISSN: 2000-0456

Available at [www.stralsakerhetsmyndigheten.se](http://www.stralsakerhetsmyndigheten.se)

This report concerns a study which has been conducted for the Swedish Radiation Safety Authority, SSM. The conclusions and viewpoints presented in the report are those of the author/authors and do not necessarily coincide with those of the SSM.

# Contents

<b>1. Summary</b> .....	<b>3</b>
<b>2. Introduction</b> .....	<b>3</b>
<b>3. Layout of the numerical campaign</b> .....	<b>5</b>
<b>4. Numerical tools</b> .....	<b>8</b>
4.1. fracod2d .....	8
4.2. phase2 .....	9
<b>5. Definition of the model</b> .....	<b>9</b>
5.1. Geometry .....	9
5.2. Geomechanical properties.....	10
5.2.1. Intact rock and fracture properties.....	10
5.2.2. Rock mass properties .....	11
5.2.3. Thermal properties.....	12
5.3. Stress conditions .....	12
5.3.1. Stress model .....	12
5.3.2. Fluid pressure .....	16
5.3.3. Swelling pressure .....	16
5.3.4. Ice cover .....	16
5.4. Temperature conditions.....	17
5.4.1. In situ temperature.....	17
5.4.2. Temperature evolution and heating scheme .....	17
5.4.3. Ice cover .....	18
5.5. Discrete fracture network DFN .....	18
<b>6. Model validation</b> .....	<b>20</b>
6.1. Rock model.....	20
6.2. Distinct fracture network model .....	20
<b>7. Results</b> .....	<b>21</b>
7.1. Overview to simulation campaign.....	21
7.2. Effect of loading history without DFN (IM-2).....	22
7.3. Evolution of fracture network DFN I under high in-situ stress field .....	26
7.4. Evolution of fracture network under low in-situ stress field .....	27
7.5. The influence of the fluid pressure from an ice cover .....	28
7.6. Evolution of fracture network DFN II .....	29
7.7. Post glacial scenario.....	30
7.8. Comparison of simulation of models with and without fracture initiation .....	31
7.9. Influence of excavation of the deposition holes .....	32
<b>8. Interpretation and Discussion</b> .....	<b>33</b>
<b>9. Conclusions</b> .....	<b>35</b>
<b>10. References</b> .....	<b>37</b>
<b>Appendix</b> .....	<b>38</b>
<b>11. Simulations</b> .....	<b>38</b>
11.1. Simulation IM-6.....	38
11.2. Simulation IM-7 .....	43
11.3. Simulation IM-9.....	49
11.4. Simulation IM-10.....	55
11.5. Simulation IA-1 .....	60
11.6. Simulation IA-2 .....	67

11.7. Simulation IA-3 .....	72
11.8. Simulation IA-4 .....	78
11.9. Simulation IIM-1 .....	84
11.10. Simulation IIA-1 .....	90
11.11. Simulation IMO-1 .....	95
11.12. Code listing examples .....	99
11.12.1. IM-2 .....	99
11.12.2. IIM-1 .....	101



# 1. Summary

The extensive numerical modelling campaign aimed at simulating the development of the distinct fracture network under the variable geomechanical boundary conditions in a repository for spent nuclear fuel at Forsmark. The models mirrored the introduction of the KBS-3V deposition concept including the backfill of the tunnel, the readjustment of the water head, the swelling of the bentonite buffer and a full sequence of heat generation from the canisters. The temperature evolution was modelled from present in situ conditions up to 75°C rock wall temperature, including a cooling phase down to repository conditions of about 10°C.

In addition a glaciation scenario was added to the simulation campaign. The glaciation scenario included the increase in vertical load due to an ice sheet of 3km thickness and the increase of fluid pressure to 34MPa due to a hydraulic connection from the surface of the ice cover.

The simulations were run for two different distinct fracture network models and two stress regimes, i.e. the stress models by Martin [2007] and Ask et al. [2007]. The understanding of the stress field at Forsmark appears to be critical for the extension of the fractures. The low magnitude stress field (Ask et al. [2007]) enhances the propagation of existing fractures in the network. The high magnitude stress field (Martin [2007]) tends to close the fractures and mobilise the frictional resistance of the fracture faces.

The results showed that during the operation, closure and thermal phase of the repository no major DFN alterations are to be expected, that may lead to hydraulic connections of the excavations. However, an increase of water head might have the most pronounced impact on the distinct fracture network evolution. A limited number of models simulating the hydraulic effect from the excess groundwater pressure of an ice sheet resulted in severe fracture propagation and connection of the fracture network.

# 2. Introduction

In classical rock mechanics, rock is viewed as a continuous flawless material. Rock strength is often described by empirical criteria based on observations of failure, mostly in the laboratory. The most frequently used criteria are the Mohr-Coulomb, Hoek-Brown, or Mogi criteria and modifications or extensions of them (Benz and Schwab [2008]).

The parameters defining the strength criteria of rock are determined by tests in the geotechnical laboratory, where the response is characterised only globally, i.e., based on measurements at the boundary that are assumed representative of the overall (homogeneous, continuous) sample response. Thus, behaviour according to classical theory may only be expected in the case of a perfectly homogeneous material undergoing perfectly uniform deformation.

However, the hypothesis of continuity does not hold for rock. Rock material is a discontinuous combination of solid matters, pores, flaws, cracks and fractures.

All analyses of the structural breakdown of rock and rock mass clearly show that a continuum based approach cannot provide a correct description of the mechanics of failure. The existence of a crack in an otherwise solid homogeneous body reduces the strength of the structure considerably. Any load acting on the body is magnified several times at the tip of such a discontinuity, so when the stress concentration at the tip of the crack reaches a critical level, it propagates. Thus, failure is governed by pre-existing discontinuities.

Discontinuities are an important feature of rock and rock mass and control not only the hydraulic properties of rock and rock mass by well-connected networks (Quesada et al. [2008]), they also govern the mechanical behaviour. When the stresses in a rock mass are altered, whether by depletion of a reservoir, sequestration of liquid or gas, increase of pressure by enhanced oil recovery operations, thermal loads or the introduction of a new excavation, the pre-existing discontinuities may grow. Their growth may create new pathways for fluid flow or, if pre-existing fractures propagate and coalesce to form larger fracture networks that intersect with an excavation or another free surface under these circumstances, the structures may lose integrity and fail.

The existence of discontinuities in rocks together with fracture and fragmentation processes limits the applicability of continuum-based models to address rock engineering problems. A way forward in understanding the overall mechanical performance of rock mass is to explicitly simulate the initiation, growth and interaction of the distinct fracture network (Backers [2010]). The software fracod2d is one of the few options to provide such analysis. fracod2d is able to explicitly simulate the development of the fracture network under varying semi-coupled THM conditions.

In a fracture mechanics modelling study performed by GeoFrames GmbH for SKI in 2008 it was shown, that extension of the pre-existing fractures and fracture sets in the rock mass can potentially lead to a hydraulic connection between neighbouring deposition holes (Backers and Stephansson [2008]). For some configurations of deposition holes and DFN, pre-existing fractures are propagating due to the increased stress field around the excavations, that leads to interconnected fractures linking up neighbouring deposition holes. These connected fractures may act as potential pathways for fluid flow and transport, not only between the deposition holes, but also between deposition holes and the deposition tunnels.

In this study, the loading history to be expected on a repository for spent nuclear fuel in Forsmark is analysed by means of a fracture mechanics based geomechanical simulation campaign using fracod2d. The existing fracture network is explicitly represented in two examples and subject to the sequence of loading cases in such a repository; e.g. excavation of the deposition holes, backfill, rising of water head, swelling from compacted bentonite, and thermal stresses from the heating of the canisters. The growth of the

individual fractures due to the changes in stresses and temperatures is simulated yielding an understanding of the potential for the coalescence of fractures, that may lead to hydraulic connections between deposition holes causing potential pathways for radionuclides. Special emphasis is also put on the possible effects of glaciation, which will add a vertical load and potentially an increase in fluid pressure to the repository.

### 3. Layout of the numerical campaign

The numerical campaign aims at mirroring the key boundary conditions and input parameters that may influence the activation of the existing DFN at Forsmark, Sweden. Some simplifications had to be made in this overview study, in particular when modelling the thermal loads, but the cornerstones of the loading path are met.

The numerical campaign comprises the following steps, which are presented in Figure 1:

- generation of the geomechanical / geometrical model and DFN model
- insertion of the excavations
- application of swelling pressure from the high-compacted bentonite
- application of constant temperature in increasing increments at deposition holes
- decrease of temperature in increments
- increase of vertical stress from ice load
- consideration of water head as caused by ice load assuming there is a hydraulic connection

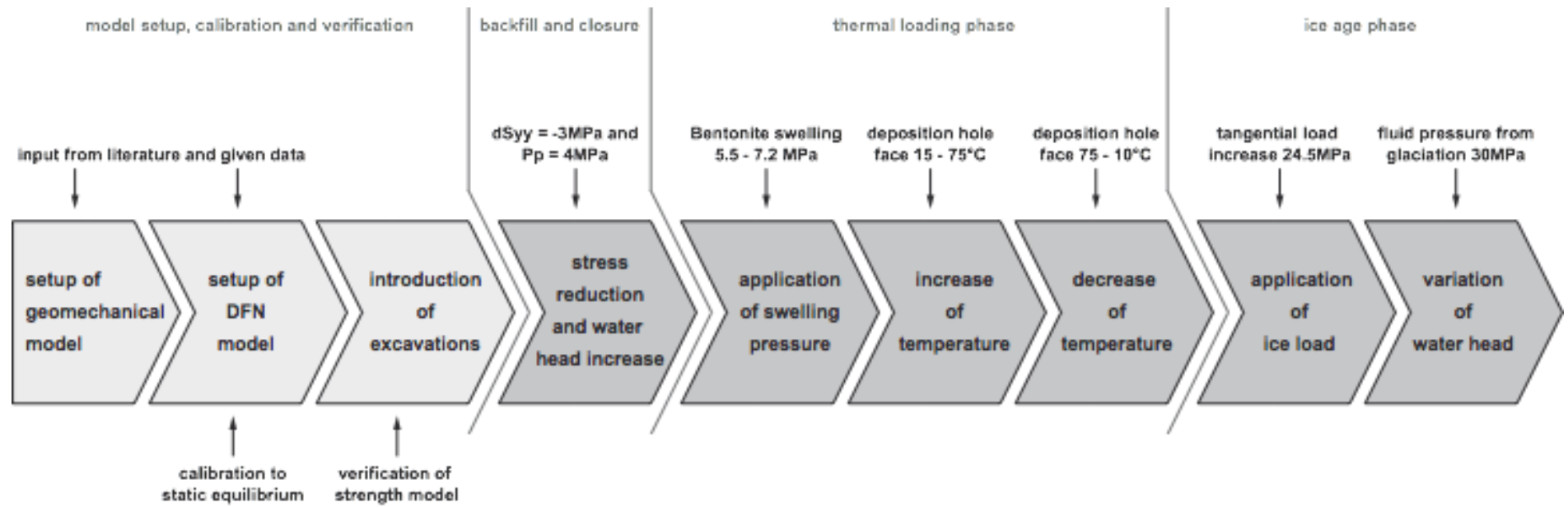


Figure 1. Workflow of the numerical simulation campaign. At first the geometry, the geomechanical models and the distinct fracture network (DFN) are defined from published data on Forsmark. The DFN model and the strength model are calibrated and verified against observations. After that the closure of the repository including the heat radiation from the canisters is simulated. Finally a cycle of ice cover is modelled and the excess water head is allowed to influence the stress condition in the repository.

The geomechanical model is set up from literature information presented by SKB. The model assumes elastic material properties up to the fracture initiation level. The fracture initiation is due to a Mohr-Coulomb criterion. Fracture propagation is modelled using a fracture mechanics based criterion incorporating fracture toughness under tensile and shear loadings. The geomechanical model includes the stresses as reported for the 420m level at Forsmark; two stress models are compared (Ask et al. [2007], Martin [2007]). The geomechanical model was validated against stable configuration.

The existing distinct fracture network (DFN) was derived from Fredriksson and Olofsson [2005]. Two DFN examples were extracted for this simulation campaign. A verification of the DFN was performed for two depth levels anticipating that no fracture propagation would occur.<sup>1</sup>

The geometrical model comprises two individual deposition holes at a centre point distance of 6m. The model domain is set to a 12m times 6m window. A variation analysis of the domain size and additional deposition holes yielded no significantly altered static stress fields. The geometrical model was validated assuming that no fracture initiation occurs in a DFN free rock mass. The initial rock temperature of the deposition hole walls is assumed to be constant at 14.5°C.

After closure of the repository two processes take place. As the tunnel is backfilled, the tangential stress around the tunnel is reduced, yielding at a reduction of the stress acting on the deposition holes. This was included in the simulations by reducing the stress acting normal to the axis of the deposition hole. Further, the water head will be increased in the repository and the bentonite backfill in the deposition holes will start swelling. This is included in the simulations also. Two different swelling pressures at constant water head pressure were simulated.

Subsequently, due to the canister heating, the temperatures in the vicinity of the deposition holes will increase and introduce thermal stresses. The complete heating sequence is not included due to computational constraints. However, a constant temperature is applied to the deposition hole walls in increasing steps (15, 15, 50, 75°C). The temperature is always kept constant for a period of 700e6s, assuming the peak temperature after roughly 150a. After each heating step the fracture propagation is simulated and the new stress state is determined and eventual fracture propagation defined.

As the heating capacity of the canisters is decaying, this is modelled by reducing the deposition hole wall temperature again stepwise (75, 50, 25, 10°C), this time applying for 9e10s. This loading sequence allows registration of remaining deformation following a heating and cooling cycle.

For Sweden an ice age can be expected in future, hence the model includes the increase of vertical load due to an ice cover of thickness 3km. This increase in vertical load is assumed not to introduce lateral stress increase. For

---

<sup>1</sup> It needs to be emphasised, that the results are valid for the given DFN and geomechanical situations only, although the results are assumed to be instructive and typical for Forsmark. Likely there exist DFN configurations that deliver more favourable or less favourable results.

the lateral stress increase several models exist, but this would have exceeded the aim of this study. A sensitivity analysis of the stress fields resulting from ice cover could be run as an extension to this study. The increase in vertical load results in a change of the tangential stress of the deposition tunnel.

Depending on the existence of permafrost in the soil, it might happen that the full water head of the ice cover will act on the repository. This is included in the simulations by adding a water pressure increase in the fractures that is equivalent to the thickness of the ice cover. Further, after the reduction of the ice cover the fluid (over-) pressure in the repository might not be reduced instantaneously; this is also considered in a simulation.

## 4. Numerical tools

Two software packages were used for the analysis. The software phase2 was used on selected stress analyses for calculation of the redistribution of the stresses around the access tunnel. The fracture mechanics based software fracod2d is used for most of the simulations.

### 4.1. fracod2d

In the context of this study the software fracod2d is used. fracod2d is a code designed to simulate fracture initiation, propagation and coalescence in hard rocks. The two-dimensional boundary element code was designed with the aim of predicting the fracture propagation and interaction of randomly distributed fractures in an elastic rock medium. It can handle both tensile and shear failures and it makes use of the Displacement Discontinuity Method (DDM). fracod2d can also be applied to study materials like concrete, glass and ceramics.

The fracture propagation criterion by Shen and Stephansson [1993] is incorporated into the code. In this criterion the resistance to fracture propagation, the fracture toughness,  $K$ , at the fracture tip is divided into two parts, one due to Mode I deformation (tensile) and one due to Mode II deformation (shear). The sum of their normalised values is used to determine the failure load and direction of fracturing. Both tensile and shear fracture propagation have been successfully simulated by fracod2d and verified by laboratory and field tests.

The input data includes the model geometry and geometry of pre-existing fractures, boundary conditions, far-field stresses, strength and elastic properties of the rock mass, fracture toughness, fracture stiffness of pre-existing and created fractures, fracture friction and cohesion. The code has the capacity of predicting fracture initiation, propagation and coalescence of pre-existing joints and newly formed fractures in the vicinity of excavations.

The code has been used in a number of research projects for the Swedish nuclear waste deposition, including the Äspö Pillar Stability Experiment

(APSE). It has also been used in modelling borehole breakouts and for the design of a drilling campaign (Moeck et al. [2007]).

## 4.2. phase2

For the analysis of the tangential stress of the access tunnel the commercial code phase2 by Rocscience Ltd (<http://www.rocscience.com/home.asp>) was used. phase2 is a 2D elasto-plastic finite element stress analysis program designed in particular for underground or surface excavations in rock or soil. It can be used for a wide range of engineering projects and includes support design, finite element slope stability and groundwater seepage analysis.

# 5. Definition of the model

This section summarises the geometrical model, the stress field models, the geomechanical models, input parameters and distinct fracture network used for the simulations.

## 5.1. Geometry

Figure 2 displays the geometry of the simulation domain. The basic layout is defined according to SKB [2009b]. The centres of the deposition holes are 6m apart, the diameter of the holes is 1.8m. The deposition holes are 8m deep. A bevel is not considered and would require an additional analysis. It is assumed that the bevel will introduce additional fracturing as it acts as a stress concentrator.

It is anticipated that the deposition tunnel is oriented parallel with the maximum horizontal stress  $S_H$ , i.e.  $S_{xx} = S_H$ ,  $S_{yy} = S_h$ , and  $S_{zz} = S_v$ , unless otherwise stated. An analysis of the influence of deposition tunnel orientation on the acting stress profile along the deposition holes is given in Eriksson et al. [2009] and SKB [2009b]. For a deposition tunnel orientation parallel with  $S_H$ , the influence of excavation is the least and the redistributed stresses at the deposition hole wall are below the assumed spalling strength. Section 5.3 derives the stresses as acting on the deposition holes from the tangential stress of the access tunnel.

The monitoring window for cross sectional simulations will be 12m x 6m wide, i.e. spanning (-6.0 ; 3.0) to (6.0 ; -3.0), fracture initiation and propagation are allowed on a reduced window size of (-4.5 ; 2.5) to (4.5 ; -2.5).

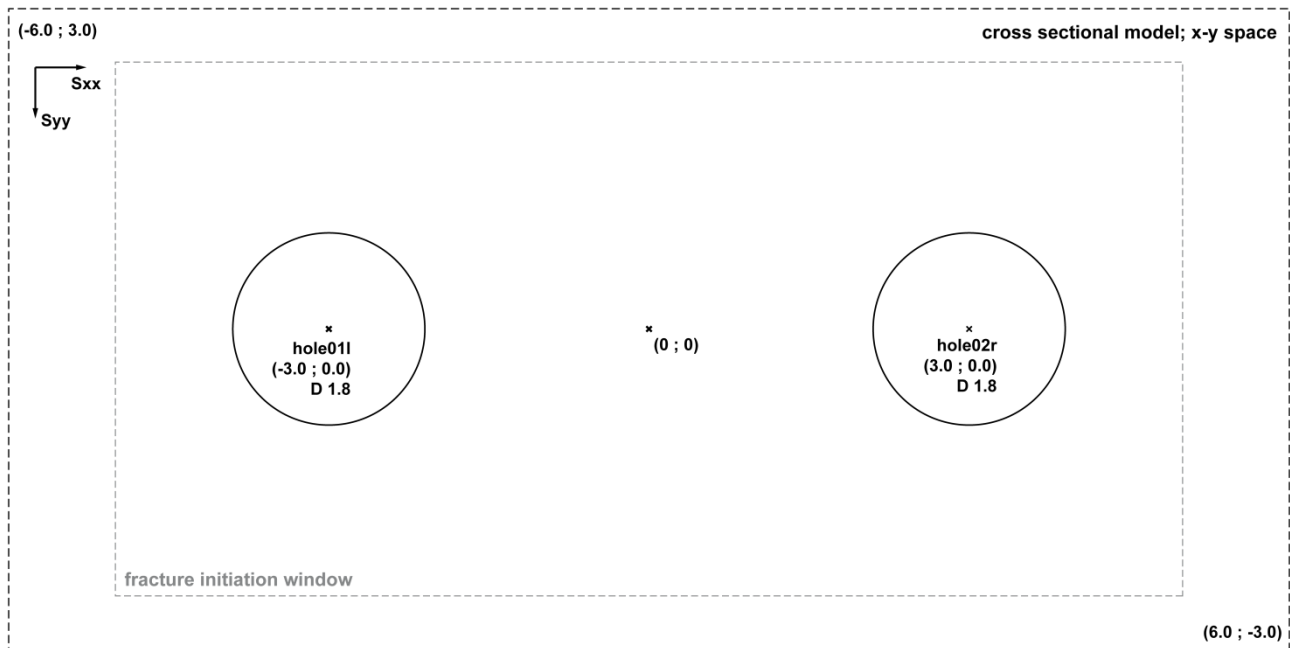


Figure 2. Geometrical layout of the model. The cross sectional cut of the model provides a computational window of 12m times 6m; fracture initiation is limited to a 9m times 5m window. The deposition holes are aligned centred with the direction of  $S_{xx} = SH$  (maximum rock stress) and are 6m apart.

## 5.2. Geomechanical properties

### 5.2.1. Intact rock and fracture properties

fracod2d uses a Mohr-Coulomb based criterion for fracture initiation. The fracture deformability is described by a linear stiffness model, and the fracture propagation is governed by a fracture toughness based fracture mechanics model. The rock behaviour is assumed linear elastic up to meeting the requirements for fracture initiation.

The values for deformation and strength properties of the intact rock material were chosen for the dominant rock type 101057 (granite to granodiorite, metamorphic, medium grained) at Forsmark site and are summarised in Table 1 (Glamheden et al. [2008], SKB [2008], SKB [2009a]). The average values are used in the models unless otherwise stated.

Table 1. Deformation and strength properties of the intact rock material (granite to granodiorite 101057) in fracture domain FFM 01. (Tab. 7-3. TR-08-05, SKB [2008]).



Parameter		value	value			comment
			min	av	max	
Young's modulus	$E$ [GPa]	69	76	83		UCS test, 50% tangent modulus
Poisson's ratio	$\nu$ [1]	0,14	0,23	0,30		
Uniaxial compressive strength	UCS [MPa]	157	226	289		
Crack initiation stress	SCI [MPa]	60	116	187		
	[%]	38 %	51 %	65 %		percent of UCS
Cohesion	$C$ [MPa]	-	28	-		Mohr Coulomb, 0-15 MPa
Friction angle	$\phi$ [°]	-	60	-		
Tensile strength	$S_T$ [MPa]	10	13	18		indirect tensile strength

The fracture mechanics parameters were determined as reported in Backers and Stephansson [2008] and are summarised in Tables 2 and 3. The Mode I and Mode II fracture toughness have been measured at ambient pressure and temperature conditions. The fracture normal stiffness has been measured on tensile fresh fractures. The fracture normal stiffness is about  $3 \cdot 10^{11}$  Pa/m. The shear stiffness is estimated from experience to  $1.5 \cdot 10^{11}$  Pa/m. The friction angle of newly formed fractures is set to  $30^\circ$ , the cohesion to 0 MPa.

Table 2. Fracture mechanics properties of the intact rock material (Backers and Stephansson [2008]).

Parameter		value	comment
Mode I fracture toughness	$K_{IC}$ [MPa $\sqrt{m}$ ]	2,5	Chevron Bend test
Mode II fracture toughness	$K_{IIC}$ [MPa $\sqrt{m}$ ]	4,0	PTS/CP experiment
Fracture normal stiffness	$k_N$ [Pa/m]	$3.0 \cdot 10^{11}$	
Fracture shear stiffness	$k_S$ [Pa/m]	$1.5 \cdot 10^{11}$	

Table 3. Fracture properties of the rock material (Tab 7-4. TR-08-05, SKB [2008]).

Parameter		value	comment
Normal stiffness	$k_{IN}$ [Pa/m]	$6.6 \cdot 10^{11}$	
Shear stiffness	$k_{IS}$ [Pa/m]	$0.3 \cdot 10^{11}$	
Peak friction angle	[°]	37	
Peak cohesion	[MPa]	0,8	
Residual friction angle	[°]	35	
Residual cohesion	[MPa]	0,3	

### 5.2.2. Rock mass properties

The values for deformation and strength properties of the rock mass were chosen for the dominant rock type 101057 (granite to granodiorite, metamorphic, medium grained) and are summarised in Table 4 (Glamheden et al. [2008], SKB [2008]). The rock mass properties are not used in the models, as the fractures are explicitly simulated.

Table 4. Rock mass properties (granite to granodiorite 101057) in fracture domain FFM 01. (SKB [2008]).

Parameter		value	value			comment
			min	av	max	
Young's modulus	$E_m$ [GPa]		39	72	76	UCS test, 50% tangent modulus
Poisson's ratio	$\nu_m$ [1]		0,12	0,23	0,30	
Uniaxial compressive strength	$UCS_m$ [MPa]		23	92	153	
Cohesion	$C_m$ [MPa]		12	27	35	Mohr Coulomb, 0-15 MPa
Friction angle	$\phi_m$ [°]		32	50	52	
Tensile strength	$S_{Tm}$ [MPa]		0,6	2,4	5,0	indirect tensile strength

### 5.2.3. Thermal properties

The thermal properties are reproduced from SKB [2008] and SKB [2009a] and are given in Table 5. The average values are used in the models unless otherwise stated.

Table 5. Thermal properties for rock type 101057 (SKB [2008], SKB [2009a]).

Parameter		value			comment
		min	av	max	
Thermal conductivity	[W/mK]	3,25	3,68	4,01	TPS method at room temperature
Heat capacity	[MJ/m <sup>3</sup> K]		2,09		TPS method
Coefficient of thermal expansion	[m/mK]	$2,1 \cdot 10^{-6}$	$7,7 \cdot 10^{-6}$	$1,5 \cdot 10^{-5}$	

## 5.3. Stress conditions

### 5.3.1. Stress model

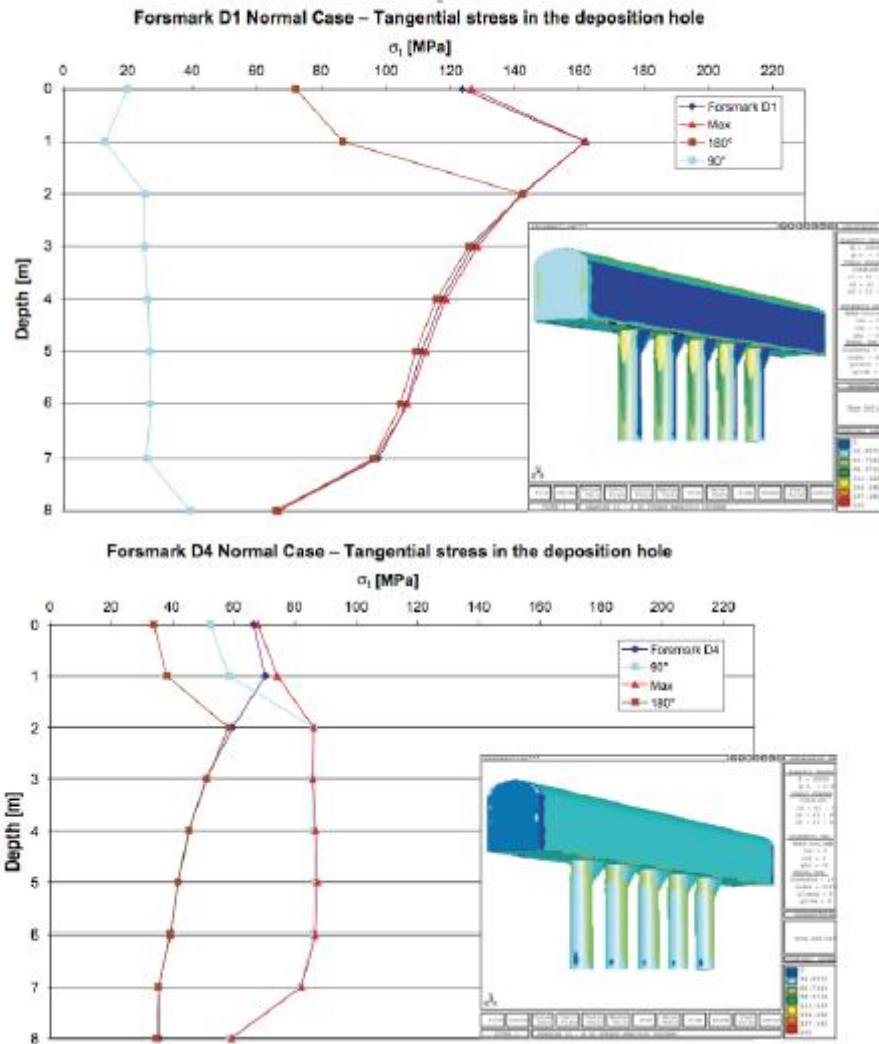
The SKB stress model for Forsmark is given in Table 6 based on Table 7-7 in SKB [2008]. The most likely values for the stresses are based on Martin [2007]. This model is used in this study unless otherwise stated. For the sake of completeness the model of Ask et al. [2007] is included in the analysis on selected simulations.

Table 6. Stress model for domains FFM01. (Ask et al. [2007], Martin [2007], SKB [2008]).

			value	comment
major horizontal stress	SH	[MPa]	$29,5 + 0,023 z$	for the depth z interval 400 - 600 m
minor horizontal stress	Sh	[MPa]	$9,2 + 0,028 z$	for the depth z interval 400 - 600 m
vertical stress	Sv	[MPa]	$0,0265 z$	for the depth z interval 400 - 600 m
orientation of SH	dirSH	[°]	145,00	for the depth z interval 400 - 600 m
<i>Martin [2007]</i>				
maximum horizontal stress (400m)	SH	[MPa]	38,7	
minimum horizontal stress (400m)	Sh	[MPa]	20,4	
vertical stress	Sv	[MPa]	10,6	
orientation of SH	dirSH	[°]	145,0	
maximum horizontal stress (500m)	SH	[MPa]	41,0	
minimum horizontal stress (500m)	Sh	[MPa]	23,2	
vertical stress	Sv	[MPa]	13,2	
orientation of SH	dirSH	[°]	145,0	
<i>Ask et al. [2007]</i>				
maximum horizontal stress (400m)	SH	[MPa]	19,2	
minimum horizontal stress (400m)	Sh	[MPa]	9,3	
vertical stress	Sv	[MPa]	10,4	
orientation of SH	dirSH	[°]	124,0	
maximum horizontal stress (500m)	SH	[MPa]	22,7	
minimum horizontal stress (500m)	Sh	[MPa]	10,2	
vertical stress	Sv	[MPa]	13,0	
orientation of SH	dirSH	[°]	124,0	

Eriksson et al. [2009] have analysed the influence of the stress redistributions around deposition tunnels on the deposition holes. Figure 3 show the tangential stress along the vertical deposition hole axis at positions 0°, 90° and 180° from the deposition tunnel direction. Please note that the bevel is included in the analysis. The influence of the bevel on the stresses reaches considerably down into the rock mass around the deposition holes. The bevel is not considered in this study, but could be analysed in terms of its fracturing potential in a dedicated study.

Figure 3. Figures A1 (left) and A4 (right) from Eriksson et al. [2009].



This campaign simulates cross sections through two neighbouring deposition holes. For this the stress redistribution from the deposition tunnel must be acknowledged. The major horizontal stress is assumed to act along the tunnel axis, and the stress redistribution from the tunnel in that direction is neglected, i.e.  $S_H = S_{xx}$ . However, the  $S_{yy}$  component in the model is influenced by the presence of the deposition tunnel.

Figure 4 shows the results from a simple phase2 simulation applying a stress state as predicted by Martin [2007] at 420m to a horse shoe tunnel of 4.2 times 4.8m. The horizontal stress below the tunnel floor varies between 30.1MPa and 22.5MPa for the interval 0 - -8m. For the modelling campaign in this study the stress at 2m below the floor will be used, i.e. 28.2MPa. The influence of a bevel is ignored.

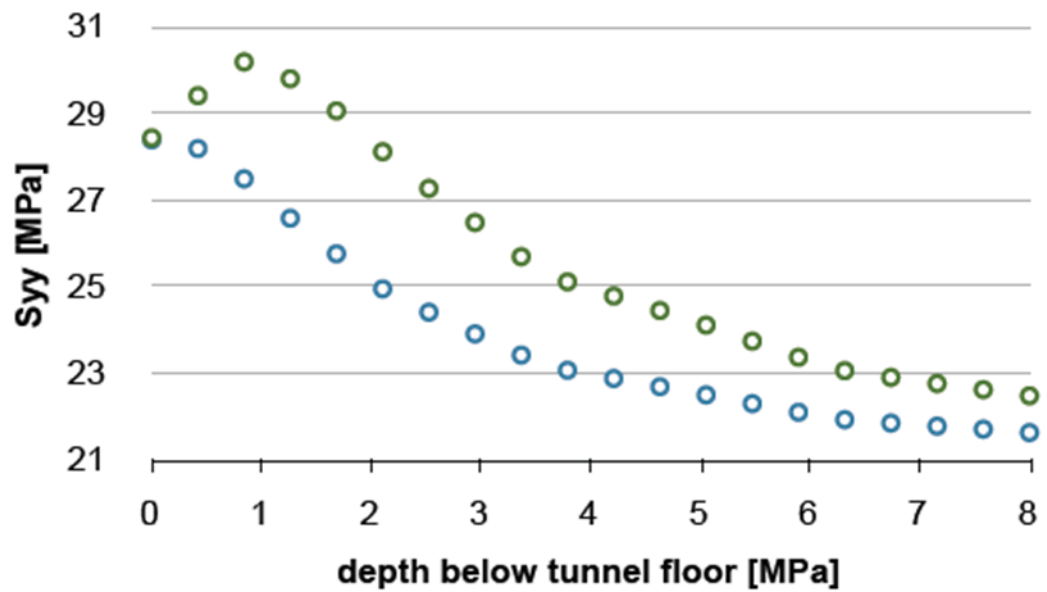


Figure 4. Horizontal stress below tunnel floor from stress redistribution at depth 420m following the stress model by Martin [2007]. green - open excavation, blue - excavation filled with bentonite.

Figure 5 shows the results from a simple phase2 simulation applying a stress state as predicted by Ask et al. [2007] at 420m to a horse shoe tunnel of 4.2 times 4.8m. The horizontal stress below the tunnel floor varies between 12.4MPa and 10.0MPa for the interval 0 - -8m. For the modelling campaign in the study the stress at 2m below the floor will be used, i.e. 12.2MPa. Also for this case a bevel is ignored.

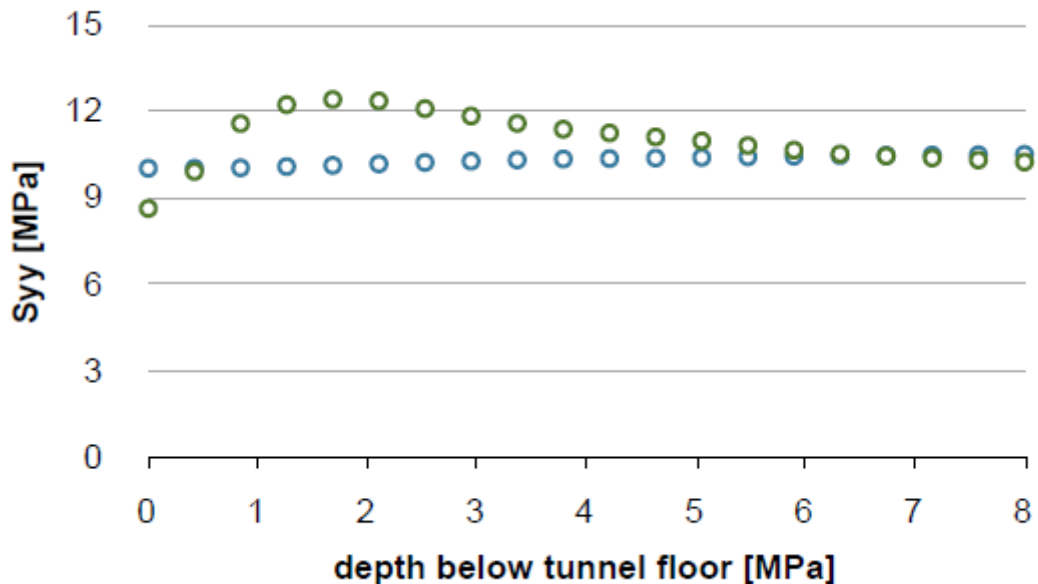


Figure 5. Horizontal stress below tunnel floor from stress redistribution at depth 420m following the stress model by Ask et al. [2007]. green - open excavation, blue - excavation filled with bentonite.

A backfill with compacted bentonite (Young's modulus approx. 100MPa) reduces the resulting horizontal stresses (cf. Figures 4 and 5). At -2m the stress is reduced by roughly 3MPa.

### 5.3.2. Fluid pressure

The fluid pressure  $P_p$  is assumed to be hydrostatic after the introduction of the bentonite and the closure of the repository. No fluid motion is considered. The fluid pressure for the respective models is set to  $P_p = 4\text{MPa}$ . For the fluid pressure  $P_p$  during the ice cover the reader is referred to the respective modelling section.

### 5.3.3. Swelling pressure

High compacted bentonite is considered one of the barriers of the multi-barrier concept. It will be emplaced between the canisters and the rock mass. The swelling pressure of the bentonite was examined by Harrington and Birchall [2007]. It was reported to be about 5.5MPa to 7.2MPa at low background pressures of the saturating fluid. The two swelling pressures are considered in the simulations.

### 5.3.4. Ice cover

It is reported that Sweden will be potentially covered by an ice cover of 3,000m thickness. This will introduce an extra vertical stress of 30MPa on the repository that superimposes to the given in situ vertical stress  $S_v = S_{zz}$ . In the models only an increase of  $S_{yy}$  is considered, ignoring other stress increasing or relieving effects. Figure 6 shows a phase2 FEM analysis looking at the influence of an ice cover dead load of increasing magnitude, i.e. 1.000m, 2.000m and 3.000m. The influence is highest below the tunnel floor, but equilibrates below -2m for the different ice cover thicknesses. For simulating the ice cover an increase of  $S_{yy}$  to 24.5MPa is anticipated;  $S_{xx}$  is kept constant ignoring potential isostatic effects.

If the soil will be frozen during the ice cover period, no significant fluid pressure increase will act on the repository levels. If the ground is not frozen the ice melting at the ground of the cover might add a fluid pressure to the reservoir that is as high as the water column at the repository depth. Hence a fluid pressure increase of  $\Delta P_p = 30\text{MPa}$  is considered.

Assuming that at an early stage of the ice age the full fluid pressure was developed, and at a later stage the soil was frozen, so the increased fluid pressure is trapped at almost full magnitude, this might introduce hydraulic fracturing at the unloading accompanying the ice melting. A simulation highlighting this scenario is presented.

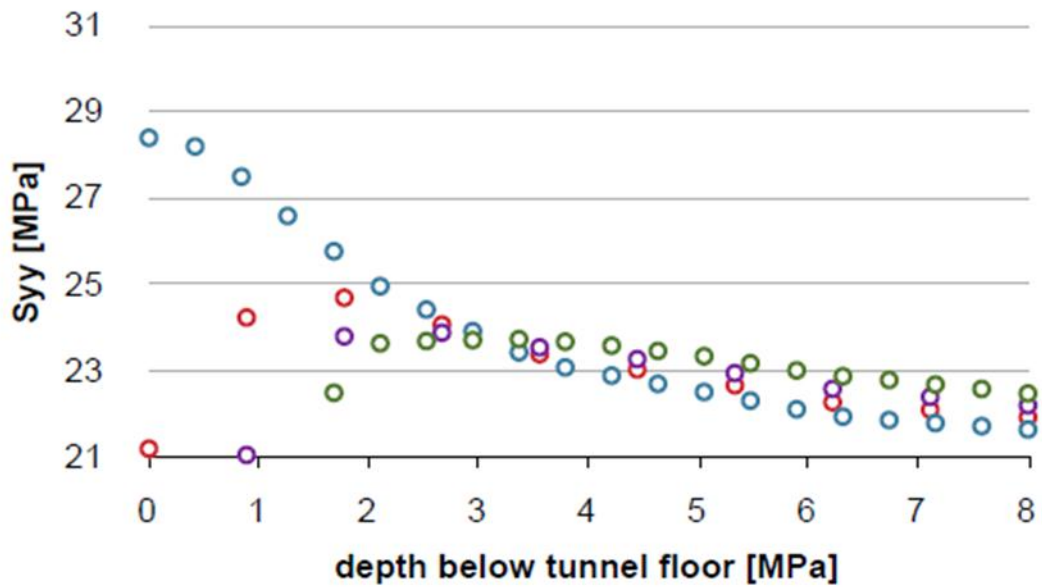


Figure 6. Influence of ice cover thickness on the  $S_{yy}$  stress below the bentonite filled tunnel floor. Only an increase of the vertical load is considered. At a distance of -2m about 24 to 25 MPa is acting in the  $S_{yy}$  direction. Blue - ice cover = 0m; 11MPa vertical; 21MPa horizontal, red - 1000; 21; 21, magenta - 2000; 31; 21, green - 3000; 41; 21.

## 5.4. Temperature conditions

### 5.4.1. In situ temperature

The in situ temperature is reported to be about 10.5°C at 400m to 12.8°C at 600m depth (SKB [2008], SKB [2009a]). The values are given in Table 7. These temperatures are used in the numerical simulations as starting temperatures for the rock mass. The air temperature is estimated at about 15°C for all depth levels.

Table 7. In situ temperatures (SKB [2008], SKB [2009a]).

Parameter		value	comment
Temperature 400m	[°]	10,5	
Temperature 500m	[°]	11,6	
Temperature 600m	[°]	12,8	

### 5.4.2. Temperature evolution and heating scheme

After the closure of the repository the waste will produce heat. It is anticipated in this modelling campaign that the temperature at the bentonite / rock contact in the deposition holes reach up to 75°C. The increase and decrease in temperature is modelled in distinct steps, i.e. 15°C, 25°C, 50°C, 75°C, 50°C, 25°C, 10°C.

### 5.4.3. Ice cover

It is assumed that the ice cover will not freeze the ground at 400m below ground or deeper. The influence of the ice cover cooling effect on the repository is ignored.

## 5.5. Discrete fracture network DFN

The rock mass usually contains a number of fractures. They are geometrically defined by length, orientation and persistence. These discontinuities may alter the fracturing behaviour of the rock mass surrounding the excavations. The fracture sets for this study are generated using the DFN by Fredriksson and Olofsson [2005]. Figure 7 shows their DFN which is used for the upcoming models. Within this DFN different locations for the excavations were tested, these are reproduced in Figures 8 and 9. Their location within the DFN model is given in Figure 10.

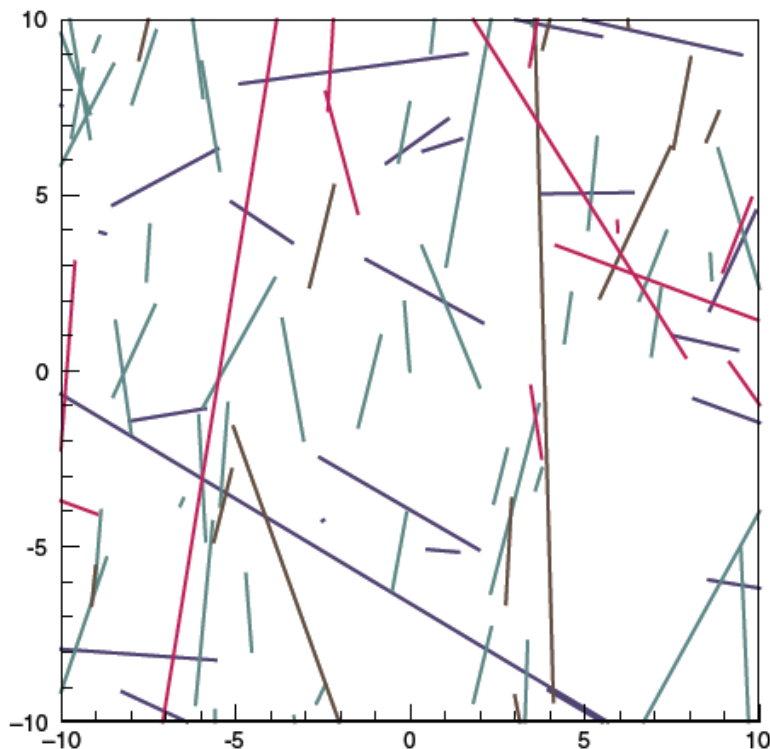


Figure 7. Fracture network by Fredriksson and Olofsson [2005]. SH is in vertical direction in their modelling campaign.

Figure 8. DFN I as used in the simulation campaign. The location within the DFN by Fredriksson and Olofsson [2005] as shown in Figure 7 is sketched in Figure 10. The numbering of the fractures refers to the numbering in the fracod2d files (Appendix).



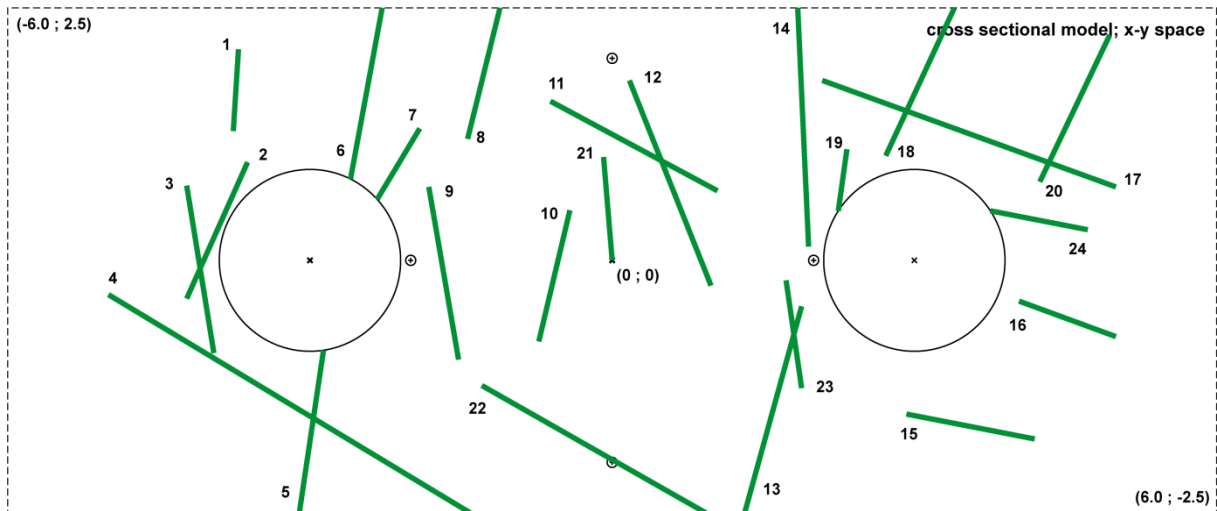


Figure 9. DFN II as used in the simulation campaign. The location within the DFN by Fredriksson and Olofsson [2005] as shown in Figure 7 is sketched in Figure 10. The numbering of the fractures refers to the numbering in the fracod2d files (Appendix).

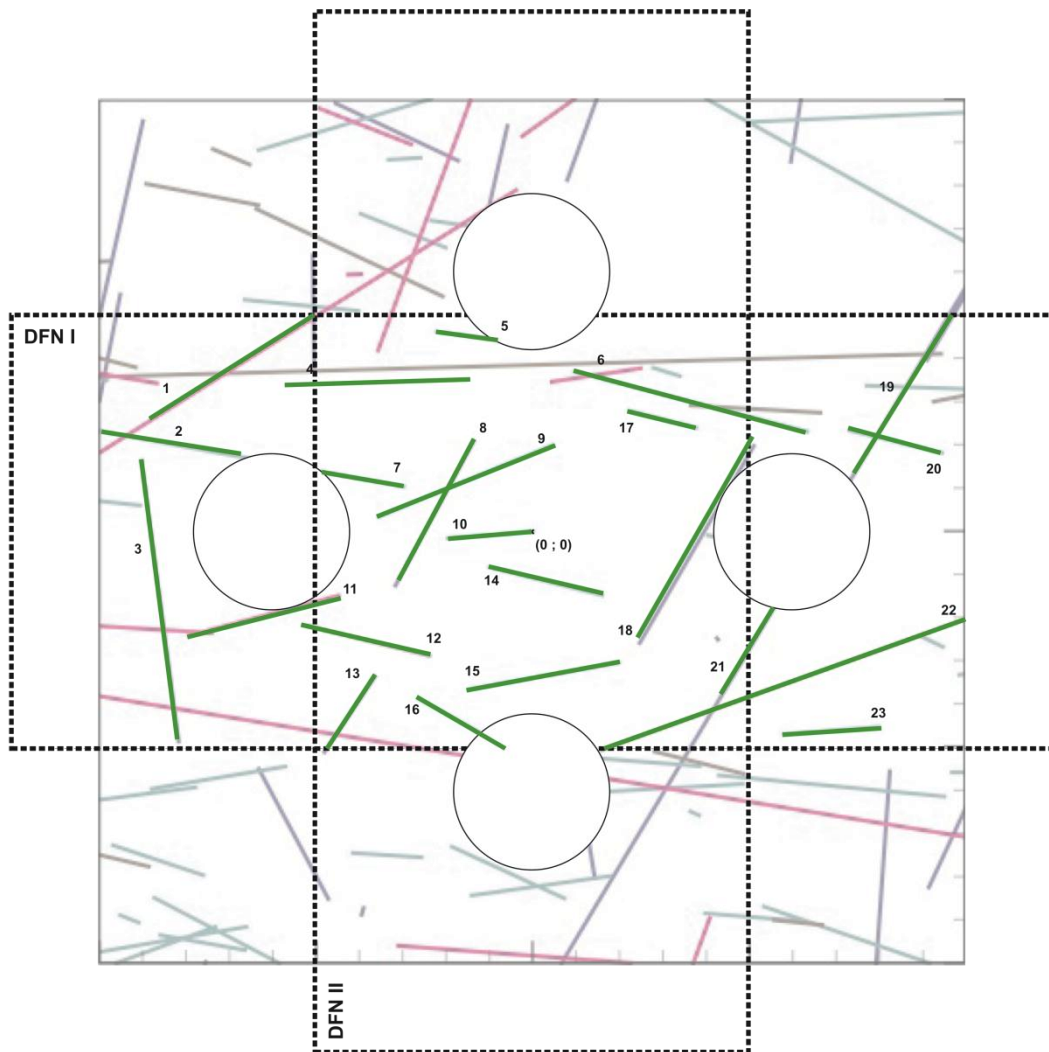


Figure 10. Location of the domains in the DFN of Fredriksson and Olofsson [2005].

## 6. Model validation

### 6.1. Rock model

The deposition holes are assumed to be stable at initial conditions, hence no significant fracture initiation should be assumed. This assumption is tested on a static model with the excavations introduced. The models show no fracturing, hence the parameter set can be granted valid (c.f. Figure 11).

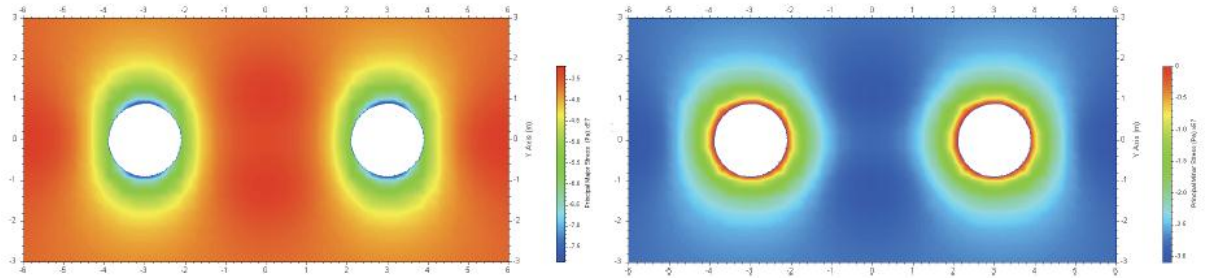


Figure 11. Simulation run with static conditions and without DFN showing no fracture initiation. The major principle stress S1 (left) and minor principle stress S3 (right) are depicted. Hence the input parameter set can be assumed valid.

From a simple Kirsch solution based calculation the maximum tangential stress  $\sigma_{\theta}$  around the canister holes is

$$\sigma_{\theta} = 3SH - S_{yy} = 3 \cdot 39\text{MPa} - 28\text{MPa} = 89\text{MPa}$$

which is well below the UCS of about 116MPa. Martin [2005] also confirmed that no significant spalling is to be expected at the 400m level.

### 6.2. Distinct fracture network model

At the in situ conditions the fracture set without any excavations can be expected to be stable, i.e. no fracturing is achieved. The DFN properties as given by SKB are used in the DFN models to test if stable conditions are achieved in the models, hence no significant fracture growth takes place. The DFN I and II (c.f. Figs. 8 to 10) were subject to the stress fields at 400m and 500m levels as given by Martin [2007] and Ask et al. [2007]. The input parameters were chosen as summarised in Chapter 5. Figure 12 displays exemplarily the DFN I at the highest stresses after the simulation showing no significant fracture growth. The same statement is valid for the other DFN model (see Tab. 8). Hence, the mechanical fracture properties as given by SKB may be used in the study.

Table 8. Results from the validation of the input parameters for the different DFN.

DFN	stress model	SH	Sh	input	stable	simulation
I	Martin [2007]	38,7	20,4	see Chapter 6	yes	dfnIvalidatemartin400
I	Martin [2007]	41,0	23,2	see Chapter 6	few wing fractures	dfnIvalidatemartin500
I	Ask et al. [2007]	19,2	9,3	see Chapter 6	yes	dfnIvalidateask400
I	Ask et al. [2007]	22,7	10,2	see Chapter 6	yes	dfnIvalidateask500
II	Martin [2007]	38,7	20,4	see Chapter 6	yes	dfnIIvalidatemartin400
II	Martin [2007]	41,0	23,2	see Chapter 6	few wing fractures	dfnIIvalidatemartin500
II	Ask et al. [2007]	19,2	9,3	see Chapter 6	yes	dfnIIvalidateask400
II	Ask et al. [2007]	22,7	10,2	see Chapter 6	yes	dfnIIvalidateask500

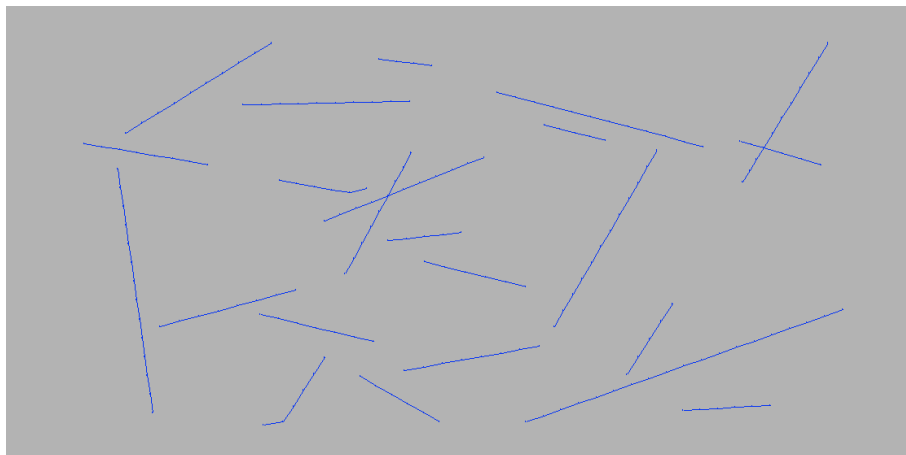


Figure 12. DFN I subject to the stress field at 500m depth as defined by Martin [2007]. No significant fracturing was introduced (i.e. only on two fractures one fracture increment) → compare to the input DFN I in Figure 8.

## 7. Results

### 7.1. Overview to simulation campaign

Table 9 summarises the simulations that are used in the results chapter. Besides, several test runs had to be performed for stability and verification reasons that yielded confirmation in the stability of the models and confidence in the results. The listings and detailed descriptions of the individual simulations are given in the appendix.

Table 9. Overview to simulations. Legend: 1) according Martin [2007]; 2) according Ask et al. [2007]; 3) unloading of ice cover load at constant high fluid pressure, appx: see appendix for figures.

ID	reference	stress field		DFN	fracture initiation	closure			heating sequence	ice cover		appx	
		Sxx	Syy			backfill	Ps	Pp		load	Pp		
		[MPa]	[MPa]			[MPa]	[MPa]	[MPa]		[MPa]	[MPa]		
IM-1	13409b21008261	38,7	28,2	<sup>1)</sup>	I	✓	-3,0	5,5	4,0	✓	24,5	34	✗
IM-2	13409b21008262	38,7	28,2	<sup>1)</sup>	✗	✓	-3,0	5,5	4,0	✓	24,5	34	✗
IM-3	13409b21008263	38,7	28,2	<sup>1)</sup>	I	✓	-3,0	7,2	4,0	✓	24,5	34	✗
IM-4	13409b21008301	38,7	28,2	<sup>1)</sup>	I	✓	-3,0	0,0	4,0	✓	24,5	34	✗
IM-5	13409b21008302	38,7	28,2	<sup>1)</sup>	I	✗	-3,0	0,0	0,0	✓	24,5	30	✗
IM-6	13409b21008311	38,7	28,2	<sup>1)</sup>	I	✗	-3,0	5,5	4,0	✗	24,5	34, +5, 60	✓
IM-7	13409b21009011	38,7	28,8	<sup>1)</sup>	I	✗	-3,0	7,2	4,0	✗	24,5	34, +5, 60	✓
IM-8	12409b21009012	38,7	28,8	<sup>1)</sup>	I	✗	-3,0	5,5	0,0	✓	24,5	30	✗
IM-9	13409b21009031	38,7	28,2	<sup>1)</sup>	I	✗	-3,0	5,5	4,0	✓	24,5	34	✓
IM-10	13409b21009032	38,7	28,2	<sup>1)</sup>	I	✗	-3,0	7,2	4,0	✓	24,5	34	✓
IA-1	13409b21009081	19,2	12,2	<sup>2)</sup>	I	✗	-3,0	5,5	4,0	✓	24,5	34	✓
IA-2	13409b21009082	19,2	12,2	<sup>2)</sup>	I	✗	-3,0	7,2	4,0	✓	24,5	34	✓
IA-3	13409b21009083	19,2	12,2	<sup>2)</sup>	I	✗	-3,0	5,5	4,0	✗	24,5	34, +5, 60	✓
IA-4	13409b21009084	19,2	12,2	<sup>2)</sup>	I	✗	-3,0	7,2	4,0	✗	24,5	34, +5, 60	✗
IA-5	13409b21009085	19,2	12,2	<sup>2)</sup>	I	✗	-3,0	5,5	0,0	✓	34,5	30	✗
IIM-1	13409b21009141	38,7	28,2	<sup>1)</sup>	II	✗	-3,0	5,5	4,0	✓	24,5	34	✓
IIA-1	13409b21009142	19,2	12,2	<sup>2)</sup>	II	✗	-3,0	5,5	4,0	✓	24,5	34	✓
IM0-1	13409b21009151	38,7	28,2	<sup>1)</sup>	I	✗	-3,0	5,5	4,0	✗	24,5	34	<sup>3)</sup> ✓
IM0-2	13409b21009161	38,7	28,2	<sup>1)</sup>	I	✗	-3,0	5,5	0,0	✗	24,5	0, +5, 50	✗

## 7.2. Effect of loading history without DFN (IM-2)

The simulation campaign highlighted in this section shows the resulting stress and temperature fields from the boundary conditions specified. No DFN is considered in these simulations; however fracture initiation according to the specified Mohr-Coulomb model is allowed.

Table 11. Conditions of the simulation IM-2 subject to the stress field according to (Martin, 2007) with a swelling pressure of 5.5MPa.

simulation	stress field		DFN	fract.ini	closure			heating	ice cover	
	Sxx	Syy			backfill	Ps	Pp		load	Pp
13409b21008262	38,7	28,2	✗	✓	-3,0	5,5	4,0	✓	24,5	34

Figure 13 shows the evolution of temperature and stress for the individual simulation steps.

The introduction of the excavations results in an increase of stresses around the deposition holes (Step A). The S1 stress field becomes elliptical due to the differential stress field applied from the access tunnel. Notice that the applied stress field mirrors a horizontal section two meters below the access

tunnel floor. The simulated temperature field is symmetric round the deposition holes, with 15°C at the hole wall and 10.5°C in the rock mass.

After the closure of the access tunnel (Step B), the tangential stress from the tunnel acting on the deposition hole is reduced assuming a full backfill with a soft material. This minor reduction has no significant effect on the stress field.

After the closure of the repository with increase of water head the bentonite in the deposition holes will start to swell (Step C). This introduces a swelling pressure that reduces the magnitude of stress redistribution.

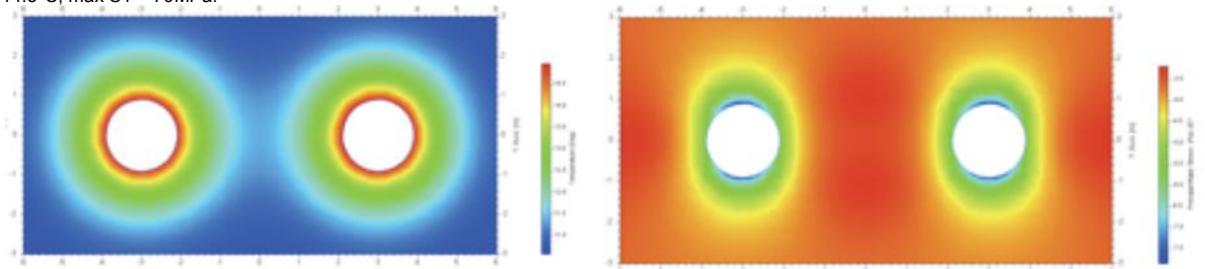
In Steps D to F the temperature of the deposition hole walls are increased quite rapidly to 75°C. The temperature in the rock mass increases and introduces increased stresses. The increase in max S1 is about  $\Delta S1 = 20\text{MPa}$ . In Steps G to I the temperature of the deposition hole walls is slowly reduced to 10°C. The highest temperatures in the simulations are between the deposition holes as a remnant of the higher temperatures at the deposition hole walls. Max S1 is reduced by  $\Delta S1 = -21\text{MPa}$ .

The application of the ice cover to the model results in a pronounced increase of S1 by  $\Delta S1 = +50\text{MPa}$  (Step J). The subsequent increase of water head reduces the S1 again (Step K).

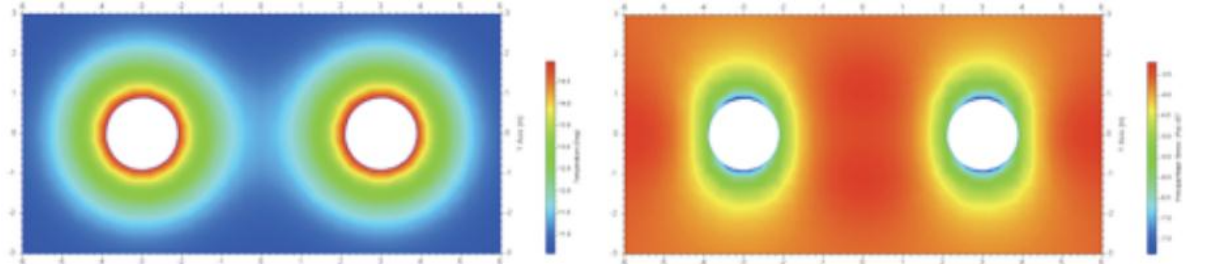
During all steps no fractures were initiated.

Figure 13. Temperature and stress evolution of model without DFN (IM-2). Thickening of lines show application of a fluid pressure. For discussion refer to the description of the steps and the main text.

Step A. The excavations are introduced in the static stress field according to Martin [2007]. The rock mass temperature is 10.5°C and the air temperature in the unsupported deposition holes is 14.5°C. // max. T = 14.5°C, max S1 = 79MPa.

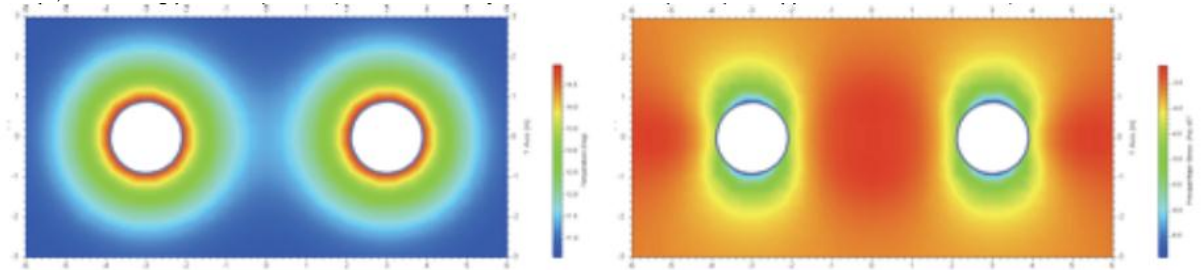


Step B. After the closure of the repository the applied stress is decreased due to the backfill of the tunnel. The temperature of the deposition hole walls is not changed. // max. T = 14.5°C, max S1 = 78MPa.

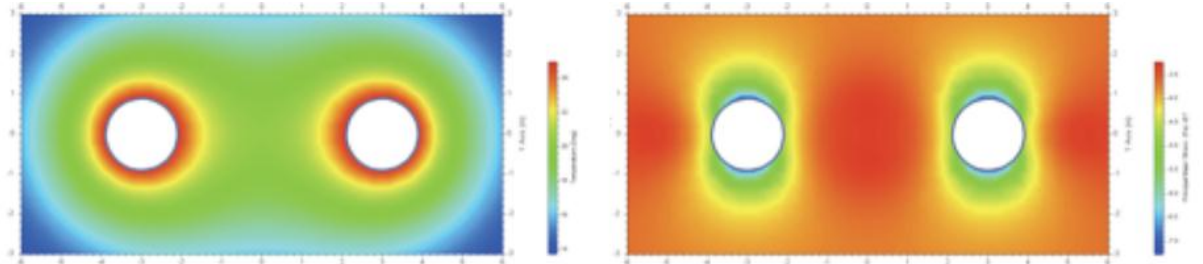




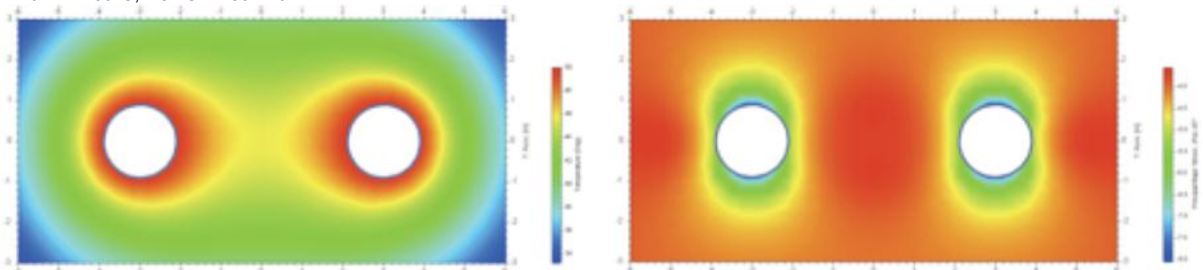
Step C. A swelling pressure (5.5MPa) and the recovery of the water head (4MPa) are applied. // max. T = 14.5°C, max S1 = 69MPa.



Step D. The temperature at the wall of the deposition holes is increased from the initial 14.5°C to 25°C. Exposition time approx. 22a. // max. T = 25°C, max S1 = 73MPa.



Step E. The temperature at the face of the deposition holes is increased to 50°C. Exposition time approx.22a. // max. T = 50°C, max S1 = 80MPa.



Step F. The temperature at the face of the deposition holes is increased to 75°C. Exposition time approx. 22a. // max. T = 75°C, max S1 = 89MPa. 134.101110.backers.09b2.fr | 73 | 10.11.2010 21.

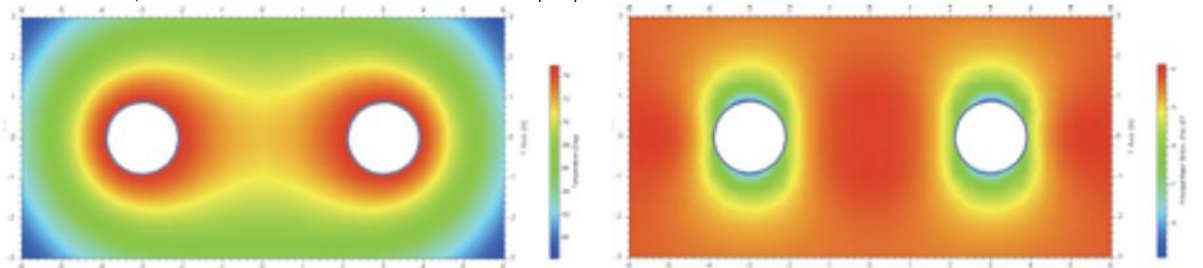
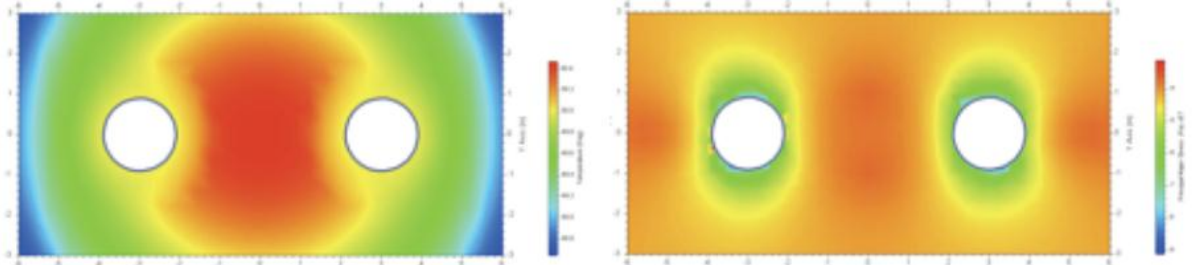
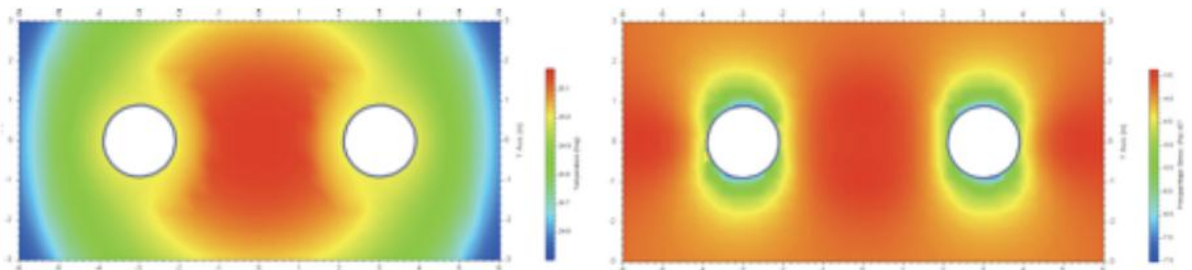


Figure 13. Temperature and stress evolution of model without DFN (IM-2). Thickening of lines show application of a fluid pressure. For discussion refer to the description of the steps and the main text.

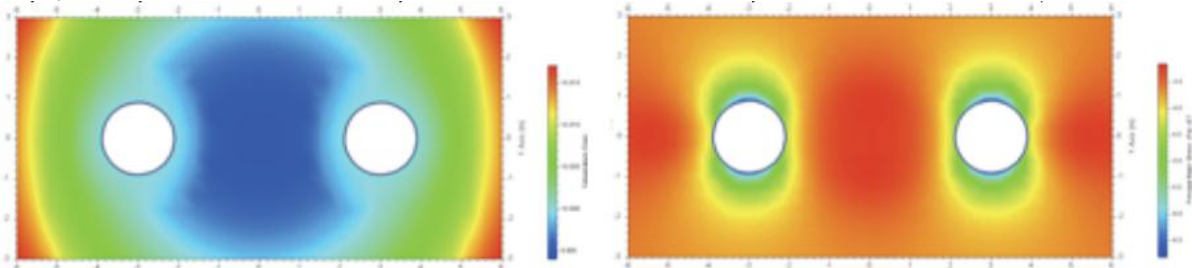
Step G. The temperature at the face of the deposition holes is decrease to 50°C. Exposition time approx. 3000a. // max. T = 51°C, max S1 = 82MPa.



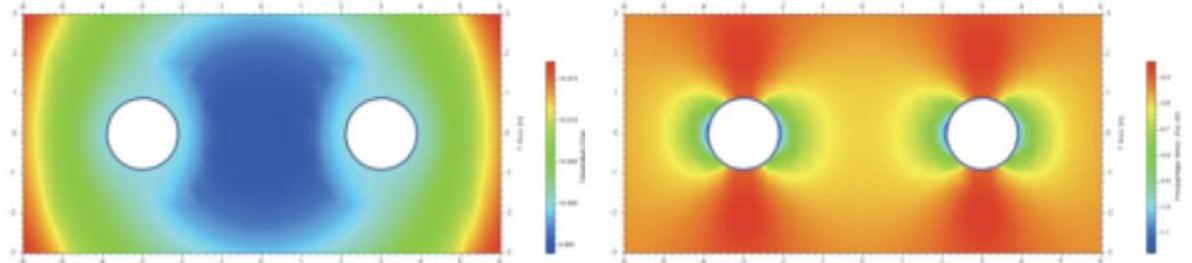
Step H. The temperature at the face of the deposition holes is decreased to 25°C. Exposition time 9e10s. // max. T = 25.2°C, max S1 = 76MPa.



Step I. The temperature at the face of the deposition holes is decreased to 10°C. Exposition time 9e10s. // T ~ 10°C, max S1 = 68MPa.

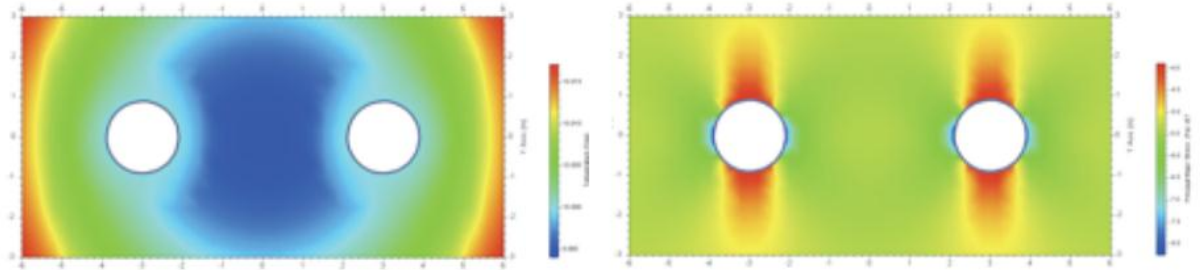


Step J. As for simulation of an ice cover of approx. 3km additional load of 24.5MPa (Syy due to redistribution around backfilled tunnel) is added. // T ~ 10°C, max S1 = 118MPa.



Step K. The water head is increased by 30MPa due to an assumed ice cover fully hydraulically connected to the repository. // T ~ 10°C, max S1 = 84MPa. 134.101110.backers.09b2.fr | 73 | 10.11.2010 22

Figure 13. Temperature and stress evolution of model without DFN (IM-2). Thickening of lines show application of a fluid pressure. For discussion refer to the description of the steps and the main text.



### 7.3. Evolution of fracture network DFN I under high in-situ stress field

The evolution of DFN I subject to the high in-situ stress field according to Martin [2005] was studied with the full heating sequence for two swelling pressures. The model parameters are given in Table 11.

Table 11. Conditions of the simulations subject to the stress field according to Martin [2007] with two swelling pressures.

ID	reference	stress field		DFN	fracture initiation	closure			heating sequence	ice cover	
		Sxx [MPa]	Syy [MPa]			backfill [MPa]	Ps [MPa]	Pp [MPa]		load [MPa]	Pp [MPa]
IM-9	13409b21009031	38,7	28,2	I	✗	-3,0	5,5	4,0	✓	24,5	34
IM-10	13409b21009032	38,7	28,2	I	✗	-3,0	7,2	4,0	✓	24,5	34

Only few fractures propagate short distances due to the stress redistribution of the excavations. The swelling pressure introduces limited additional stable fracturing irrespective of magnitude. Neither the backfill nor heating sequence results in significant fracture propagation. The increase in load from the ice cover introduces only minor fracturing. The increase in fluid pressure from the top of the ice sheet causes some fracturing that may lead to potential flow paths between the deposition holes. Figure 14 shows an example of the developed fracture pattern.



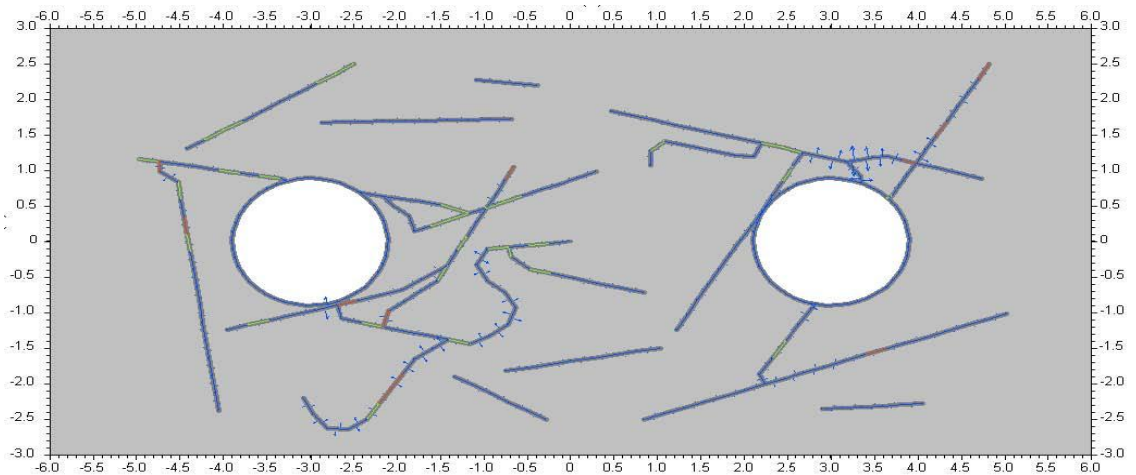


Figure 14. Example of the fracture evolution in a stress field according to Martin [2005]. (simulation IM-9, last stage).

#### 7.4. Evolution of fracture network under low in-situ stress field

The evaluations of rock stresses at Forsmark by Ask et al. [2007] have yielded a significantly lower in-situ stress field compared to Martin [2007]. Assuming the loading history will be the same from the reduced starting values of Ask et al. [2007], and as the ice age has shown to significantly enhance fracturing, a series of simulations at low in-situ stress values was conducted. The conditions of the model are given in Table 12.

Table 12. Conditions of the simulations subject to the stress field according to Ask et al. [2007] for two swelling pressures.

ID	reference	stress field		DFN	fracture initiation	closure			heating sequence	ice cover	
		Sxx [MPa]	Syy [MPa]			backfill [MPa]	Ps [MPa]	Pp [MPa]		load [MPa]	Pp [MPa]
IA-1	13409b21009081	19,2	12,2	I	x	-3,0	5,5	4,0	✓	24,5	34
IA-2	13409b21009082	19,2	12,2	I	x	-3,0	7,2	4,0	✓	24,5	34

The introduction of the excavations and the reduction of Syy due to the backfill only show minor fracture propagation. But already the combination of swelling pressure and in particular water pressure after the closure of the repository results according to the simulations in significant fracture growth connecting the deposition holes. Addition of thermal loads enhances fracture growth. It appears that fracture growth at peak temperature seems to be unstable<sup>2</sup> - hence additional study of this case should be performed. Figure 15 shows an example of a developed fracture pattern.

<sup>2</sup> The five cycles of fracture growth appear not to be sufficient to reduce the energy in the system sufficiently. Hence, additional computing would be required to study the influence of the peak temperature. As an artefact of this instability of the computational step fracturing is proceeding in the cooling phase.

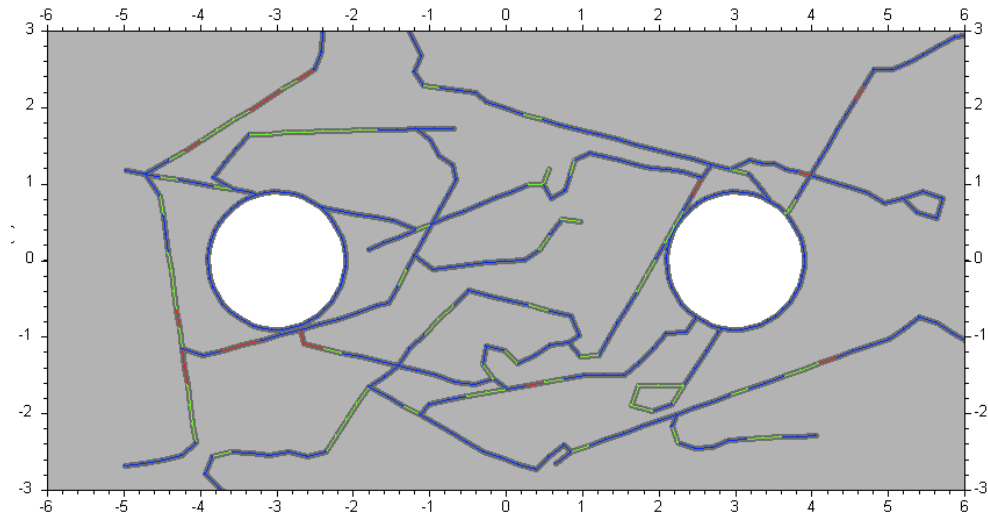


Figure 15. Example of the fracture evolution in a stress field according to Ask et al. [2007] with increased water head from an ice sheet. (simulation IA-2, last stage).

## 7.5. The influence of the fluid pressure from an ice cover

The previous analyses have shown that the fluid pressure resulting from an ice cover has the highest impact on the fracture growth of DFN I. Therefore, the fluid pressure under ice cover load is stepwise increased in the following simulations. Table 13 summarises the boundary conditions.

Table 13. Conditions of the simulations aiming at studying the influence of the ice cover. Legend: <sup>1)</sup> according Martin [2007]; <sup>2)</sup> according Ask et al. [2007].

ID	reference	stress field		DFN	fracture initiation	closure			heating sequence	ice cover		
		Sxx [MPa]	Syy [MPa]			backfill [MPa]	Ps [MPa]	Pp [MPa]		load [MPa]	Pp [MPa]	
IM-6	13409b21008311	38,7	28,2	<sup>1)</sup>	I	✗	-3,0	5,5	4,0	✗	24,5	34, +5, 60
IM-7	13409b21009011	38,7	28,8	<sup>1)</sup>	I	✗	-3,0	7,2	4,0	✗	24,5	34, +5, 60
IA-3	13409b21009083	19,2	12,2	<sup>2)</sup>	I	✗	-3,0	5,5	4,0	✗	24,5	34, +5, 60
IA-4	13409b21009084	19,2	12,2	<sup>2)</sup>	I	✗	-3,0	7,2	4,0	✗	24,5	34, +5, 60

At the conditions of high in-situ stress only few fractures propagate short distances due to the stress redistribution from the excavations. Neither the backfill, swelling pressure nor heating sequence gave significant fracture propagation. While the increase in load from the ice cover introduces only minor fracturing, the additional increase in fluid pressure introduces some fracturing that may lead to potential connection of the deposition holes. The hydraulic connection in the example is achieved above  $P_p > 44\text{MPa}$ .

At low in-situ stress condition also only few fracture propagate short distances due to the stress redistribution of the excavations. The increase in  $P_p$

due to recovery of water head already introduces significant fracture propagation and DFN development. Hydraulic connection is already achieved at  $P_p < 4\text{MPa}$ . The increase in load due to the ice cover stabilises the fractures slightly, the increase in fluid pressure due to the ice cover introduces severe fracturing again. At some point almost all fractures have run into an arrester position so that a further increase in  $P_p$  does not introduce additional fracture propagation. As the initiation of new fractures is not activated it may be discussed if new fractures would be created; this is beyond the scope of this study, as the applied  $P_p$  from the ice cover can already be assumed quite high.

It has to be emphasised that this is valid for the given DFN. The results so far have shown the great potential of this loading to introduce full hydraulic connection. Therefore additional simulations should be performed to determine the potential of this scenario.

Figure 16 compares the DFN after a water head of 60MPa was applied.

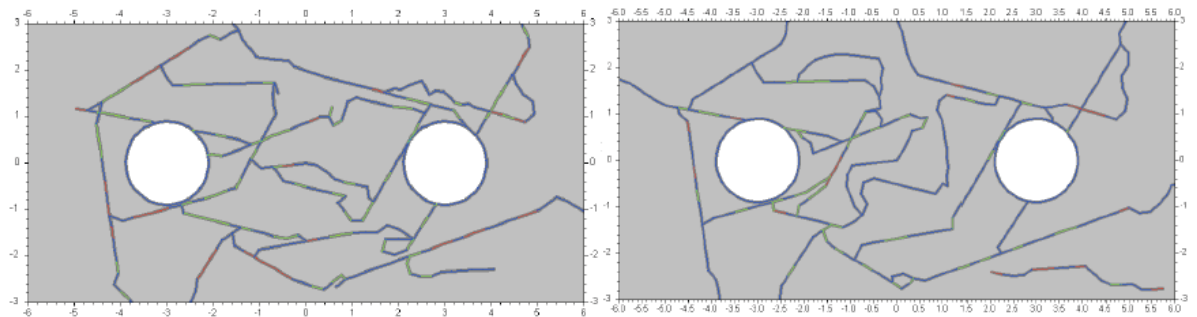


Figure 16. Comparison of DFN development at high (left, Martin [2005], simulation IM-7) and low (right, Ask et al. [2007], simulation IA-4) in-situ stresses after application of additional water head up to 60MPa. Both models show hydraulic connection of the deposition holes.

## 7.6. Evolution of fracture network DFN II

For comparison DFN II (see Fig. 9) is implemented to see if the fracture evolution is changed due to the orientation of the majority of fractures perpendicular to  $SH = S_{xx}$ . Table 14 summarises the boundary conditions.

Table 14. Overview of simulations of the DFN II development. Legend: <sup>1)</sup> according Martin [2007]; <sup>2)</sup> according Ask et al. [2007].

ID	reference	stress field		DFN	fracture initiation	closure			heating sequence	ice cover		
		$S_{xx}$ [MPa]	$S_{yy}$ [MPa]			backfill [MPa]	$P_s$ [MPa]	$P_p$ [MPa]		load [MPa]	$P_p$ [MPa]	
IIM-1	13409b21009141	38,7	28,2	<sup>1)</sup>	II	✗	-3,0	5,5	4,0	✓	24,5	34
IIA-1	13409b21009142	19,2	12,2	<sup>2)</sup>	II	✗	-3,0	5,5	4,0	✓	24,5	34

At the conditions of the stress field by Martin [2005] only few fractures propagate short distances due to the loading history until the increased water

pressure from the ice cover is applied. The water head from an ice cover might introduce hydraulic fracture growth of individual fractures.

At conditions of the low stress field Ask et al. [2007] few fractures propagate short distances due to the loading history until the ice cover induced increase in  $S_{yy}$ . The  $S_{yy}$  increase without increase in  $P_p$  resulted in some fracture growth. The additional water head from an ice cover might introduce severe hydraulic fracture growth. Due to the orientation of the fractures in DFN II perpendicular to  $S_{xx}$  a direct hydraulic connection is less pronounced as with DFN I.

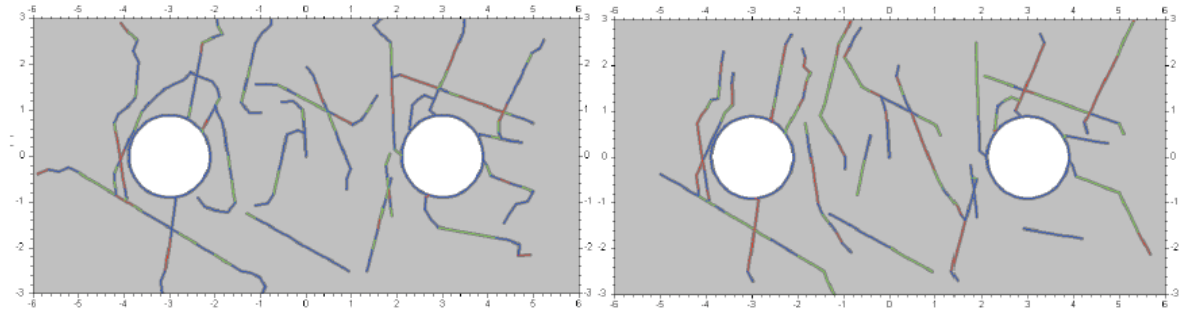


Figure 17. Comparison of DFN II development at high (left, Martin [2005], simulation IIM-1) and low (right, Ask et al. [2007], simulation IIA-1) in-situ stresses after application of a complete 3km additional water head.

## 7.7. Post glacial scenario

Simulations of the scenario for glaciation so far has shown minor influence of the increase in vertical load, resulting in a tangential stress increase affecting the deposition holes, but a strong influence of the accompanied increase of water pressure on the fracture growth and in particular in the low in-situ stress scenario. The increase in vertical load from the ice sheet should compensate to some extent for the increase in water pressure. Assuming that on the melting of the ice cover the water pressure is not reducing as fast as is the vertical load, this might be e.g. due to a permafrost zone, a simulation is run that takes the vertical load due to the ice cover off the model, but maintains the water pressure. The results are given in Figure 18.

The model in this simulation includes DFN I and is subject to the stress field by Martin [2007]. After the introduction of the excavations and the closure of the repository, the ice cover load is applied. No heating sequence was modelled, as this showed minor influence in comparable models. After the increase in  $S_{yy}$ , the water pressure is increased to  $P_p = 34\text{MPa}$ , afterwards the  $S_{yy}$  is reduced by  $24,5\text{MPa}$  at maintaining the increased  $P_p$  at  $34\text{MPa}$ . The simulation resulted in a complete hydraulic connection between the deposition hole. Although the loading sequence is extreme, it clearly shows the influence of a high pore pressure.

Table 15. Conditions of the simulations subject to the stress field according to Martin [2007] without heating scenario but reduction of  $S_{yy}$  at high pore pressure.

ID	reference	stress field		DFN	fracture initiation	closure			heating sequence	ice cover	
		$S_{xx}$	$S_{yy}$			backfill	$P_s$	$P_p$		load	$P_p$
		[MPa]	[MPa]								
IM0-1	13409b21009151	38,7	28,2	I	X	-3,0	5,5	4,0	X	24,5	34

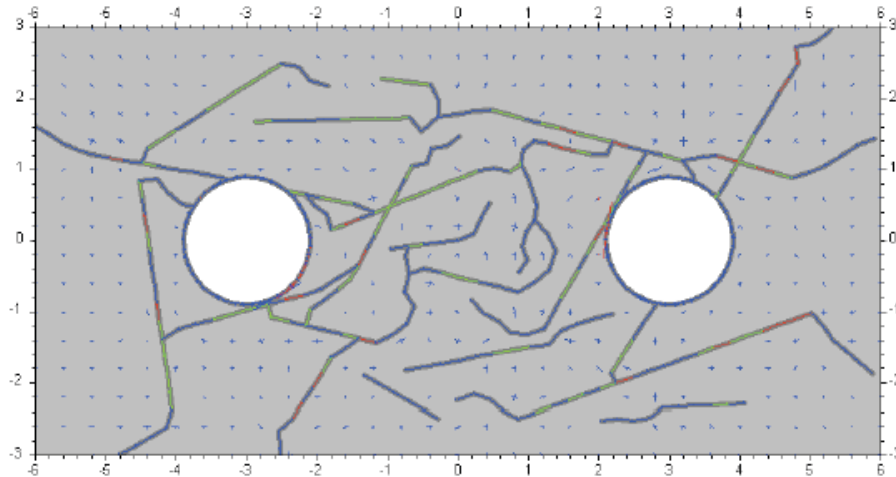


Figure 18. Fracture network for an overpressure scenario from the glaciation. At full  $P_p = 34\text{MPa}$  the load of the ice cover is removed, hence the stress field is again as defined by Martin [2007]. However, the water pressure  $P_p$  is assumed trapped, introducing severe fracturing and formation of hydraulic connection of the deposition holes.

## 7.8. Comparison of simulation of models with and without fracture initiation

The majority of simulations were run without the option of new fractures to be initiated. This was due to computational costs; without the fracture initiation option activated the simulations took about 40% less computing time. Figure 19 depicts a comparison of two simulations that were run through the complete simulation at identical options except for the option of new fractures to be initiated. The general outcome of the two simulations is similar. In the immediate vicinity of the excavations some additional fractures were initiated, changing the general fracture pattern only minor. Comparison of the results of additional simulations on DFN I has confirmed the outcome. The deformation takes place mainly on the fractures, hence the increase in stresses close to the deposition holes is not so pronounced and hence no spalling is introduced.

Table 15. Conditions of the simulations subject to the stress field according to (Martin, 2007) with and without fracture initiation.

ID	reference	stress field		DFN	fracture initiation	closure			heating sequence	ice cover	
		Sxx	Syy			backfill	Ps	Pp		load	Pp
		[MPa]	[MPa]								
IM-1	13409b21008261	38,7	28,2	I	✓	-3,0	5,5	4,0	✓	24,5	34
IM-9	13409b21009031	38,7	28,2	I	✗	-3,0	5,5	4,0	✓	24,5	34

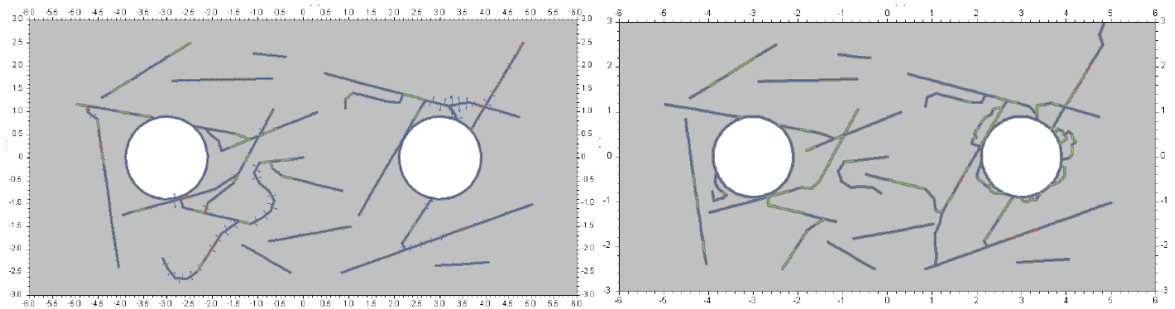


Figure 19. Comparison of DFN development in otherwise intact rock with and without fracture initiation. model IM-1 (left) vs IM-9 (right - with fracture initiation). The figures show the fracture network, and the type of fracture. Colour code: blue - currently not loaded, green - shear loaded, red - open. Thickening of lines show application of a fluid pressure. Note the initiation of minor fracturing at the right deposition hole in the (right) picture where fracture initiation was activated.

## 7.9. Influence of excavation of the deposition holes

Figure 20 compares for DFN I and DFN II the influence of the excavation of the deposition holes in the two stress scenarios. Irrespective of the in-situ stress scenario the fracturing is minor. The potential for fracture growth is low, as the fractures are predominantly neither loaded in shear nor in tensile; hence their activation potential is low.

Table 16. Conditions of the simulations subject to different stress fields and DFNs under consideration of the excavation of the deposition holes.

ID	reference	stress field		DFN	fracture initiation	closure			heating sequence	ice cover	
		Sxx	Syy			backfill	Ps	Pp		load	Pp
		[MPa]	[MPa]								
IM-9	13409b21009031	38,7	28,2	I	✗	-3,0	5,5	4,0	✓	24,5	34
IA-1	13409b21009081	19,2	12,2	I	✗	-3,0	5,5	4,0	✓	24,5	34
IIM-1	13409b21009141	38,7	28,2	II	✗	-3,0	5,5	4,0	✓	24,5	34
IIA-1	13409b21009142	19,2	12,2	II	✗	-3,0	5,5	4,0	✓	24,5	34

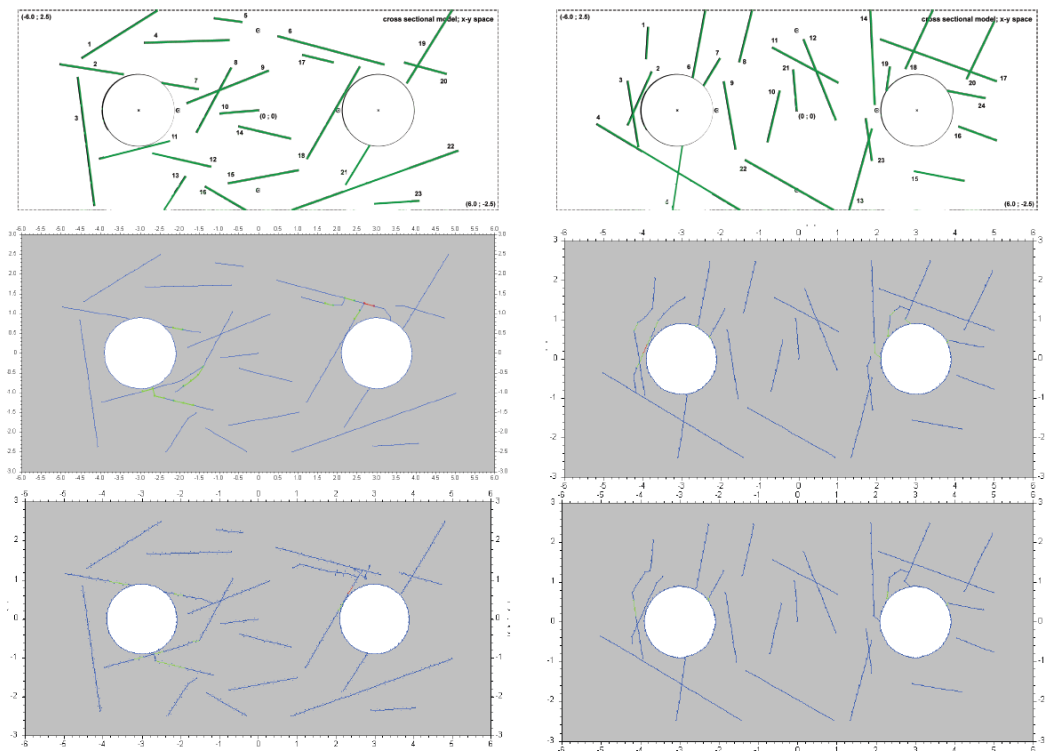


Figure 20. Excavation of the deposition holes generates only little fracture growth in the vicinity of the deposition holes. Left from top to bottom: original DFN I - simulation IM-9, stress by Martin [2007] - simulation IA-1, stress by Ask et al. [2007]; right from top to bottom: original DFN II - simulation IIM-1, stress by Martin [2007] - simulation IIA-1, stress by Ask et al. [2007]. The figures show the fracture network, and the type of fracture. Colour code: blue - currently not loaded, green - shear loaded, red - open.

## 8. Interpretation and Discussion

The simulations incorporate the complete assumed loading history of a repository at Forsmark in the configuration of two neighbouring deposition holes. The loading sequence includes the closure of the repository including the backfill of the tunnel, the swelling pressure of the compacted bentonite in the deposition holes, a full thermal cycle up to 75°C and following cooling, and subsequently the increase of vertical in-situ stress from an ice cover of thickness 3,000m in combination with the increase in fluid pressure in the repository due to a hydraulic connection to the top of the ice sheet. The analysis was performed for two stress scenarios; i.e. the scenarios by Martin [2007] and Ask et al. [2007].

In general it can be concluded that the increase of fluid pressure has the most significant influence on the development of the fracture network and hence has the highest potential to create fluid pathways for radionuclides between deposition holes. Figure 21 interprets the principle results.



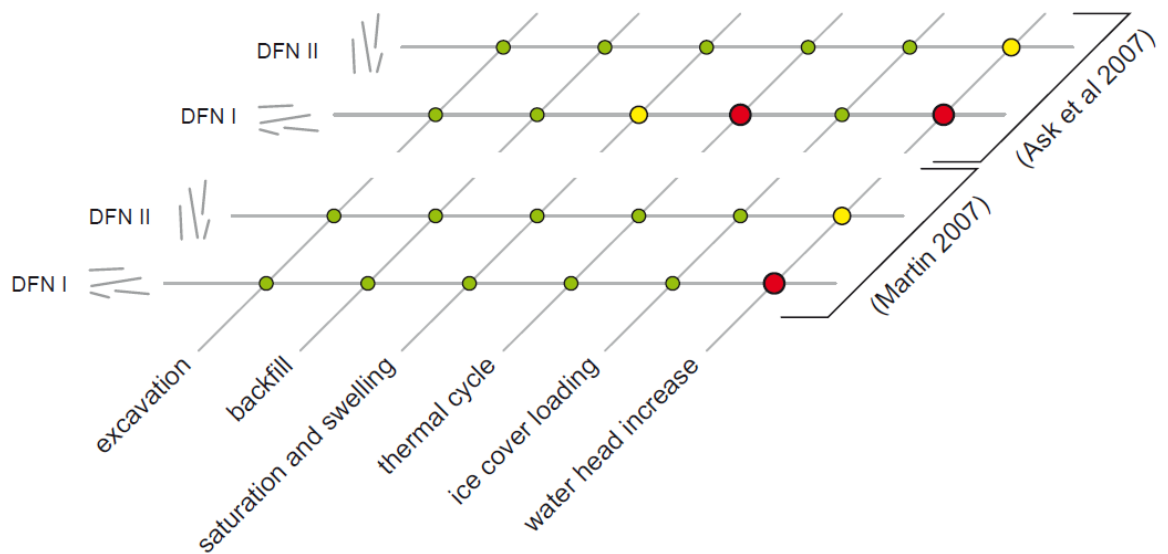


Figure 21. Summary of the principle modelling results. The different phases of the simulation are given along the horizontal direction, while the two assumed DFN are given in the vertical. The bottom lines are for the stress field by Martin [2007], the top lines by Ask et al. [2007]. The diagram shows that DFN I subjected to water head increase during glaciation is the most severe case at both stress field scenarios. The low stress field scenario by Ask et al. [2007] enhances fracturing during the thermal cycle also.

The distinct fracture network was generated from the data provided by SKB. The DFNs were loaded with the provided in-situ stress conditions and showed no significant fracture growth, i.e. the DFNs are stable under the given conditions as should be expected for existing in-situ conditions. The majority of fractures showed no sign of tensile or tractile loading. Hence the DFN model used for this study is assumed valid. A sensitivity analysis of the different parameters describing the fractures of the DFNs is beyond the scope of this study.

The simulations have shown that the excavation of the deposition holes only activates few fractures in the vicinity of the deposition holes (Figure 20). The potential for fracture growth appears low. Spalling is also not predicted; the majority of deformations appear to take place on the fractures.

Also, the change of stress field as may be expected from backfill of the tunnels shows no effect on the DFN. The backfill reduces the tangential stress on the access tunnel and hence reduces the  $S_{yy}$  stress on the deposition holes. Although the difference in  $S_{yy}$  and  $S_{xx}$  is reduced and hence changes the minimum and maximum tangential stress on the deposition holes no significant fracture growth was initiated.

The swelling pressure, irrespective of magnitude, reduces the tangential stresses on the deposition holes and no significant fracture growth was observed. However, rising of the fluid pressure in the repository to the hydrostatic head resulted in fracture growth at the low in-situ stress scenario as reported by Ask et al. [2007].

The excavation of the deposition holes and the backfill of the repository with subsequent increase of hydrostatic pressure and swelling pressure mark the



beginning of the increase of temperature from the waste canisters in the simulation sequence. The stepwise increase and decrease of temperature can be assumed to deliver realistic thermal stresses that may lead to fracture growth. However, the results show that the thermally introduced stresses in the vicinity of the deposition holes cause limited impact on the DFN development in case of the high in-situ stress field as presented by Martin [2007]. In contrast, at low in-situ stresses the thermal load will propagate the fractures leading to a hydraulic connection between the deposition holes, this even without the releveling of the hydrostatic pressure (simulation IA-5).

The increase of  $S_{yy}$  due to an ice load has in all models shown minor influence on the DFN development. It has to be emphasised that the increase of vertical stress due to an ice cover has been considered without allowing for an increase of the horizontal stresses at deposition level. Hence, the influence of the ice sheet loading on  $S_{xx}$  in the models is ignored. It can be assumed that the horizontal stress might be increased with implications for the DFN stability.

An increase of water head in combination with an ice cover from future glaciation has shown the most prominent effect on the DFN development. For the high in-situ stress regime (Martin [2007]) the hydraulically introduced fracture growth is moderate; under the assumption of low in-situ stresses (Ask et al. [2007]) the fracture network is severely extended forming potential hydraulic connections between the deposition holes. Further, it was shown that if the increase in stress field from the ice cover is reducing faster than the fluid pressure there is a potential for hydraulic driven fracture growth also for the case of a high in-situ stress regime.

## 9. Conclusions

The numerical modelling campaign aimed at simulating the development of the distinct fracture network under variable geomechanical boundary conditions in a KBS-3V repository for spent nuclear fuel at Forsmark, Sweden. The models mirror the excavation of the deposition holes, the backfill of the tunnel, the readjustment of the water head, the swelling of the bentonite buffer and a full sequence of heat generation from the canisters. The temperature evolutions was modelled from in-situ conditions up to 75°C rock wall temperature, including a cooling phase down to repository conditions of about 10°C. The simulations were run for two different distinct fracture network models and two stress regimes, i.e. the stress models by Martin [2007] and Ask et al. [2007].

In addition a glaciation scenario was added to the modelling campaign. The glaciation scenario included the increase in vertical load due to an ice cover of 3km thickness and the increase of fluid pressure to 34MPa due to a hydraulic connection with the ice cover.

The simulation results show that during the operation, closure and thermal phase of the repository no major DFN alterations are observed, that may lead to hydraulic connections of the excavations. An increase of water head has

been shown to have the most pronounced impact on the distinct fracture network evolution at the given boundary conditions.

The understanding of the stress field at Forsmark appears to be critical for the extension of the fractures. The low magnitude stress field (Ask et al. [2007]) enhances the propagation of existing fractures in the network. The high magnitude stress field (Martin [2007]) tends to close the fractures and mobilise the frictional resistance of the fracture faces.

## 10. References

- Ask, D., F. Cornet, et al. (2007). Stress measurements with hydraulic methods in boreholes KFM07A, KFM07C, KFM08A, KFM09A and KFM09B. SKB Report, SKB.
- Backers, T. (2010). "Applications of fracture mechanics numerical modelling in rock engineering." First Break 28.
- Backers, T. and O. Stephansson (2008). Modelling of Fracture Initiation, Propagation and Creep of a KBS-3V and KBS-3H Repository in Sparsely Fractured Rock with Application to the Design at Forsmark Candidate Site. GeoFrames Report: 175.
- Benz, T. and R. Schwab (2008). "A quantitative comparison of six rock failure criteria." International Journal of Rock Mechanics and Mining Sciences 45(7): 1176-1186.
- Eriksson, M., J. Petersson, et al. (2009). Underground design Forsmark Layout D2 - Rock mechanics and rock support. SKB Report, SKB: 54.
- Fredriksson, A. and I. Olofsson (2005). Rock mechanics site descriptive model- theoretical approach. Preliminary site description Forsmark area – version 1.2. SKB Report, SKB: 56.
- Glamheden, R., F. Lanaro, et al. (2008). Rock mechanics Forsmark Modelling stage 2.3 - Complementary analysis and verification of the rock mechanics model. SKB Report, SKB: 81.
- Harrington, J. and D. Birchall (2007). Sensitivity of total stress to changes in externally applied water pressure in KBS-3 buffer bentonite. SKB Technical Report, SKB.
- Martin, C. D. (2007). Quantifying in situ stress magnitudes and orientations for Forsmark. Forsmark stage 2.2. SKB Report, SKB: 95.
- Martin, D. (2005). Preliminary assessment of potential underground stability (wedge and spalling) at Forsmark, Simpevarp and Laxemar sites. SKB Report, SKB.
- Moeck, I., T. Backers, et al. (2007). Assessment of Mechanical Wellbore Stability by Numerical Analysis of Fracture Growth. EAGE 69th Conference & Exhibition. London, EAGE.
- Quesada, D., D. Picard, et al. (2008). "The role of the interbed thickness on the step-over fracture under overburden pressure." International Journal of Rock Mechanics and Mining Sciences In Press, Corrected Proof.
- Shen, B. and O. Stephansson (1993). "Modification of the G-criterion of crack propagation in compression." Int. J. Eng. Fract. Mech. **47**: 177-189.
- SKB (2008). Site description of Forsmark at completion of the site investigation phase, SDM-Site Forsmark. SKB Technical Report, SKB: 545.
- SKB (2009a). Site engineering report Forsmark - Guidelines for underground design step D2. SKB Report, SKB: 142.
- SKB (2009b). Underground design Forsmark. SKB Report, SKB: 128.

# Appendix

## 11. Simulations

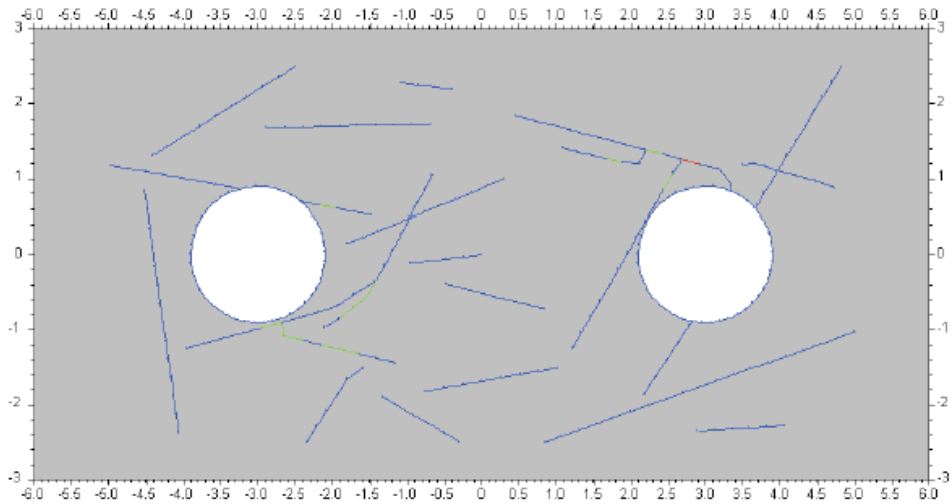
### 11.1. Simulation IM-6

The model in this simulation includes DFN I and is subject to the stress field according to Martin [2007]. It features only a limited loading history including low swelling pressure  $P_s$ , but no heating sequence. As the fluid pressure has shown pronounced effect on the fracture growth, the fluid pressure under ice cover load is stepwise increased.

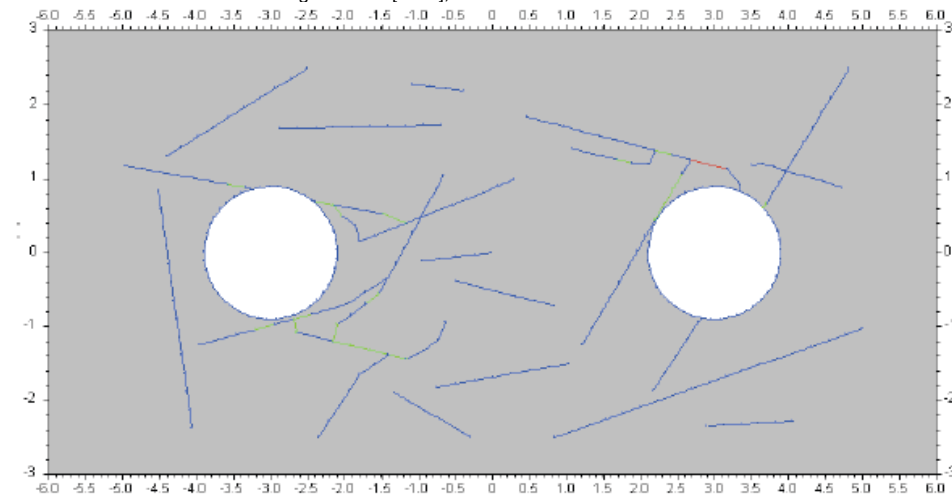
simulation	stress field		DFN	fract.ini	closure			heating	ice cover		
	Sxx	Syy			backfill	Ps	Pp		load	Pp	
13409b21008311	38,7	28,2	<sup>1)</sup>	I	X	-3,0	5,5	4,0	X	24,5	34, +5, 60

Only few fractures propagate short distances due to the stress redistribution of the excavations. Neither the backfill, swelling pressure nor heating sequence show significant fracture propagation. While the increase in load from the ice cover introduces only minor fracturing, the increase in fluid pressure introduces some fracturing that may lead to potential connection of the deposition holes. The hydraulic connection in the example is achieved above  $P_p > 44\text{MPa}$ . It has to be emphasised that this is valid for the given DFN. The results so far have shown the great potential of this loading to introduce full hydraulic connection.

Figure a. Fracture network evolution (13409b21008311). Stress field according to Martin [2007], DFN I, low swelling pressure, no heating sequence, ice cover and extended ice load fluid pressure. The figures show the fracture network and the type of fracture. Colour code: blue - currently not loaded, green - shear loaded, red - open. Thickening of lines show application of a fluid pressure.

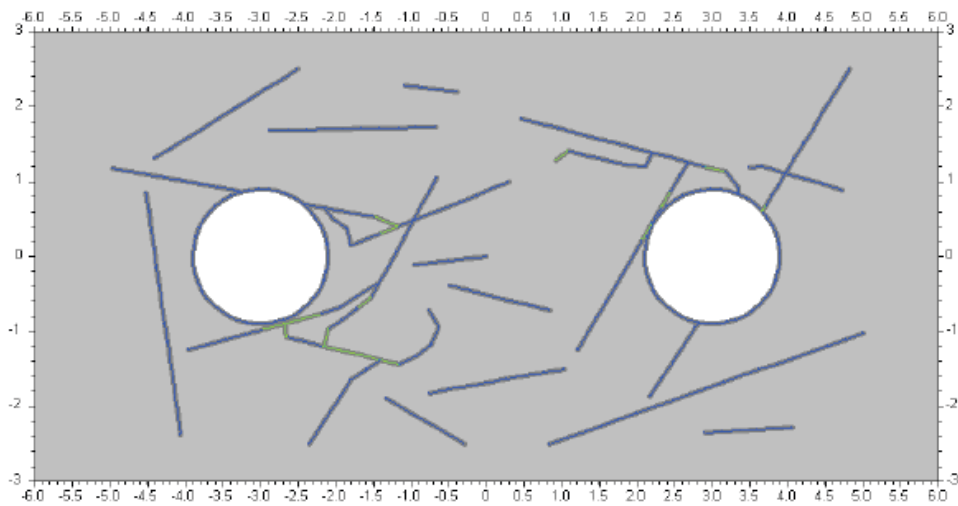


Fracture network after introduction of the excavations. Only few fractures propagated due to the redistribution of the stresses. Stress field according to Martin [2007]; DFN I.

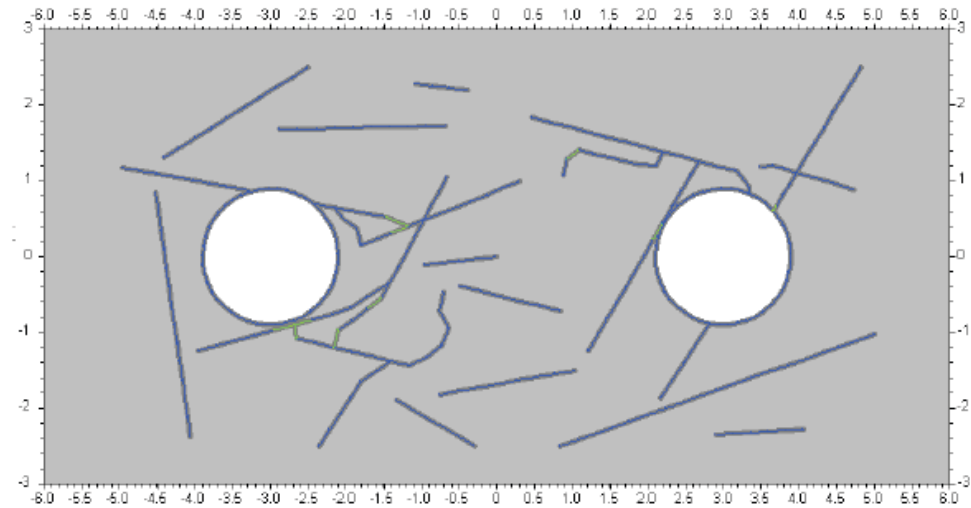


After the closure of the repository the applied stress is increased due to the backfill of the tunnel. This has no significant impact on the DFN.

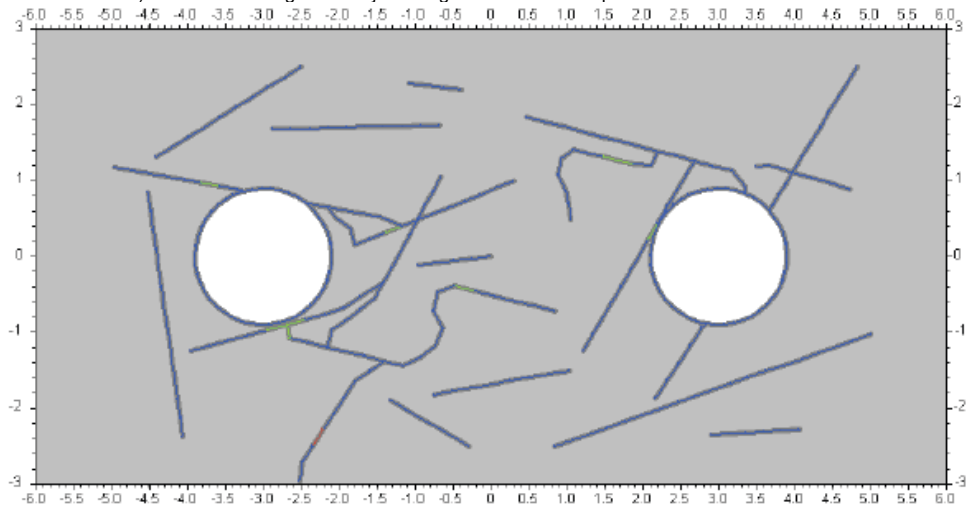
Figure a. Fracture network evolution (13409b21008311). Stress field according to Martin [2007], DFN I, low swelling pressure, no heating sequence, ice cover and extended ice load fluid pressure. The figures show the fracture network and the type of fracture. Colour code: blue - currently not loaded, green - shear loaded, red - open. Thickening of lines show application of a fluid pressure.



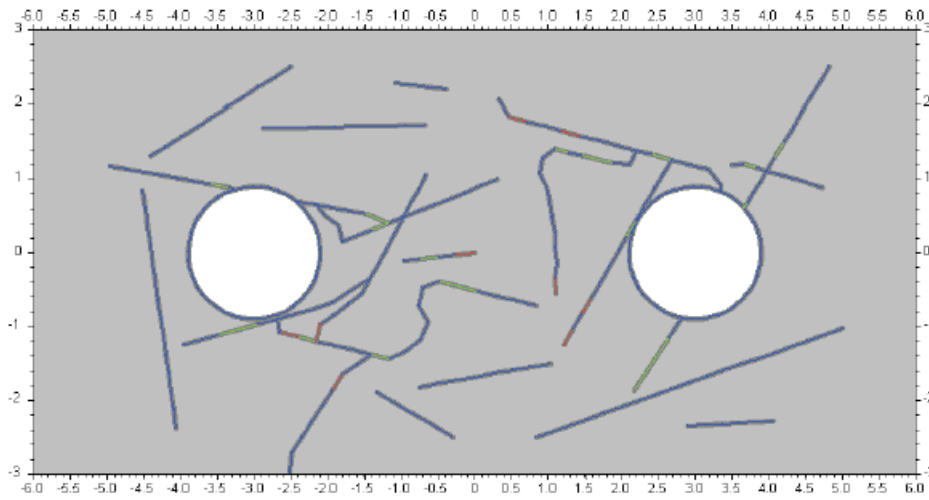
The swelling pressure (5.5MPa) and the recovery of a water head (4MPa) show no impact on the DFN.



As for simulation of an ice cover of approx. 3km additional load of 24.5MPa ( $S_{yy}$  due to redistribution around backfilled tunnel) is added resulting in no major changes of the DFN or aperture.

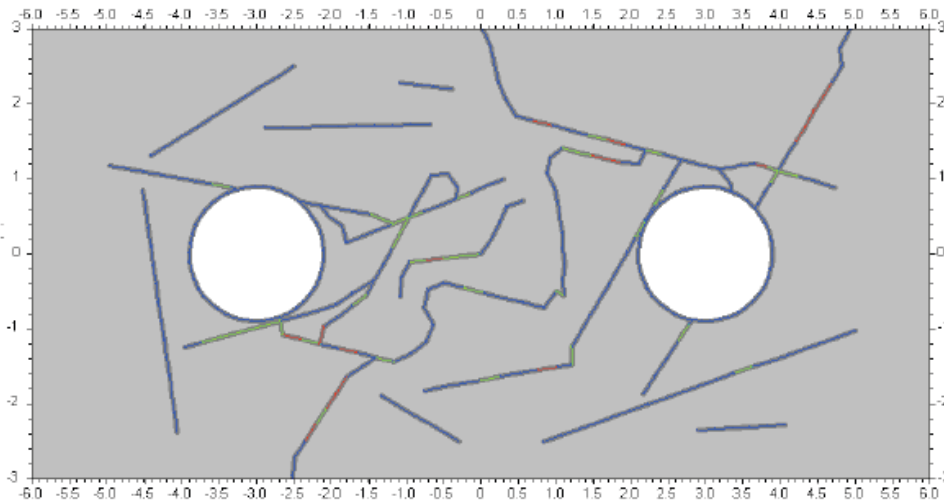


The water pressure acting on the deposition holes and the fractures is increased from  $P_p = 34\text{MPa}$  in steps of 5MPa.  $P_p = 39\text{MPa}$

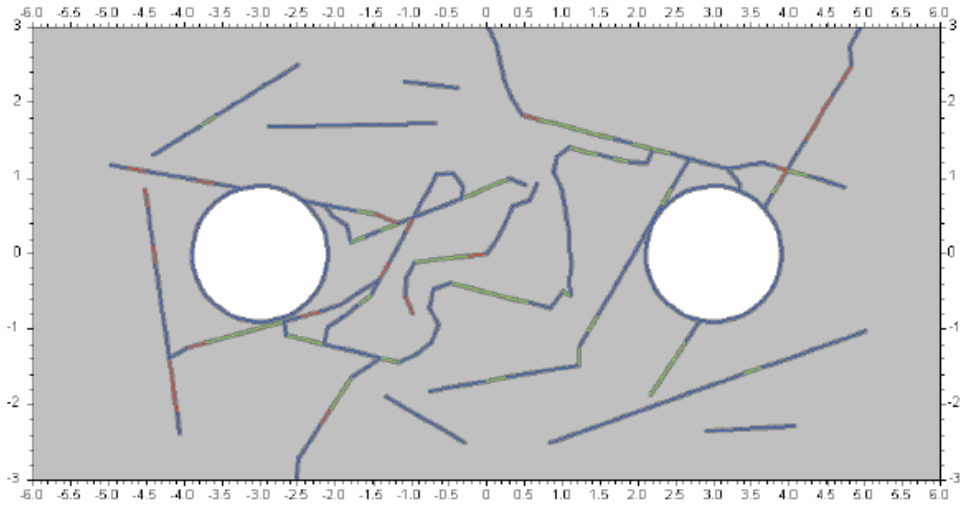


$P_p = 44\text{MPa}$ . Fracture growth.

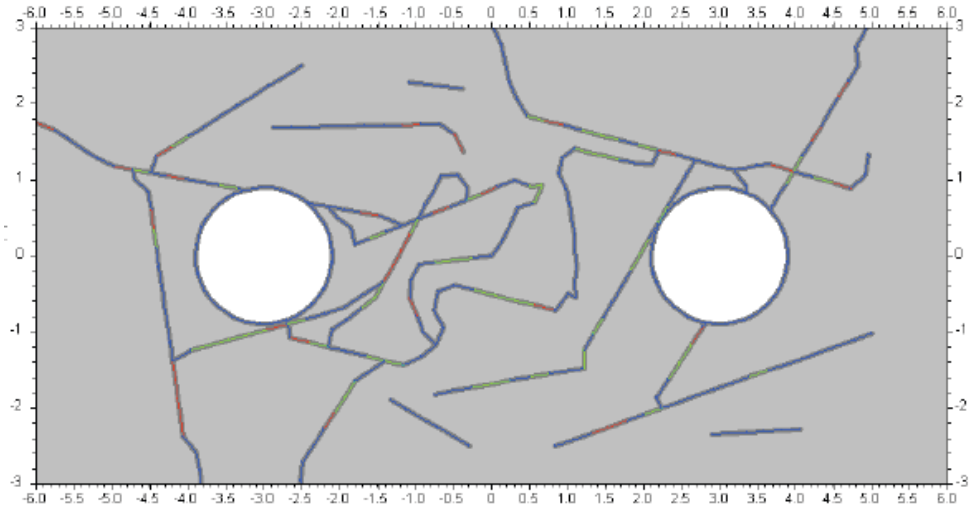
Figure a. Fracture network evolution (13409b21008311). Stress field according to Martin [2007], DFN I, low swelling pressure, no heating sequence, ice cover and extended ice load fluid pressure. The figures show the fracture network and the type of fracture. Colour code: blue - currently not loaded, green - shear loaded, red - open. Thickening of lines show application of a fluid pressure.



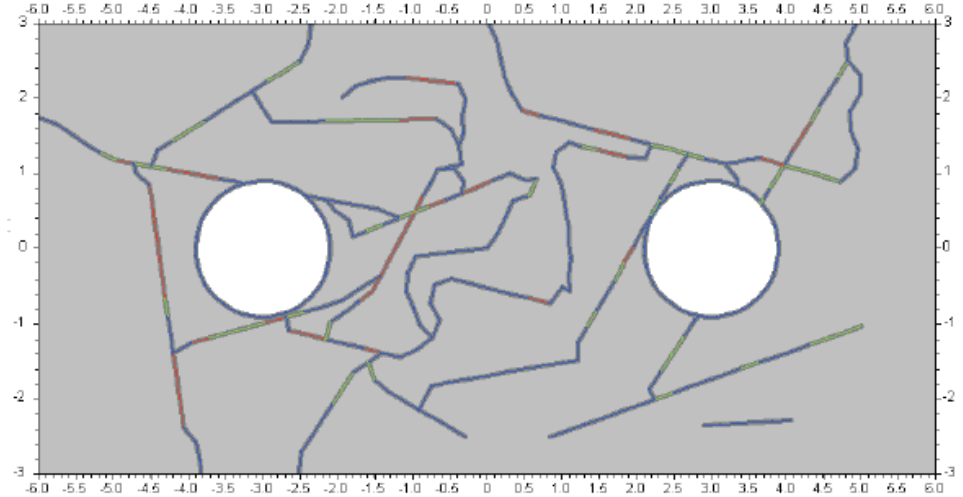
$P_p = 49\text{MPa}$ . Fracture growth.



$P_p = 54\text{MPa}$ . Fracture growth.



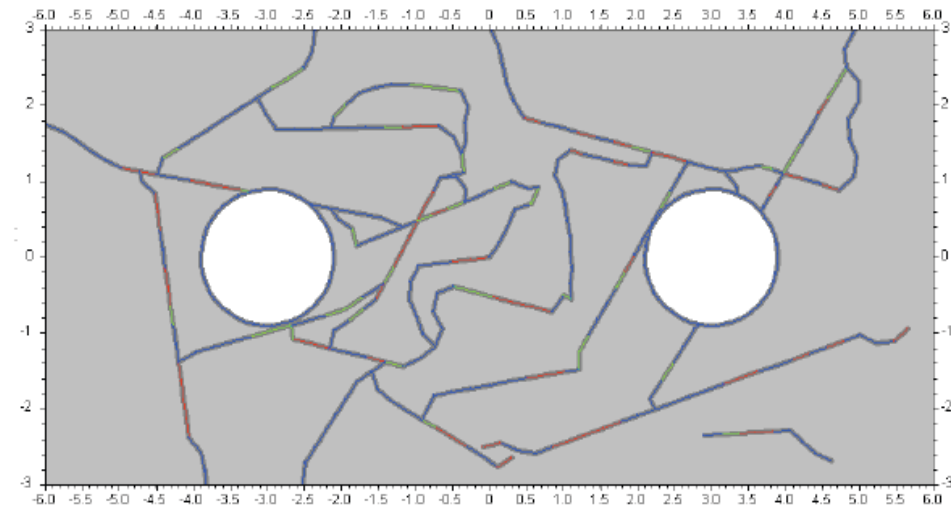
$P_p = 59\text{MPa}$ . Fracture growth.



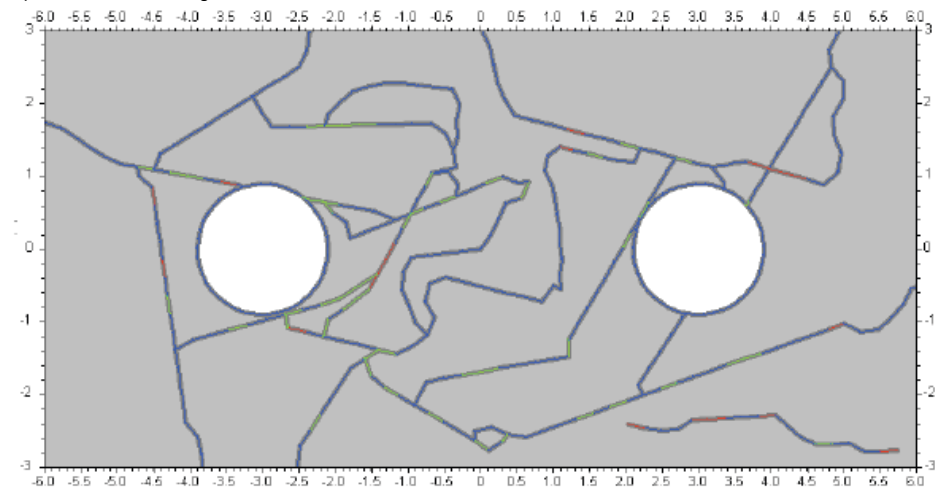
$P_p = 64\text{MPa}$ . Fracture growth.



Figure a. Fracture network evolution (13409b21008311). Stress field according to Martin [2007], DFN I, low swelling pressure, no heating sequence, ice cover and extended ice load fluid pressure. The figures show the fracture network and the type of fracture. Colour code: blue - currently not loaded, green - shear loaded, red - open. Thickening of lines show application of a fluid pressure.



Pp = 69MPa. Fracture growth.



Pp = 74MPa. Fracture growth.

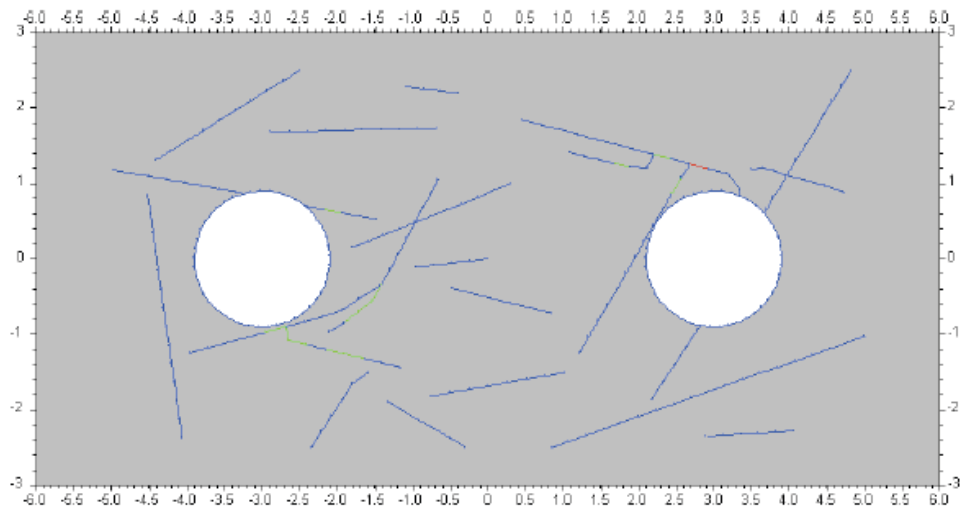
## 11.2. Simulation IM-7

The model in this simulation includes DFN I and is subject to the stress field according to Martin [2007]. It features only a limited loading history including high swelling pressure  $P_s$ , but no heating sequence. As the fluid pressure has shown pronounced effect on the fracture growth, the fluid pressure under ice cover load is stepwise increase.

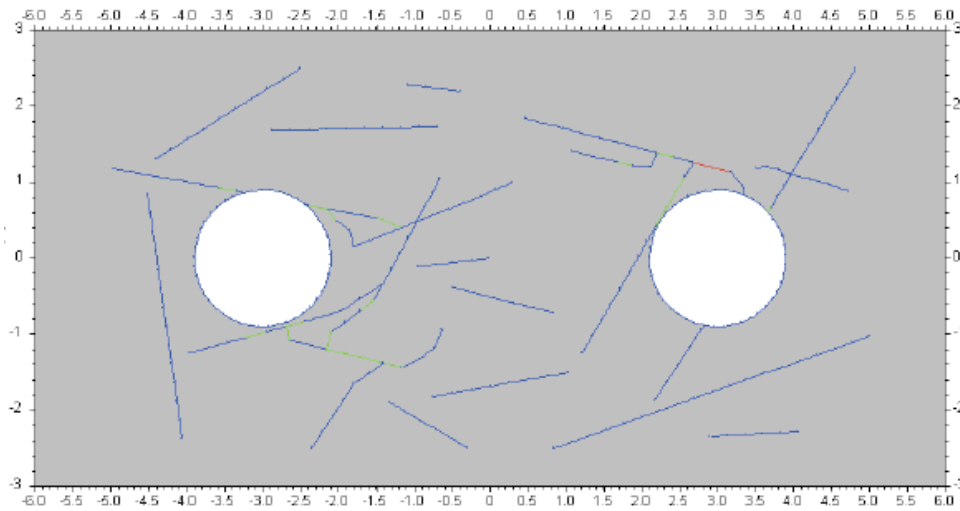
simulation	stress field		DFN	fract.ini	closure			heating	ice cover	
	Sxx	Syy			backfill	$P_s$	$P_p$		load	$P_p$
13409b21009011	38,7	28,2 <sup>1)</sup>	I	x	-3,0	7,2	4,0	x	24,5	34, +5, 60

Only few fractures propagate short distances due to the stress redistribution of the excavations. Neither the backfill, swelling pressure nor heating sequence show significant fracture propagation. While the increase in load from the ice cover introduces only minor fracturing, the increase in fluid pressure introduces some fracturing that may lead to potential connection of the deposition holes. The hydraulic connection in the example is achieved above  $P_p > 44\text{MPa}$  as it was also at the low swelling pressure of  $5.5\text{MPa}$ . It has to be emphasised that this is valid for the given DFN. The results so far have shown the great potential of this loading to introduce full hydraulic connection.

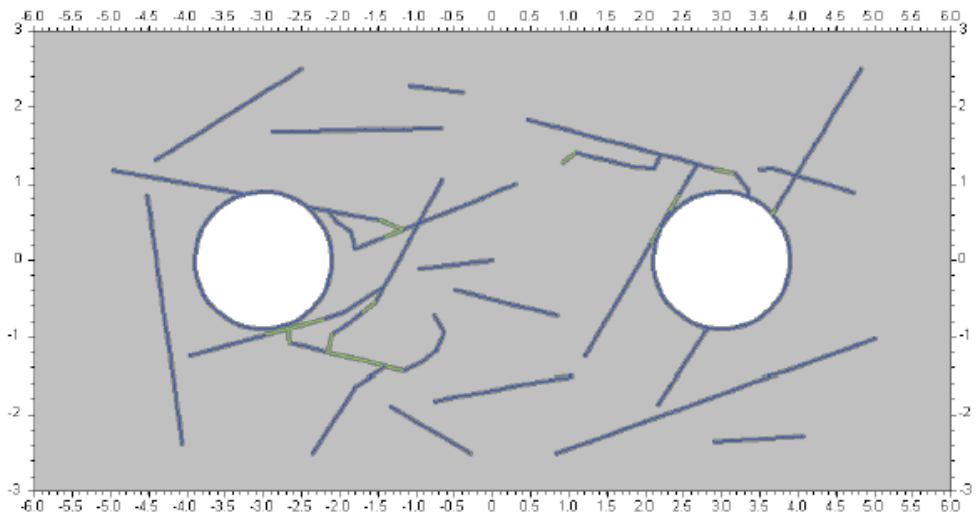
Figure b. Fracture network evolution (13409b21009011). Stress field according to Martin [2007], DFN I, high swelling pressure, no heating sequence, ice cover and extended ice load fluid pressure. The figures show the fracture network and the type of fracture. Colour code: blue - currently not loaded, green - shear loaded, red - open. Thickening of lines show application of a fluid pressure.



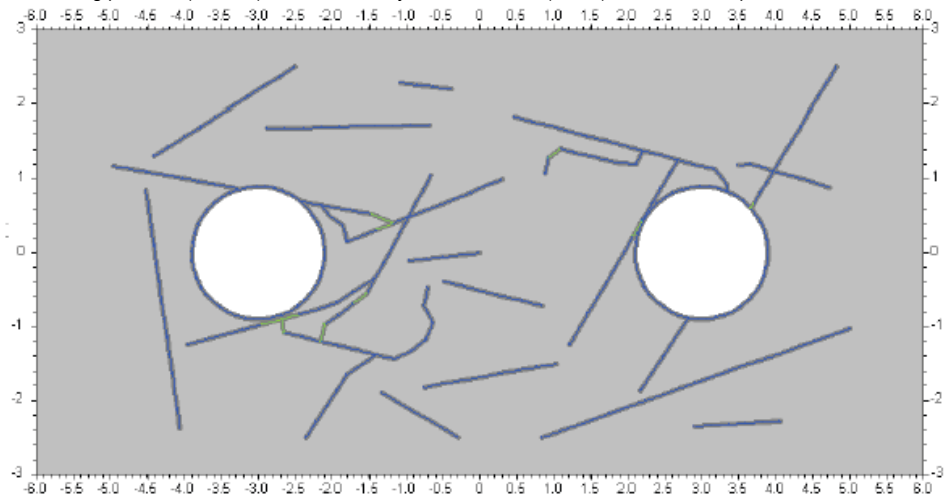
Fracture network after introduction of the excavations. Only few fractures propagated due to the redistribution of the stresses. Stress field according to Martin [2007]; DFN I.



After the closure of the repository the applied stress is increased due to the backfill of the tunnel. This has no significant impact on the DFN.

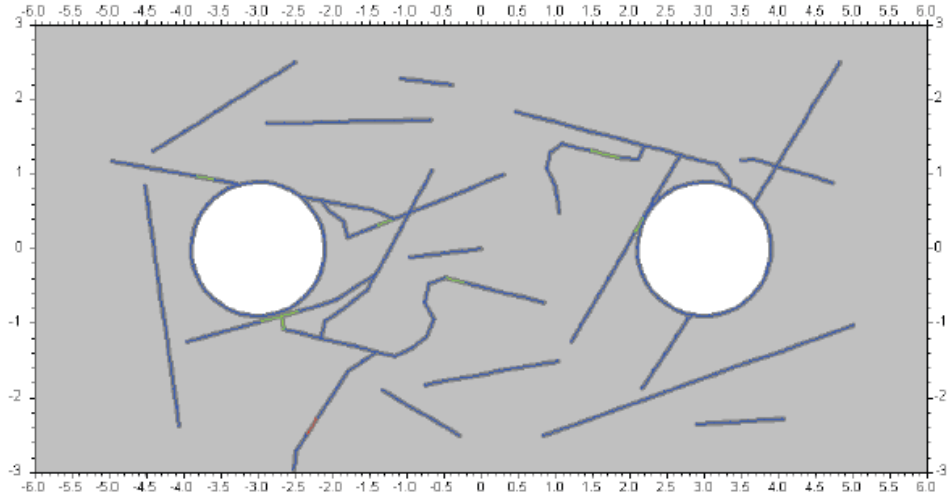


The swelling pressure (7.2MPa) and the recovery of a water head (4MPa) show limited impact on the DFN.

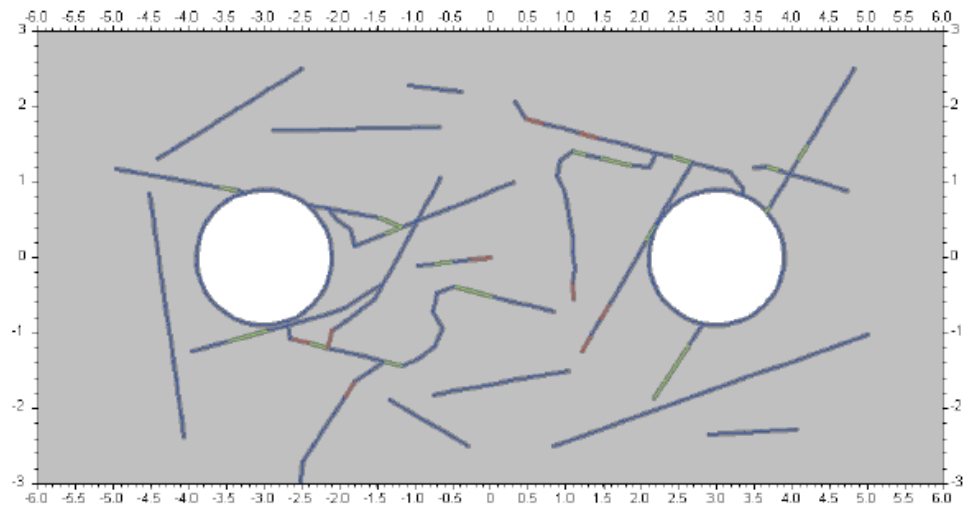


As for simulation of an ice cover of approx. 3km additional load of 24.5MPa ( $S_{yy}$  due to redistribution around backfilled tunnel) is added resulting in no major changes of the DFN or aperture.

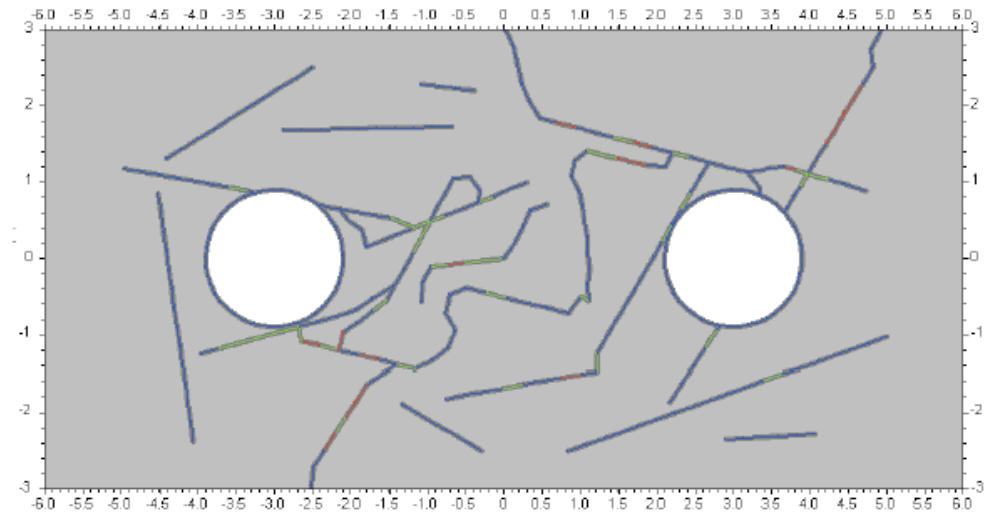
Figure b. Fracture network evolution (13409b21009011). Stress field according to Martin [2007], DFN I, high swelling pressure, no heating sequence, ice cover and extended ice load fluid pressure. The figures show the fracture network and the type of fracture. Colour code: blue - currently not loaded, green - shear loaded, red - open. Thickening of lines show application of a fluid pressure.



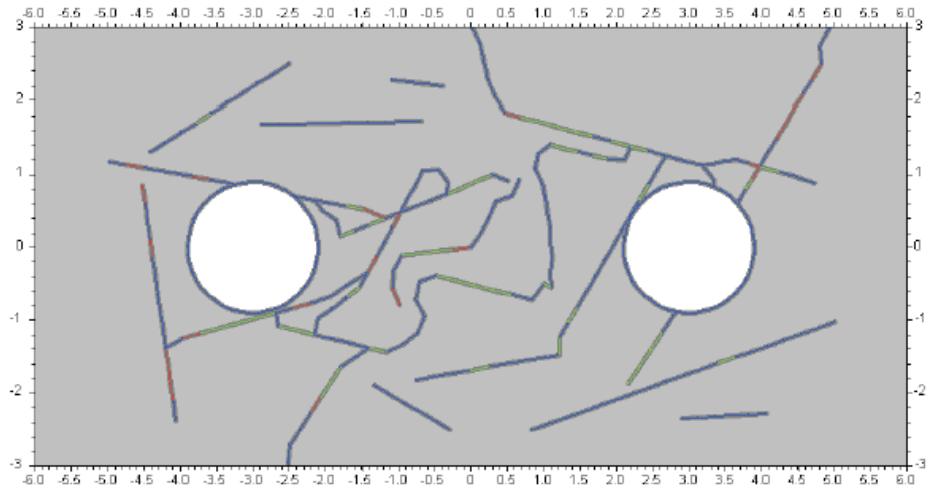
The water pressure acting on the deposition holes and the fractures is increased from  $P_p = 34\text{MPa}$  in steps of  $5\text{MPa}$ .  $P_p = 39\text{MPa}$



$P_p = 44\text{MPa}$ . Fracture growth.

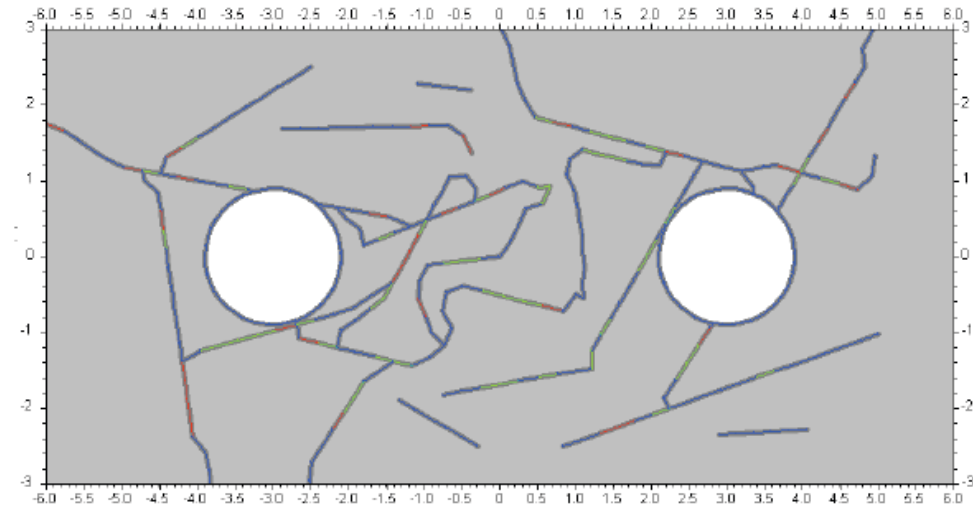


$P_p = 49\text{MPa}$ . Fracture growth.

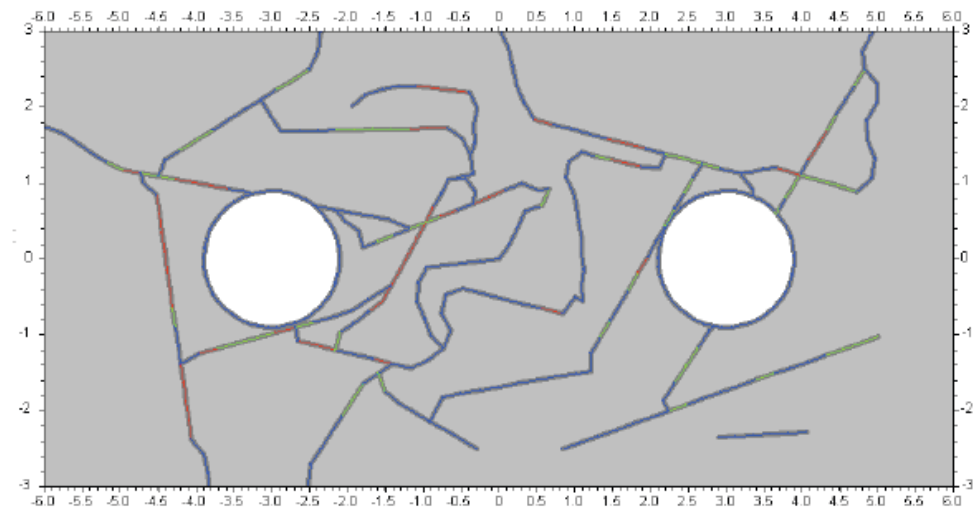


$P_p = 54\text{MPa}$ . Fracture growth.

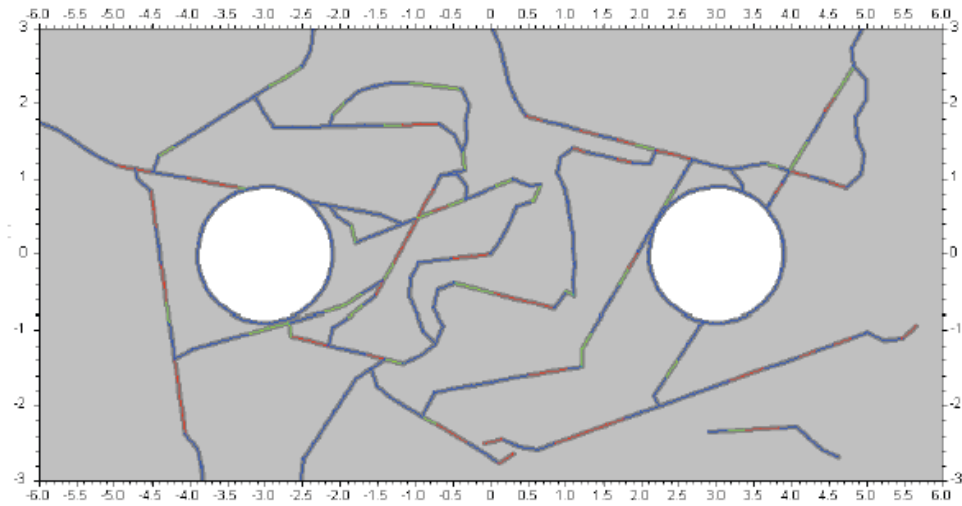
Figure b. Fracture network evolution (13409b21009011). Stress field according to Martin [2007], DFN I, high swelling pressure, no heating sequence, ice cover and extended ice load fluid pressure. The figures show the fracture network and the type of fracture. Colour code: blue - currently not loaded, green - shear loaded, red - open. Thickening of lines show application of a fluid pressure.



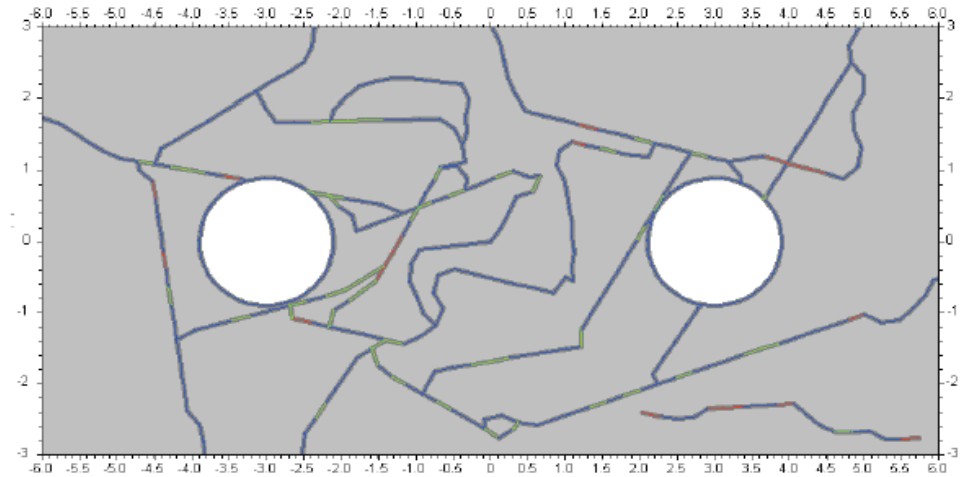
$P_p = 59\text{MPa}$ . Fracture growth.



$P_p = 64\text{MPa}$ . Fracture growth.



Pp = 69MPa. Fracture growth.



Pp = 74MPa. Fracture growth.

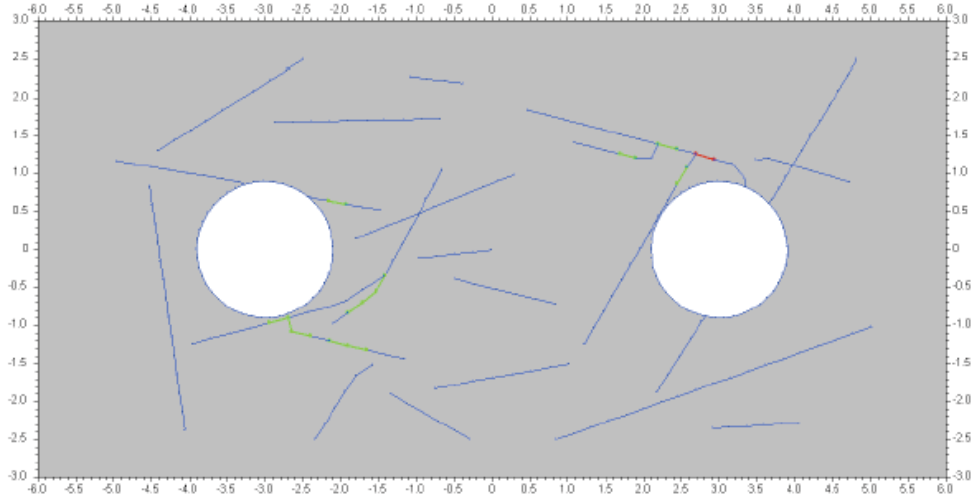
### 11.3. Simulation IM-9

The model in this simulation includes DFN I and is subject to the stress field according to Martin [2007]. It features the full loading history including low swelling pressure Ps, the heating sequence up to 75°C and the ice cover.

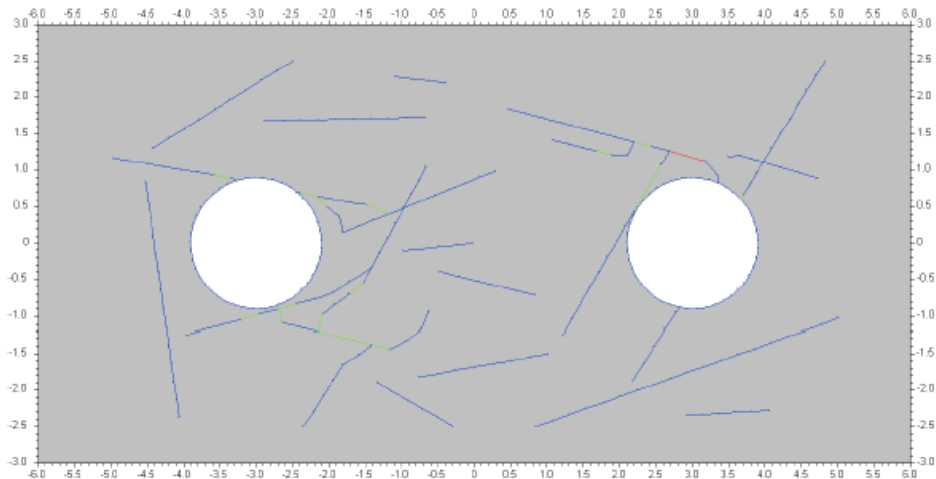
simulation	stress field		DFN	fract.ini	closure			heating	ice cover	
	Sxx	Syy			backfill	Ps	Pp		load	Pp
13409b21009031	38,7	28,2 <sup>1)</sup>	I	x	-3,0	5,5	4,0	✓	24,5	34

Only few fractures propagate short distances due to the stress redistribution of the excavations. Neither the backfill, swelling pressure nor heating sequence show significant fracture propagation. The increase of load due to the ice cover in combination with the increase in fluid pressure introduces some fracturing that may lead to potential connection of the deposition holes.

Figure c. Fracture network evolution (13409b21009031). Stress field according to Martin [2007], DFN I, low swelling pressure, heating sequence and ice cover. The figures show the fracture network and the type of fracture. Colour code: blue - currently not loaded, green - shear loaded, red - open. Thickening of lines show application of a fluid pressure.



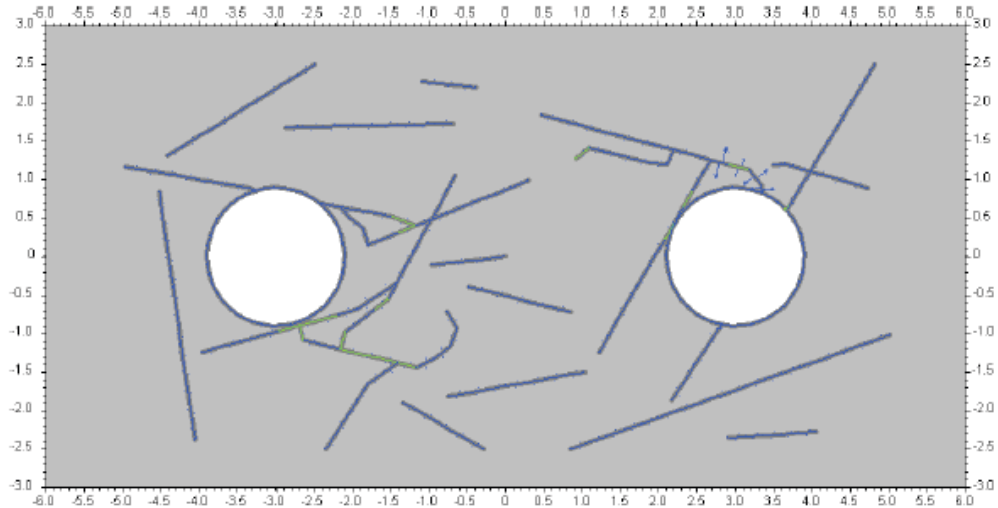
Fracture network after introduction of the excavations. Only few fractures propagated due to the redistribution of the stresses. Stress field according to Martin [2007]; DFN I.



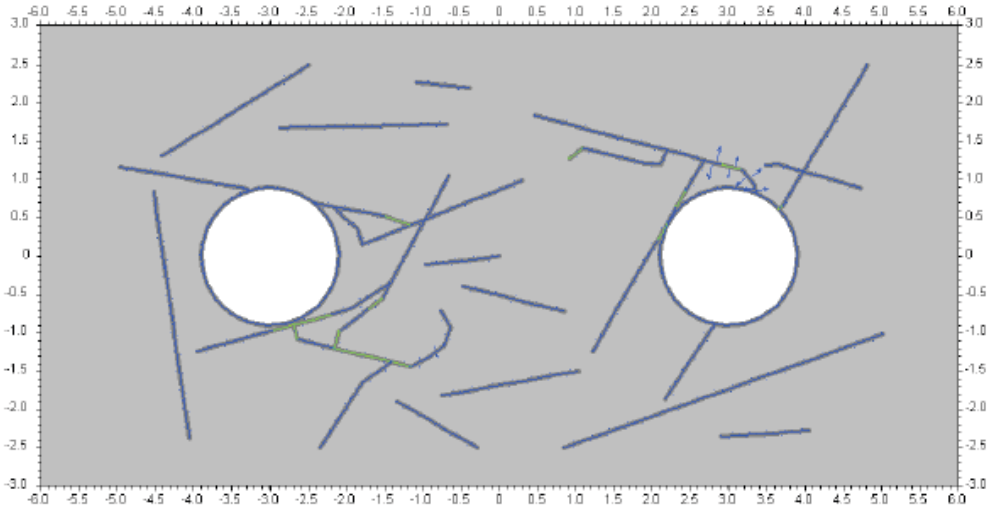
After the closure of the repository the applied stress is increased due to the backfill of the tunnel. This has no significant impact on the DFN.



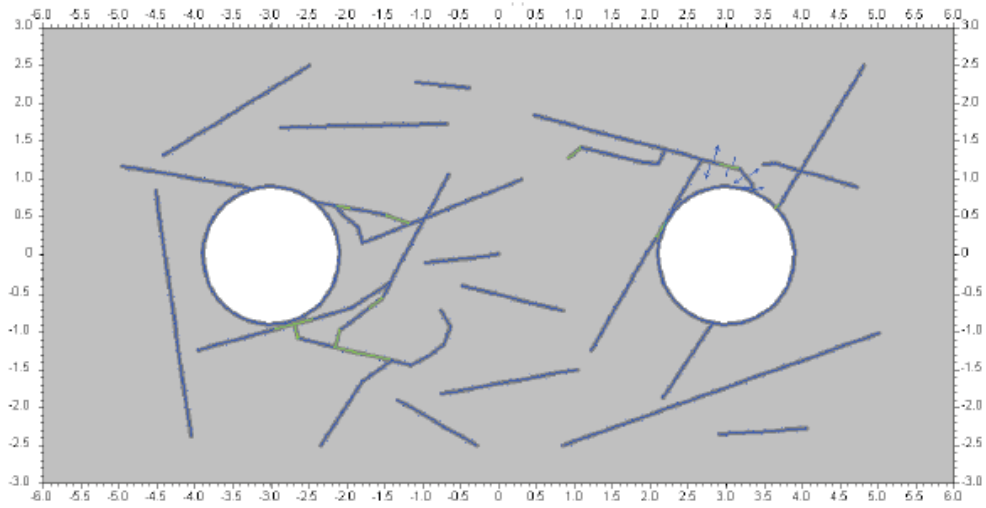
Figure c. Fracture network evolution (13409b21009031). Stress field according to Martin [2007], DFN I, low swelling pressure, heating sequence and ice cover. The figures show the fracture network and the type of fracture. Colour code: blue - currently not loaded, green - shear loaded, red - open. Thickening of lines show application of a fluid pressure.



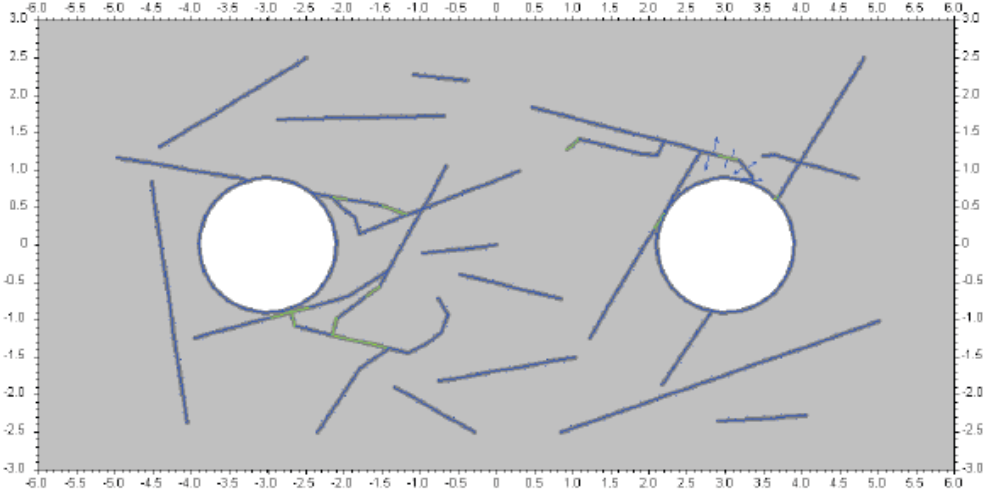
The swelling pressure (5.5MPa) and the recovery of a water head (4MPa) show no impact on the DFN.



The temperature at the face of the deposition holes is increased from the initial 14.5°C to 25°C. This shows no impact on the DFN.

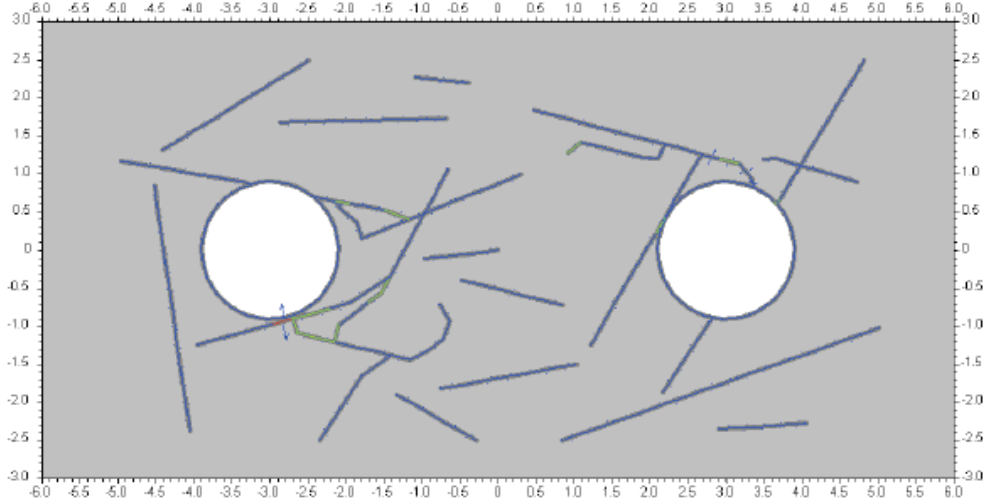


Temperature at the deposition hole face is increased to 50°C. No impact.

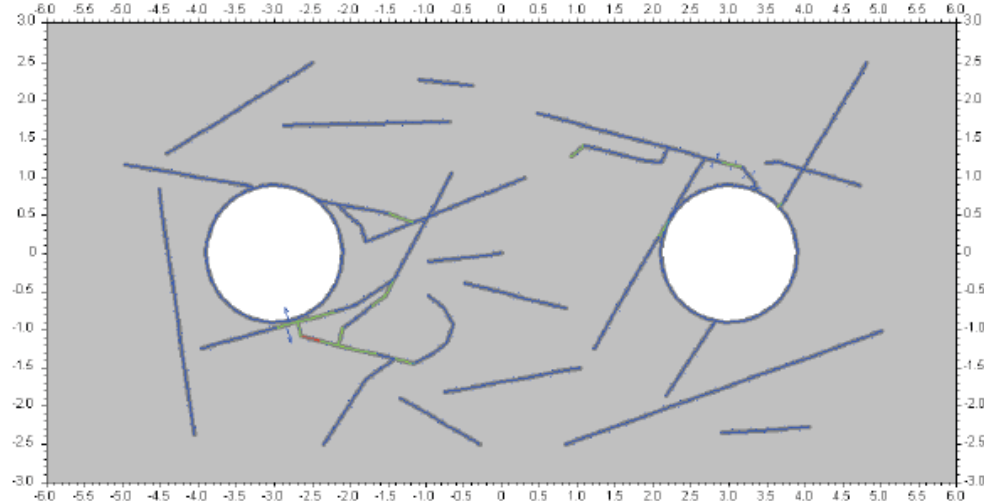


Temperature at the deposition hole face is increased to 75°C. No impact.

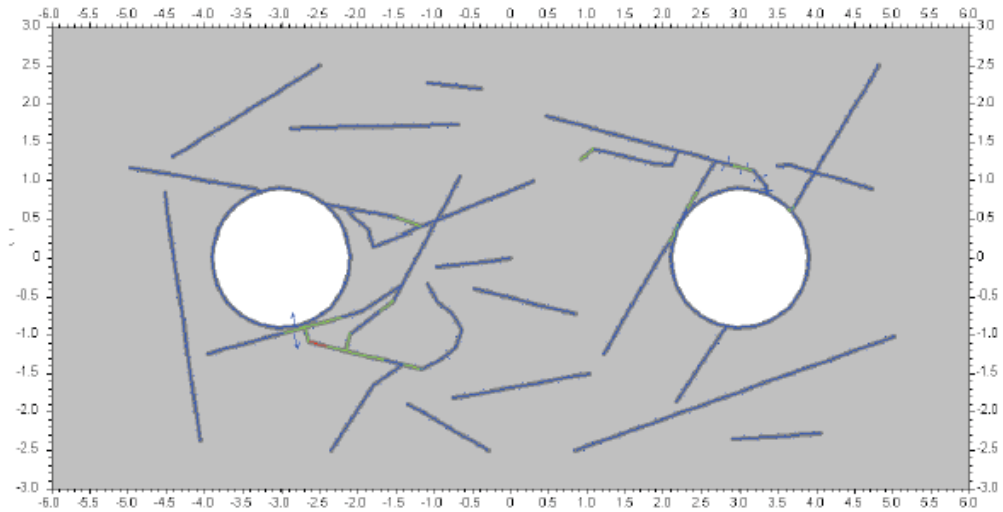
Figure c. Fracture network evolution (13409b21009031). Stress field according to Martin [2007], DFN I, low swelling pressure, heating sequence and ice cover. The figures show the fracture network and the type of fracture. Colour code: blue - currently not loaded, green - shear loaded, red - open. Thickening of lines show application of a fluid pressure.



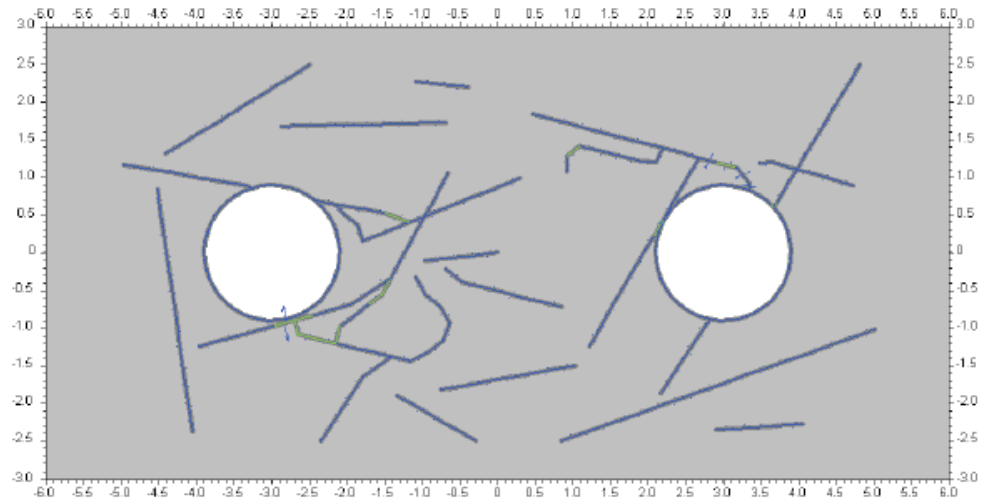
Temperature at the deposition hole face is decreased to 50°C. The aperture of selected fractures reduces. No impact on DFN.



Temperature at the deposition hole face is decreased to 25°C. No impact.

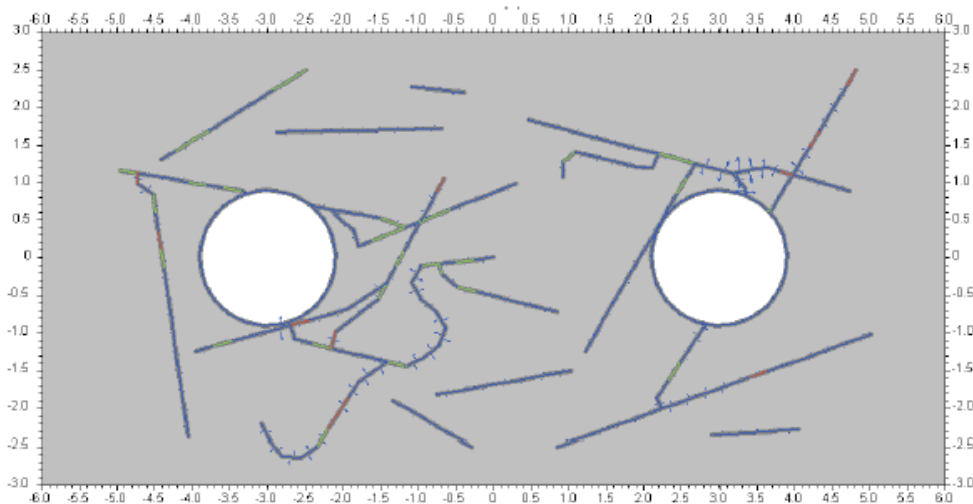


Temperature at the deposition hole face is decreased to 10°C. The aperture of selected fractures reduces. No impact on DFN.



As for simulation of an ice cover of approx. 3km additional load of 24.5MPa ( $S_{yy}$  due to redistribution around backfilled tunnel) is added resulting in no major changes of the DFN or aperture.

Figure c. Fracture network evolution (13409b21009031). Stress field according to Martin [2007], DFN I, low swelling pressure, heating sequence and ice cover. The figures show the fracture network and the type of fracture. Colour code: blue - currently not loaded, green - shear loaded, red - open. Thickening of lines show application of a fluid pressure.



The water head is increased to 34MPa due to an assumed ice cover fully hydraulically connected to the repository. The fractures show higher apertures and additional fracturing is introduced.

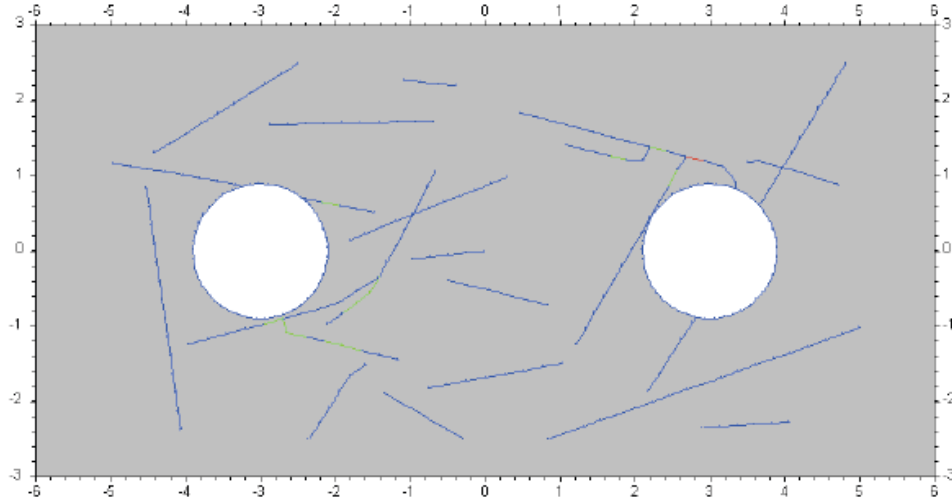
#### 11.4. Simulation IM-10

The model in this simulation includes DFN I and is subject to the stress field according to Martin [2007]. It features the full loading history including high swelling pressure  $P_s$ , the heating sequence up to 75°C and the ice cover.

simulation	stress field		DFN	fract.ini	closure			heating	ice cover	
	Sxx	Syy			backfill	Ps	Pp		load	Pp
13409b21009032	38,7	28,2 <sup>1)</sup>	I	X	-3,0	7,2	4,0	✓	24,5	34

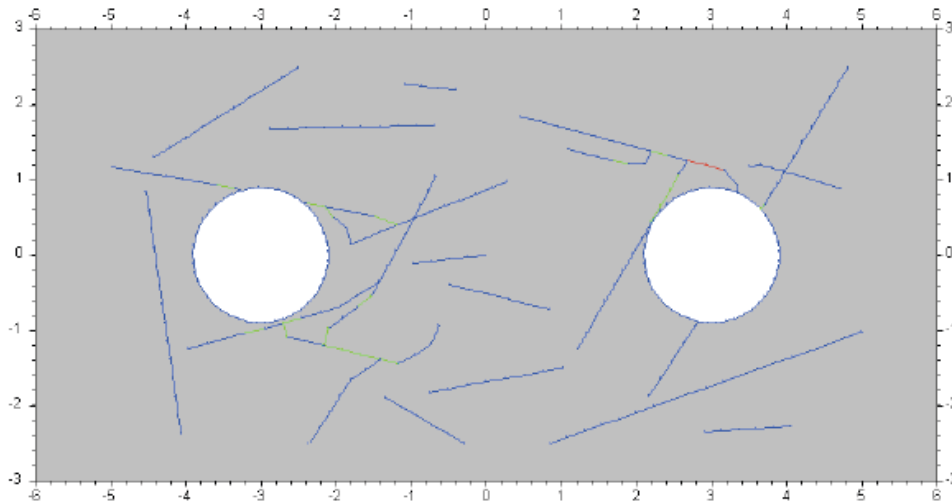
Only few fractures propagate short distances due to the stress redistribution of the excavations. The swelling pressure introduces limited additional stable fracturing. Neither the backfill nor heating sequence results in significant fracture propagation. While the increase in load from the ice cover introduces only minor fracturing, the increase in fluid pressure introduces some fracturing that may lead to potential connection of the deposition holes.

Figure d. Fracture network evolution (13409b21009032). Stress field according to Martin [2007], DFN I, high swelling pressure, heating sequence and ice cover. The figures show the fracture network and the type of fracture. Colour code: blue - currently not loaded, green - shear loaded, red - open. Thickening of lines show application of a fluid pressure

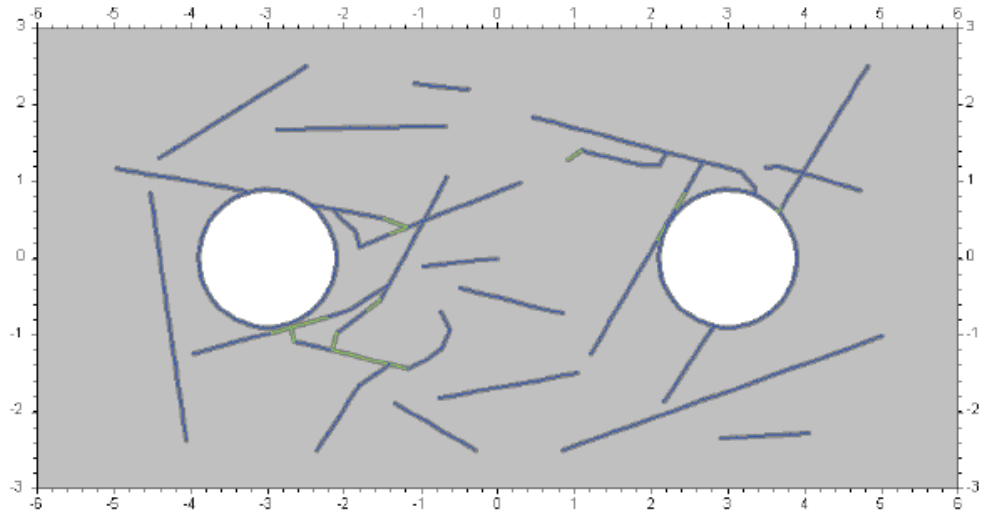


Fracture network after introduction of the excavations. Only few fractures propagated due to the redistribution of the stresses. Stress field according to Martin [2007]; DFN I.

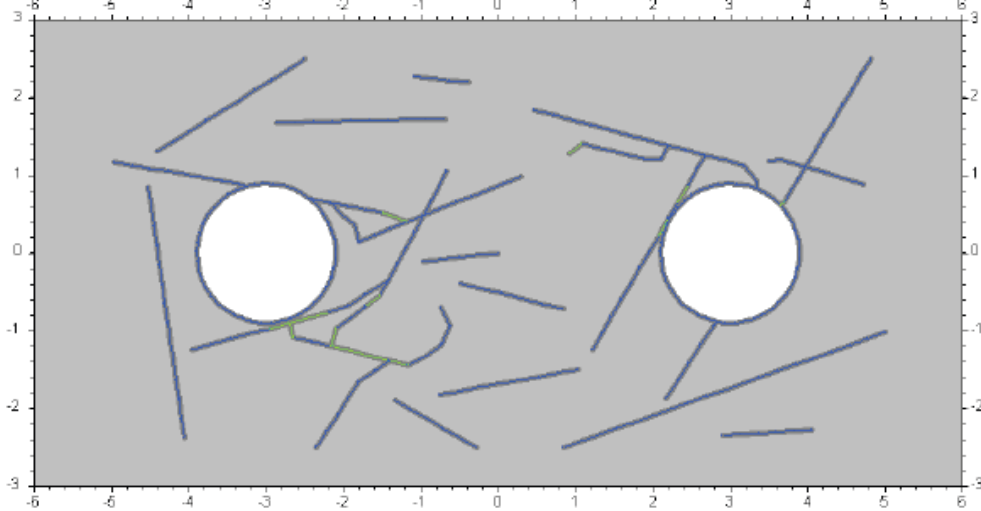
Figure d. Fracture network evolution (13409b21009032). Stress field according to Martin [2007], DFN I, high swelling pressure, heating sequence and ice cover. The figures show the fracture network and the type of fracture. Colour code: blue - currently not loaded, green - shear loaded, red - open. Thickening of lines show application of a fluid pressure.



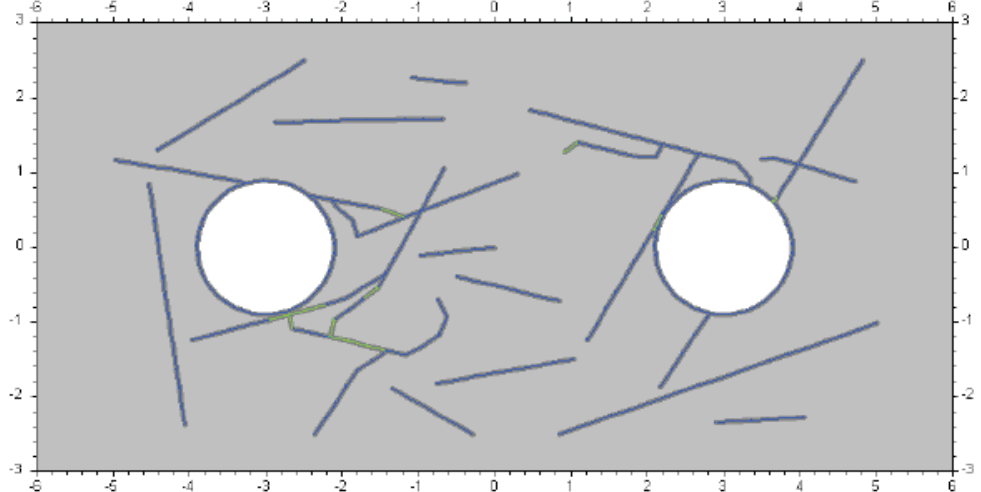
After the closure of the repository the applied stress is increased due to the backfill of the tunnel. This has no significant impact on the DFN.



The swelling pressure (7.2MPa) and the recovery of a water head (4MPa) show no impact on the DFN.

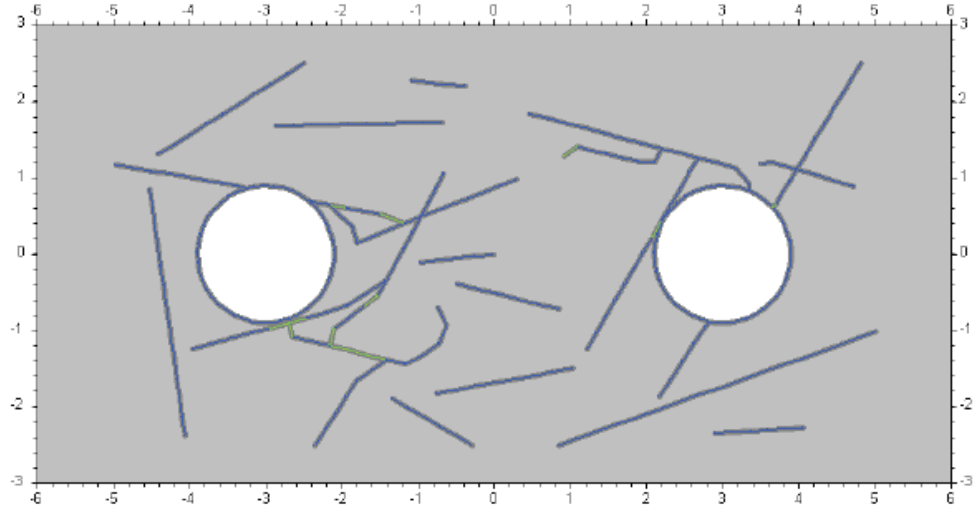


The temperature at the face of the deposition holes is increased from the initial 14.5°C to 25°C. This shows no impact on the DFN.

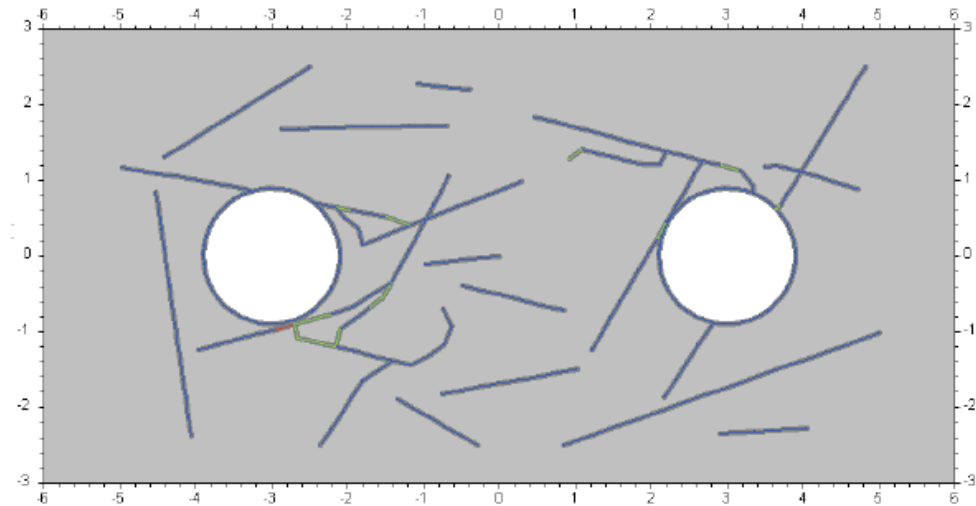


Temperature at the deposition hole face is increased to 50°C. No impact.

Figure d. Fracture network evolution (13409b21009032). Stress field according to Martin [2007], DFN I, high swelling pressure, heating sequence and ice cover. The figures show the fracture network and the type of fracture. Colour code: blue - currently not loaded, green - shear loaded, red - open. Thickening of lines show application of a fluid pressure.

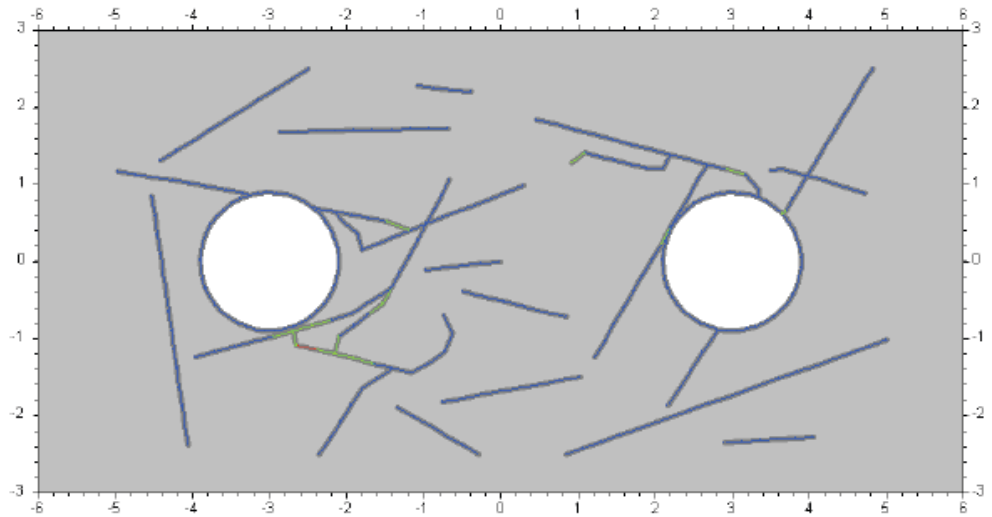


Temperature at the deposition hole face is increased to 75°C. No impact.

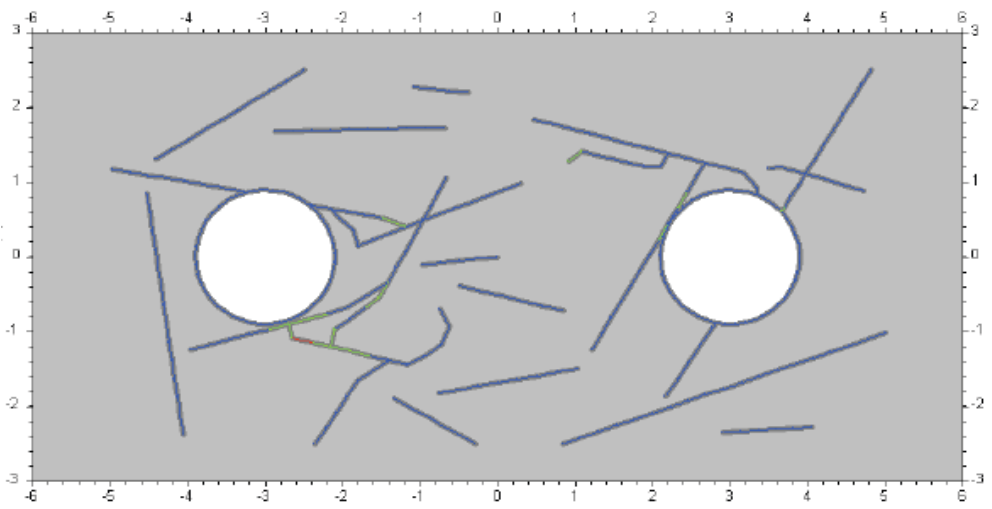


Temperature at the deposition hole face is decreased to 50°C. The aperture of selected fractures reduces. No impact on DFN.



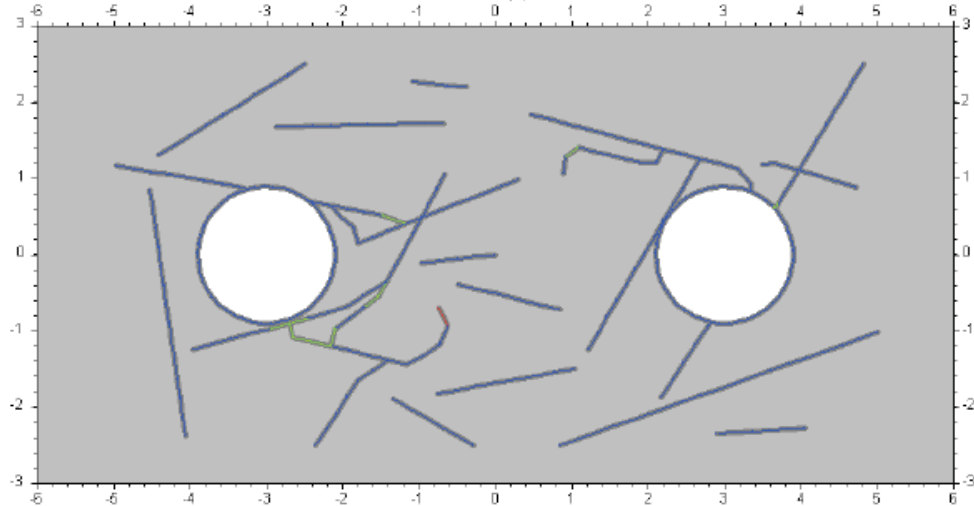


Temperature at the deposition hole face is decreased to 25°C. No impact.

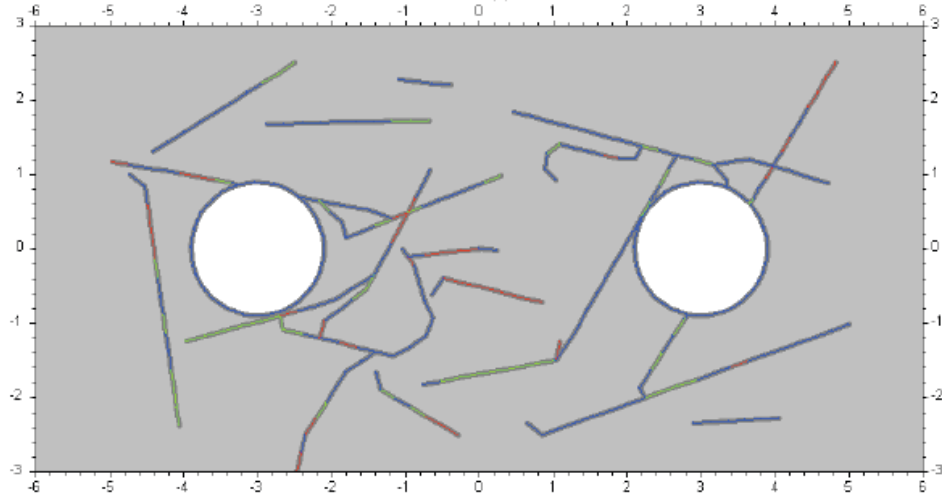


Temperature at the deposition hole face is decreased to 10°C. The aperture of selected fractures reduces. No impact on DFN.

Figure d. Fracture network evolution (13409b21009032). Stress field according to Martin [2007], DFN I, high swelling pressure, heating sequence and ice cover. The figures show the fracture network and the type of fracture. Colour code: blue - currently not loaded, green - shear loaded, red - open. Thickening of lines show application of a fluid pressure.



As for simulation of an ice cover of approx. 3km additional load of 24.5MPa ( $S_{yy}$  due to redistribution around backfilled tunnel) is added resulting in no major changes of the DFN or aperture.



The water head is increased to 34MPa due to an assumed ice cover fully hydraulically connected to the repository. The fractures show higher apertures and additional fracturing is introduced.

## 11.5. Simulation IA-1

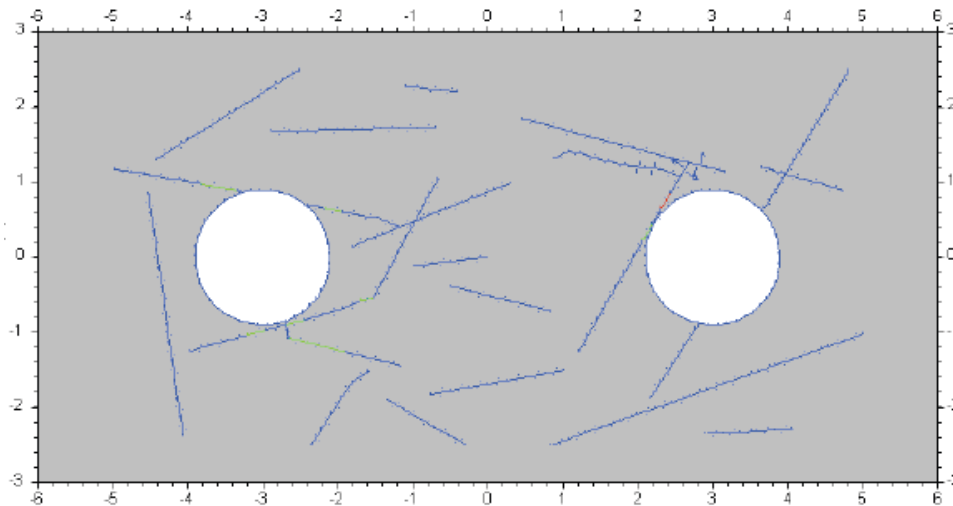
The model in this simulation includes DFN I and is subject to the stress field according to Ask et al. [2007]. It features the full loading history including low swelling pressure  $P_s$ , the heating sequence up to 75°C and the ice cover.

simulation	stress field		DFN	fract.ini	closure			heating	ice cover		
	$S_{xx}$	$S_{yy}$			backfill	$P_s$	$P_p$		load	$P_p$	
13409b21009081	19,2	12,2	2)	I	X	-3,0	5,5	4,0	✓	24,5	34

The introduction of the excavations and the reduction of  $S_{yy}$  due to the backfill only show minor fracture propagation. But already the combination of swelling pressure and in particular water pressure after the closure of the repository results according to the simulations in significant fracture growth connecting the deposition holes. Addition of thermal loads enhances fracture growth. It appears that fracture growth at peak temperature seems to be unstable<sup>3</sup>.

Most of the fractures have connected to other fractures already after the thermal phase so that the fracture propagation under the additional ice cover loads is limited but the fractures appear still under high loads.

Figure e. Fracture network evolution (13409b21009081). Stress field according to Ask et al. [2007], DFN I, low swelling pressure, heating sequence and ice cover. The figures show the fracture network and the type of fracture. Colour code: blue - currently not loaded, green - shear loaded, red - open. Thickening of lines show application of a fluid pressure.



Fracture network after introduction of the excavations. Only few fractures propagated due to the redistribution of the stresses. Stress field according to Ask et al. [2007]; DFN I.

<sup>3</sup> The five cycles of fracture growth appear not to be sufficient to reduce the energy in the system sufficiently. Hence additional computing would be required to study the influence of the peak temperature. As an artefact of this instability of the computational step fracturing is ongoing into the cooling phase.

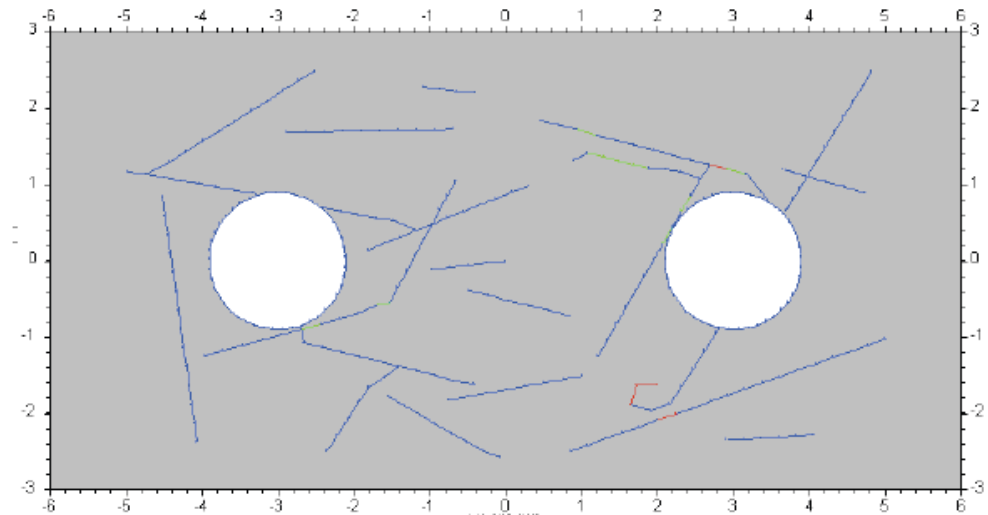
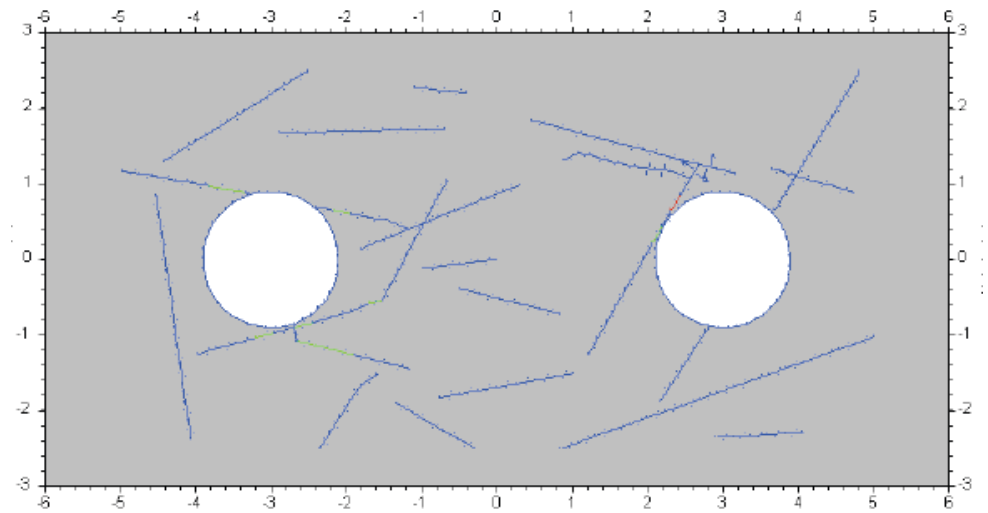
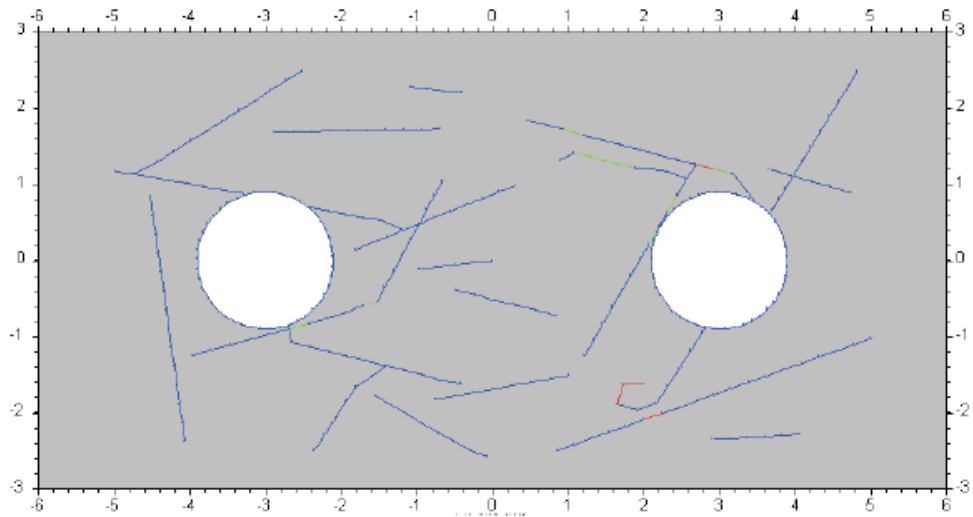


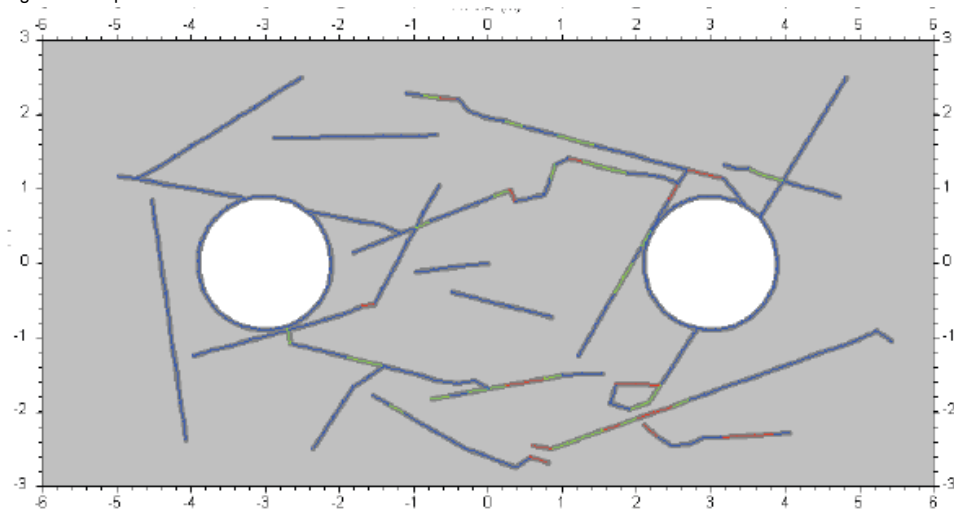
Figure e. Fracture network evolution (13409b21009081). Stress field according to Ask et al. [2007], DFN I, low swelling pressure, heating sequence and ice cover. The figures show the fracture network and the type of fracture. Colour code: blue - currently not loaded, green - shear loaded, red - open. Thickening of lines show application of a fluid pressure.



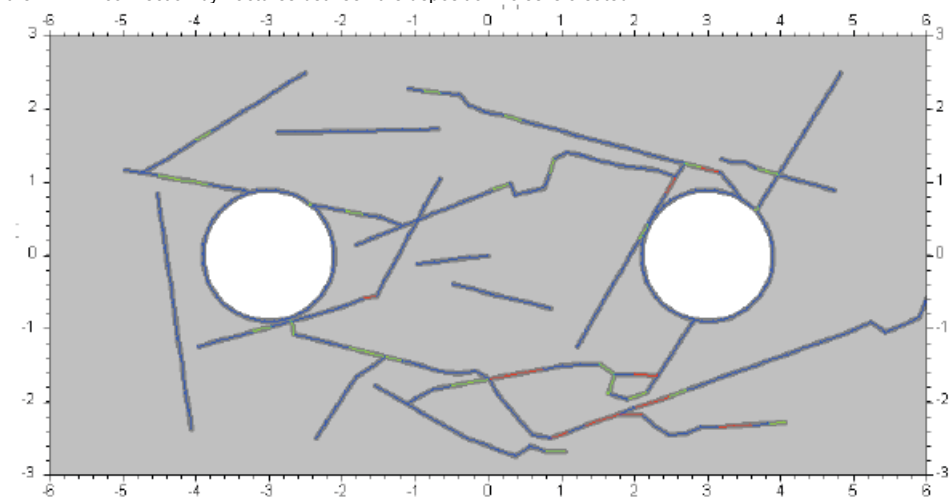
Fracture network after introduction of the excavations. Only few fractures propagated due to the redistribution of the stresses. Stress field according to Ask et al. [2007]; DFN I.



After the closure of the repository the applied stress is increased due to the backfill of the tunnel. This has no significant impact on the DFN.

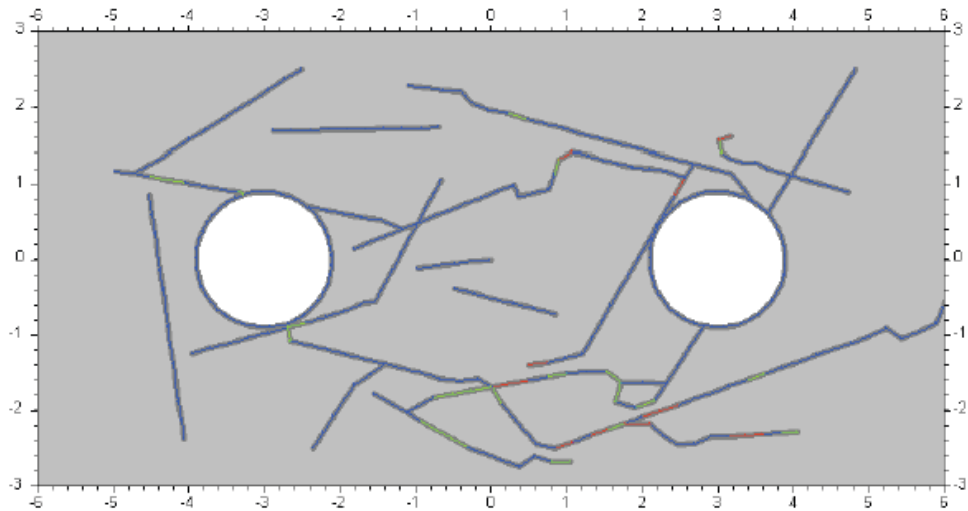


The swelling pressure (5.5MPa) and the recovery of a water head (4MPa) show already significant impact on the DFN. A connection by fractures between the deposition holes is created.

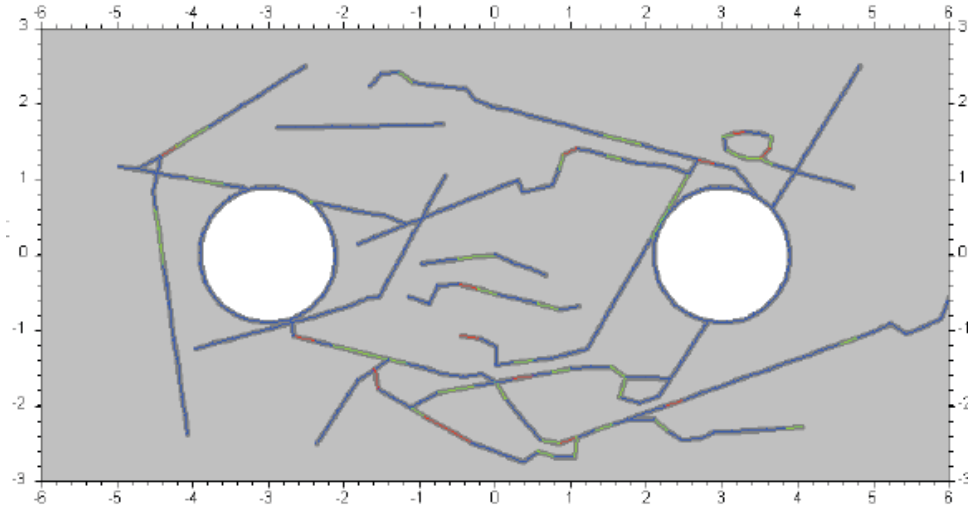


The temperature at the face of the deposition holes is increased from the initial 14.5°C to 25°C. Further fracture growth creates potential fluid pathways.

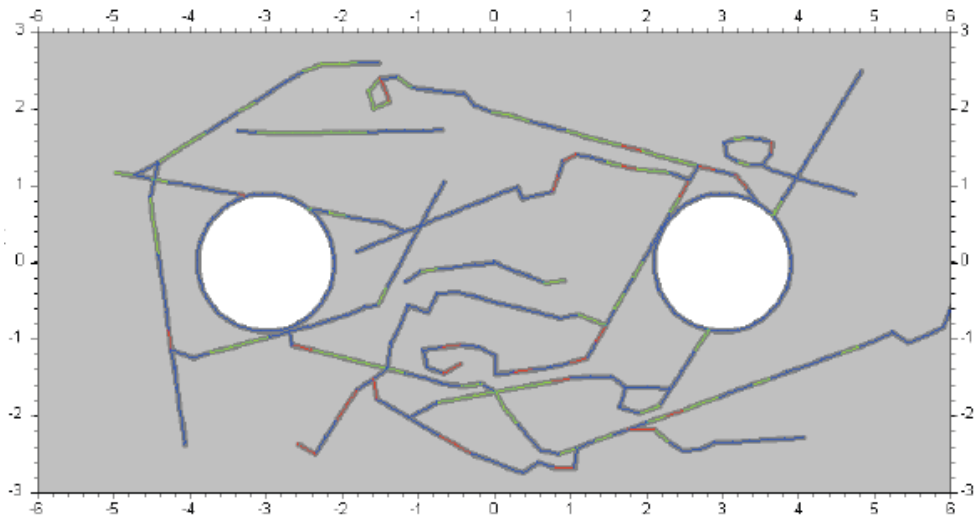
Figure e. Fracture network evolution (13409b21009081). Stress field according to Ask et al. [2007], DFN I, low swelling pressure, heating sequence and ice cover. The figures show the fracture network and the type of fracture. Colour code: blue - currently not loaded, green - shear loaded, red - open. Thickening of lines show application of a fluid pressure.



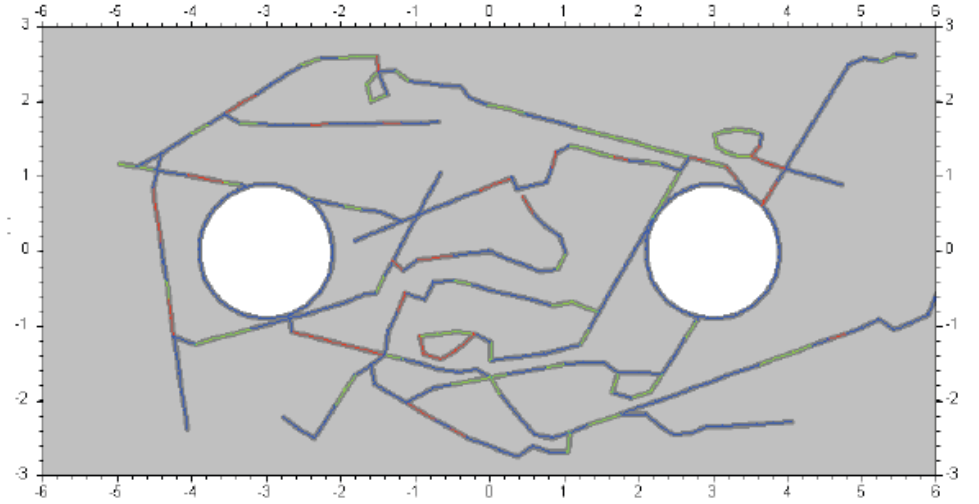
Temperature at the deposition hole face is increased to 50°C. Minor impact.



Temperature at the deposition hole face is increased to 75°C. Further fracture growth.

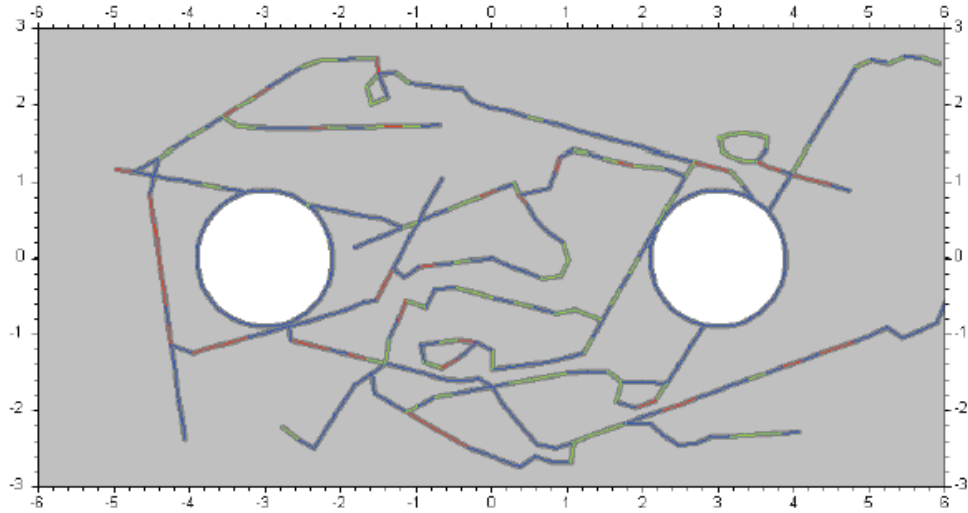


Temperature at the deposition hole face is decreased to 50°C. No stabilisation of the model.

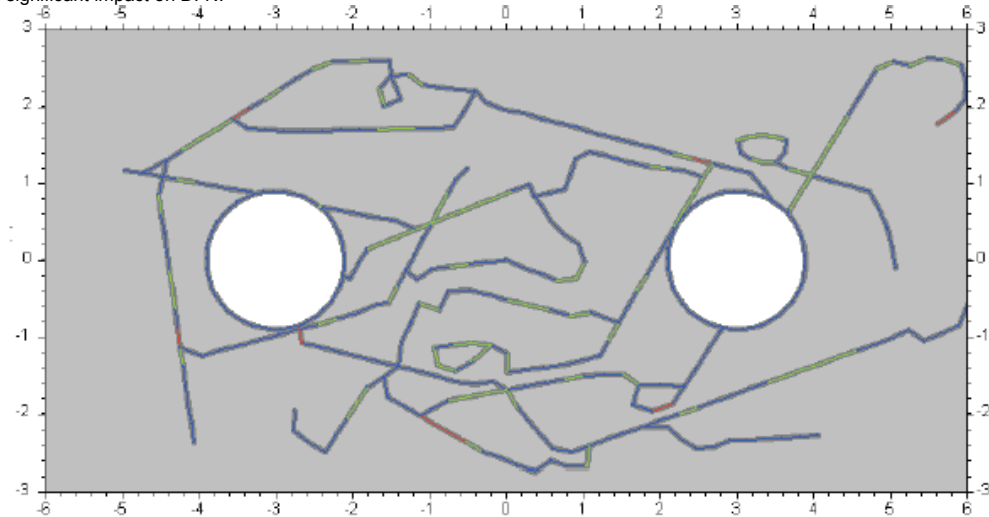


Temperature at the deposition hole face is decreased to 25°C. Still fracture growth.

Figure e. Fracture network evolution (13409b21009081). Stress field according to Ask et al. [2007], DFN I, low swelling pressure, heating sequence and ice cover. The figures show the fracture network and the type of fracture. Colour code: blue - currently not loaded, green - shear loaded, red - open. Thickening of lines show application of a fluid pressure.

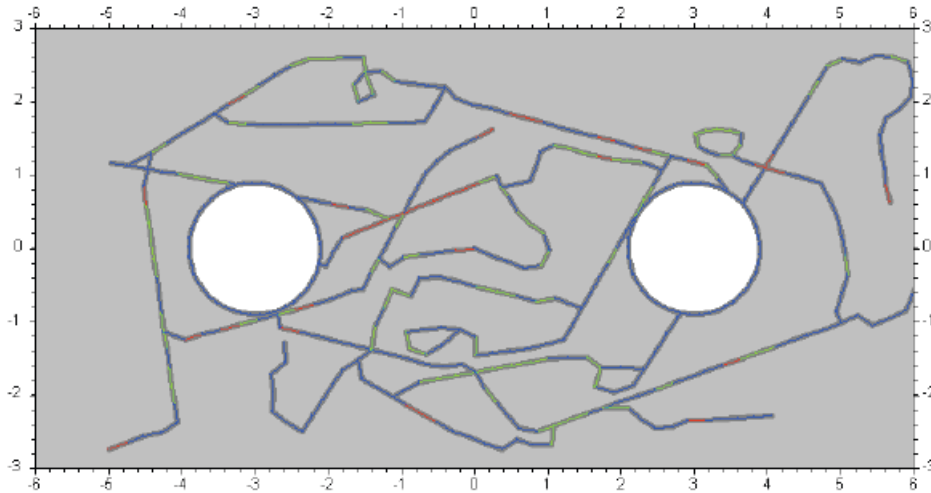


Temperature at the deposition hole face is decreased to 10°C. The aperture of selected fractures reduces. No significant impact on DFN.



As for simulation of an ice cover of approx. 3km additional load of 24.5MPa ( $S_{yy}$  due to redistribution around backfilled tunnel) is added resulting in no major changes of the DFN.





The water head is increased to 34MPa due to an assumed ice cover fully hydraulically connected to the repository. And additional fracturing is introduced.

## 11.6. Simulation IA-2

The model in this simulation includes DFN I and is subject to the stress field according to Ask et al. [2007]. It features the full loading history including high swelling pressure  $P_s$ , the heating sequence up to 75°C and the ice cover.

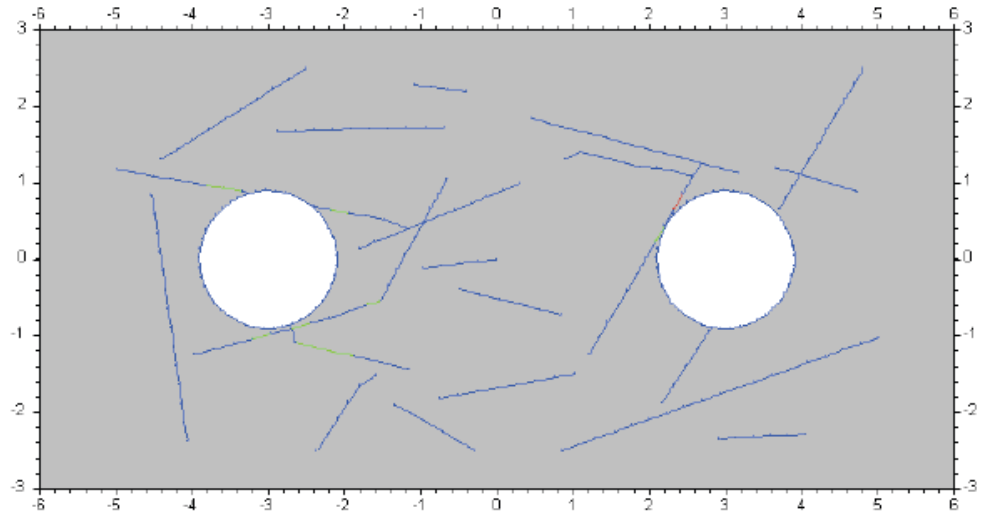
simulation	stress field		DFN	fract.ini	closure			heating	ice cover	
	Sxx	Syy			backfill	$P_s$	$P_p$		load	$P_p$
13409b21009082	19,2	12,2 <sup>2)</sup>	I	X	-3,0	7,2	4,0	✓	24,5	34

The introduction of the excavations and the reduction of  $S_{yy}$  due to the backfill only show minor fracture propagation. But already the combination of swelling pressure and in particular water pressure after the closure of the repository results according to the simulations in significant fracture growth connecting the deposition holes. Addition of thermal loads enhances fracture growth. It appears that fracture growth at peak temperature seems to be unstable<sup>4</sup>.

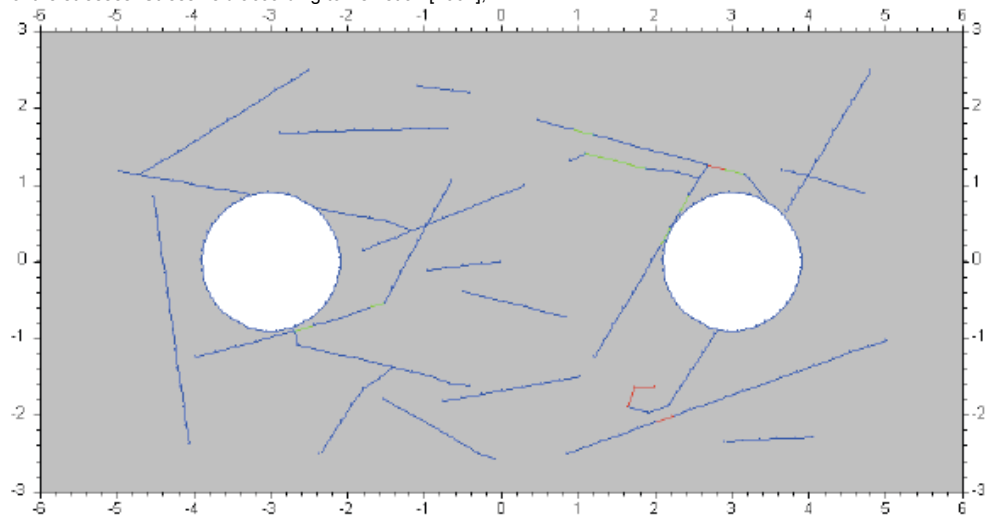
Most of the fractures have connected to other fractures already after the thermal phase so that the fracture propagation under the additional ice cover loads is limited but the fractures appear still under high loads.

<sup>4</sup> The five cycles of fracture growth appear not to be sufficient to reduce the energy in the system sufficiently. Hence additional computing would be required to study the influence of the peak temperature. As an artefact of this instability of the computational step fracturing is ongoing into the cooling phase.

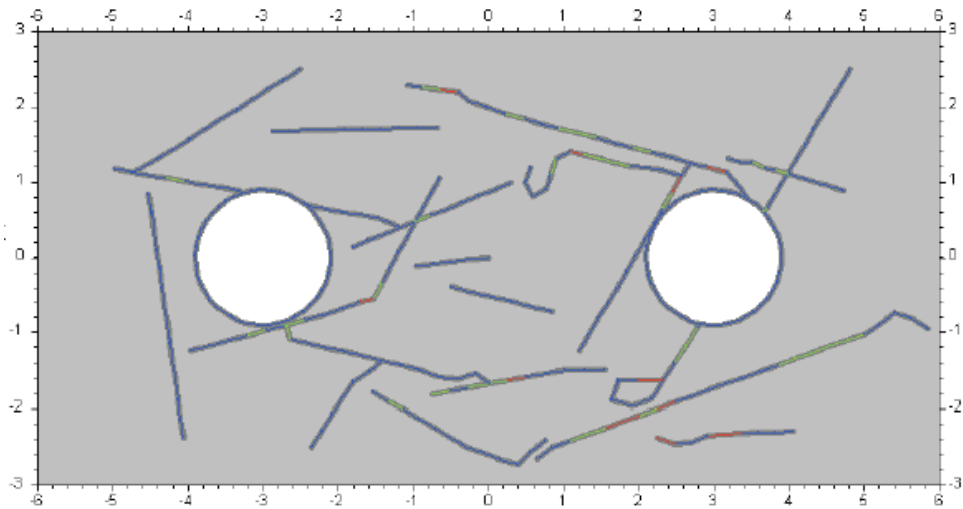
Figure f. Fracture network evolution (13409b21009082). Stress field according to Ask et al. [2007], DFN I, high swelling pressure, heating sequence and ice cover. The figures show the fracture network and the type of fracture. Colour code: blue - currently not loaded, green - shear loaded, red - open. Thickening of lines show application of a fluid pressure.



Fracture network after introduction of the excavations. Only few fractures propagated due to the redistribution of the stresses. Stress field according to Ask et al. [2007]; DFN I.

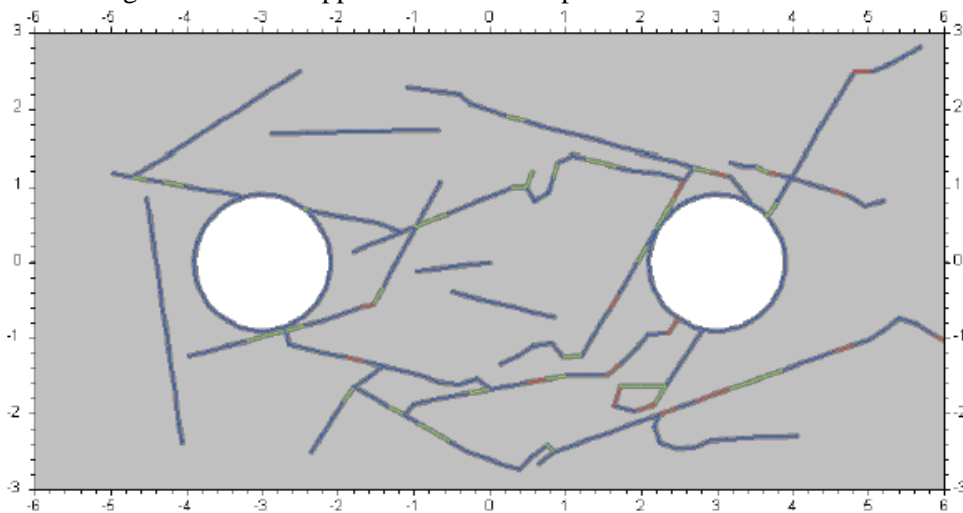


After the closure of the repository the applied stress is increased due to the backfill of the tunnel. This has no significant impact on the DFN.

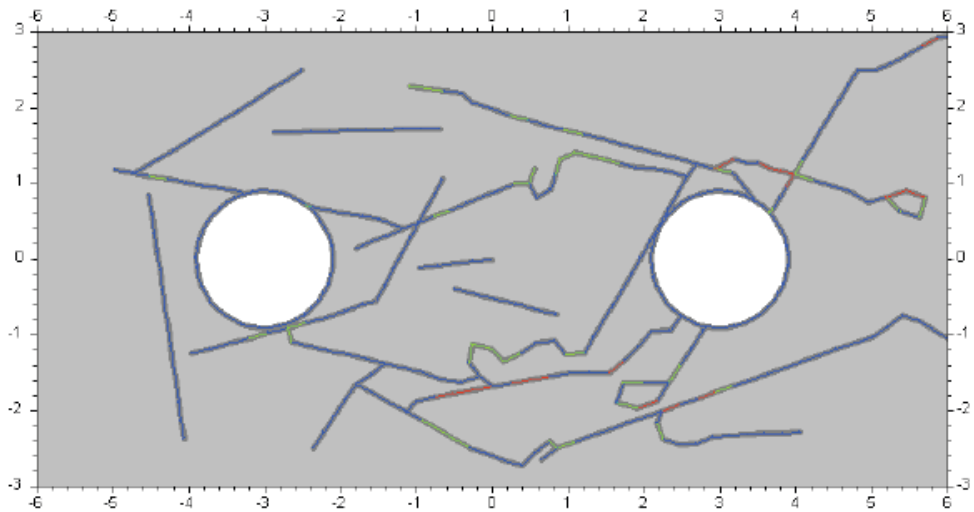


The swelling pressure (7.2MPa) and the recovery of a water head (4MPa) show already significant impact on the DFN. A connection by fractures between the deposition holes is created.

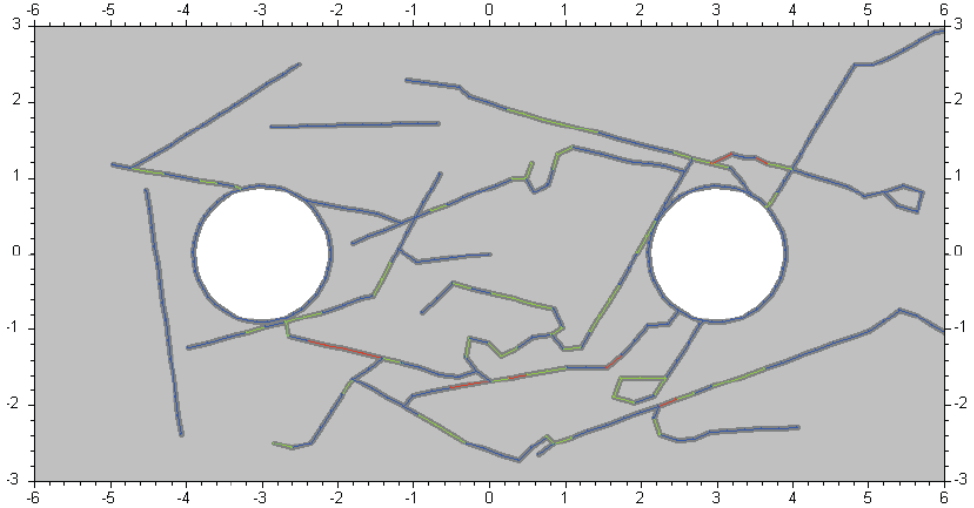
Figure f. Fracture network evolution (13409b21009082). Stress field according to Ask et al. [2007], DFN I, high swelling pressure, heating sequence and ice cover. The figures show the fracture network and the type of fracture. Colour code: blue - currently not loaded, green - shear loaded, red - open. Thickening of lines show application of a fluid pressure.



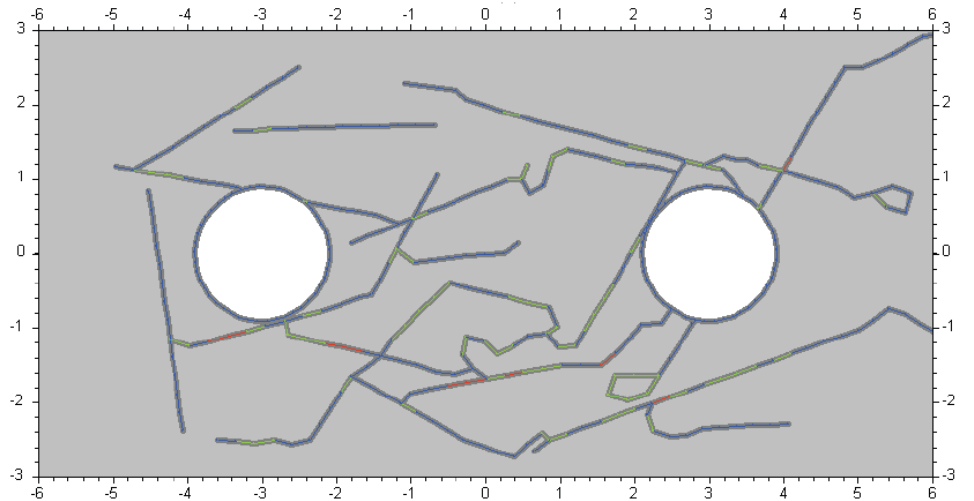
The temperature at the face of the deposition holes is increased from the initial 14.5°C to 25°C. Further fracture growth creates potential fluid pathways.



Temperature at the deposition hole face is increased to 50°C. Minor impact.

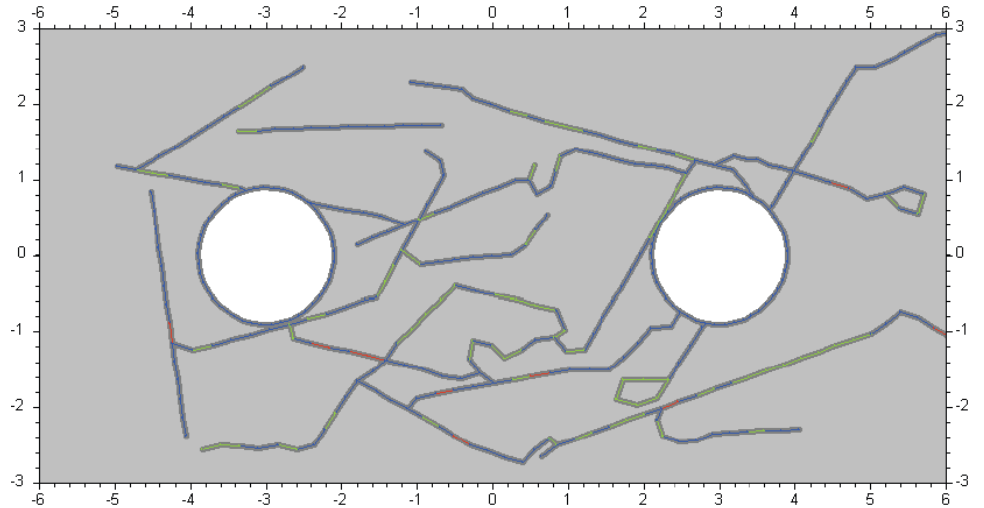


Temperature at the deposition hole face is increased to 75°C. Further fracture growth.

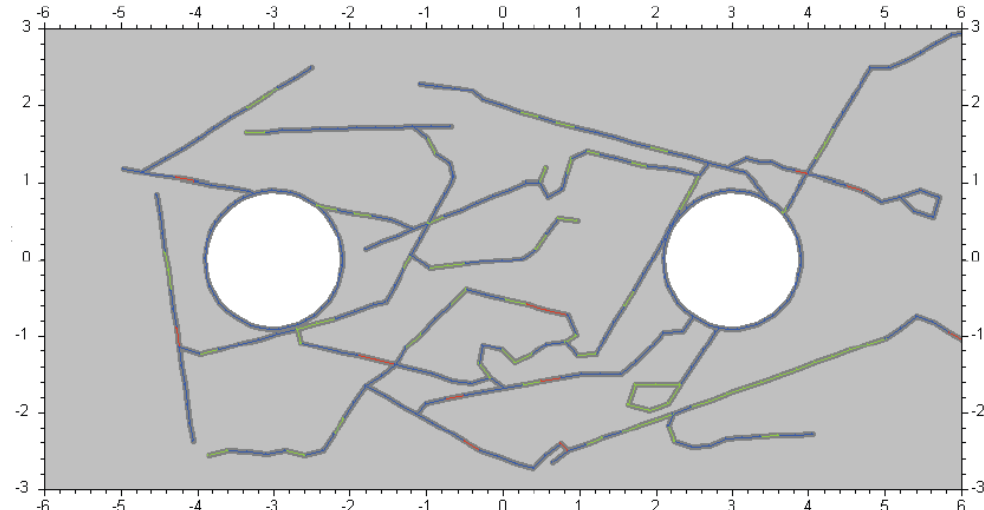


Temperature at the deposition hole face is decreased to 50°C. No stabilisation of the model.

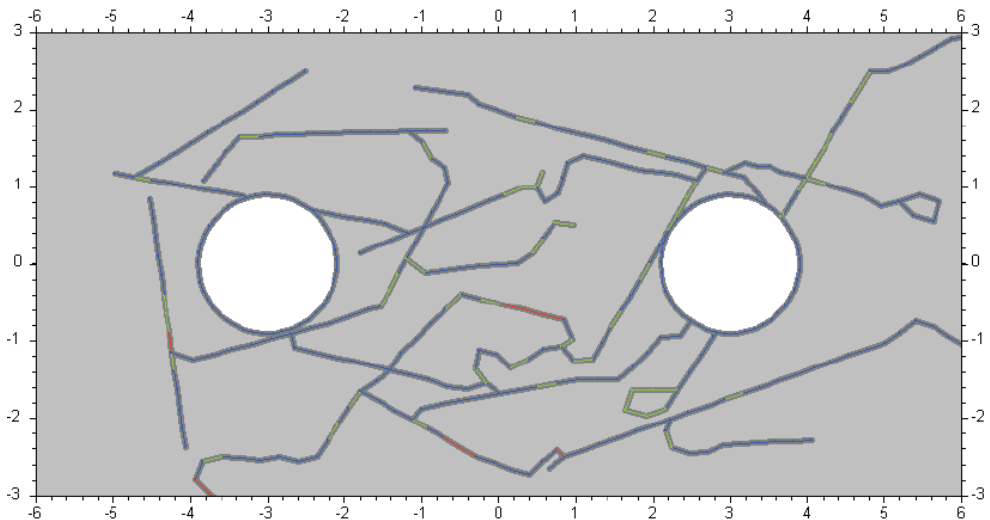
Figure f. Fracture network evolution (13409b21009082). Stress field according to Ask et al. [2007], DFN I, high swelling pressure, heating sequence and ice cover. The figures show the fracture network and the type of fracture. Colour code: blue - currently not loaded, green - shear loaded, red - open. Thickening of lines show application of a fluid pressure.



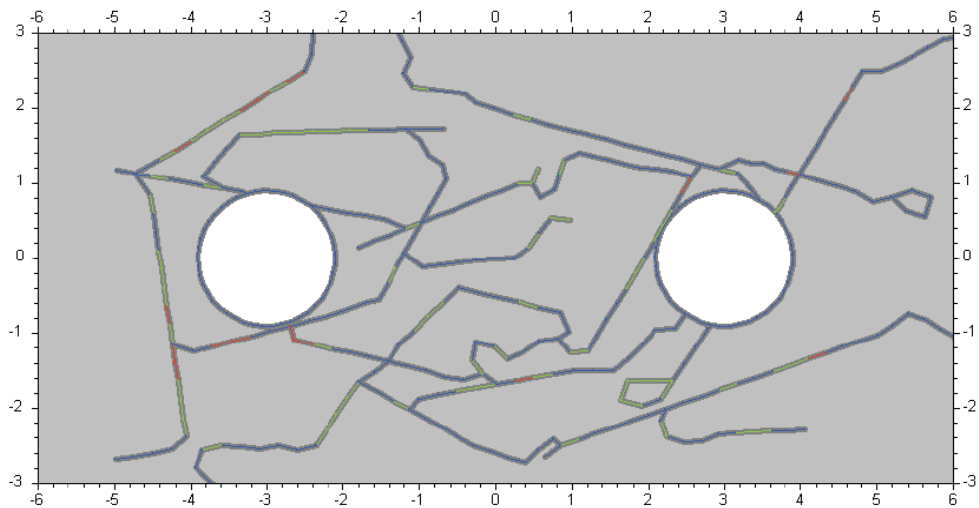
Temperature at the deposition hole face is decreased to 25°C. Still fracture growth.



Temperature at the deposition hole face is decreased to 10°C. The aperture of selected fractures reduces. No significant impact on DFN.



As for simulation of an ice cover of approx. 3km additional load of 24.5MPa ( $S_{yy}$  due to redistribution around backfilled tunnel) is added resulting in no major changes of the DFN.



The water head is increased to 34MPa due to an assumed ice cover fully hydraulically connected to the repository. Additional fracturing is introduced.

### 11.7. Simulation IA-3

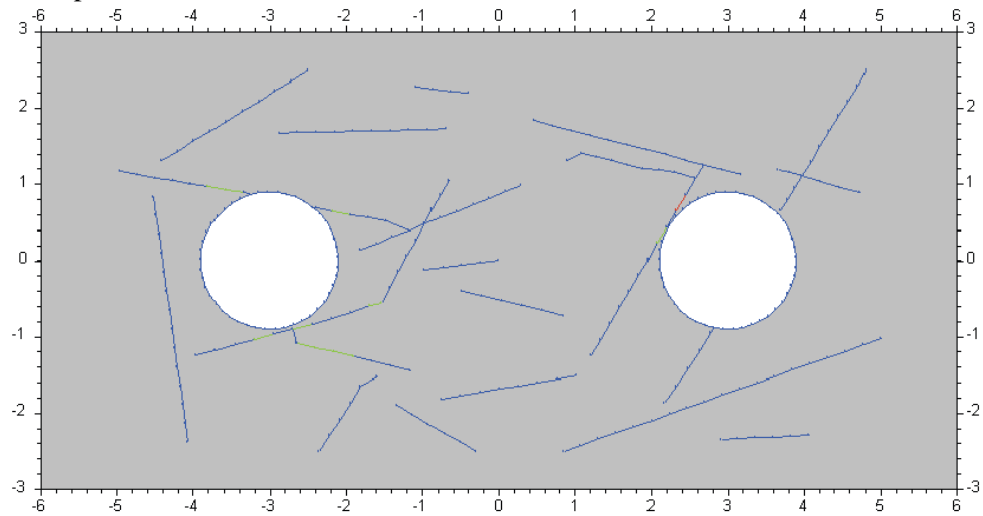
The model in this simulation includes DFN I and is subject to the stress field according to Ask et al. [2007]. It features only a limited loading history including low swelling pressure  $P_s$ , but no heating sequence. As the fluid pressure has shown pronounced effect on the fracture growth, the fluid pressure under ice cover load is stepwise increase.

simulation	stress field		DFN	fract.ini	closure			heating	ice cover	
	Sxx	Syy			backfill	$P_s$	$P_p$		load	$P_p$
13409b21009083	19,2	12,2 <sup>2)</sup>	I	X	-3,0	5,5	4,0	X	24,5	34, +5, 60

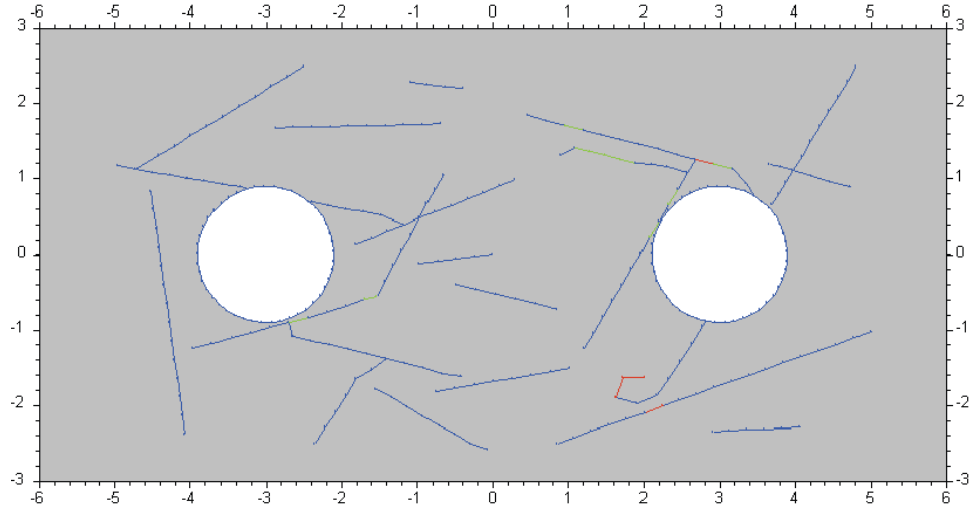
Only few fractures propagate short distances due to the stress redistribution of the excavations. The increase in  $P_p$  due to recovery of water head already introduces significant fracture propagation and DFN development. The in-

crease in load due to the ice cover stabilises the fractures slightly, the increase in fluid pressure due to the ice cover introduces severe fracturing again. At some point almost all fractures have run into an arrester position so that a further increase in  $P_p$  does not introduce additional fracture propagation. As the initiation of new fractures is not activated it may be discussed if new fractures would be created; this is beyond the scope of this study, as the applied  $P_p$  from the ice cover can already be assumed quite high.

Figure g. Fracture network evolution (13409b21009083). Stress field according to Ask et al. [2007], DFN I, low swelling pressure, no heating sequence, ice cover and extended ice load fluid pressure. The figures show the fracture network and the type of fracture. Colour code: blue - currently not loaded, green - shear loaded, red - open. Thickening of lines show application of a fluid pressure.

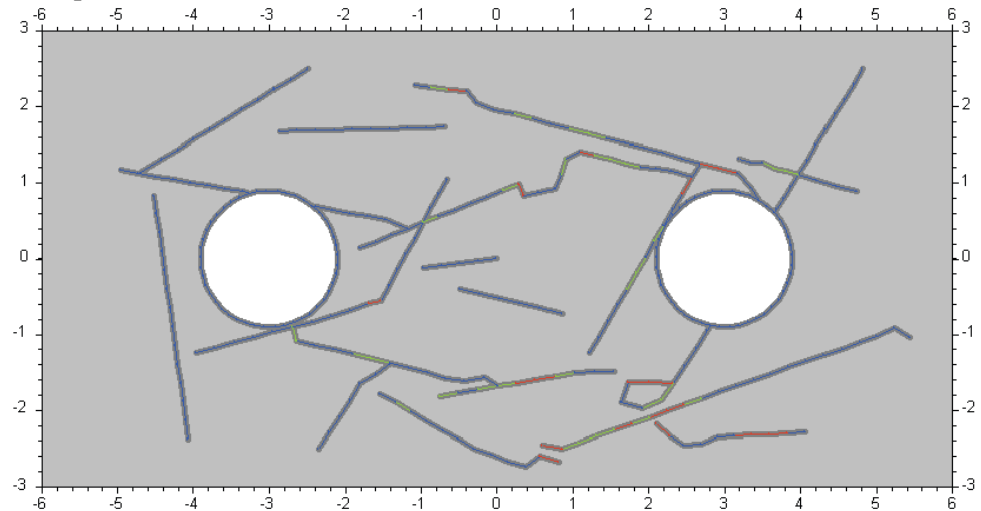


Fracture network after introduction of the excavations. Only few fractures propagated due to the redistribution of the stresses. Stress field according to Ask et al. [2007]; DFN I.

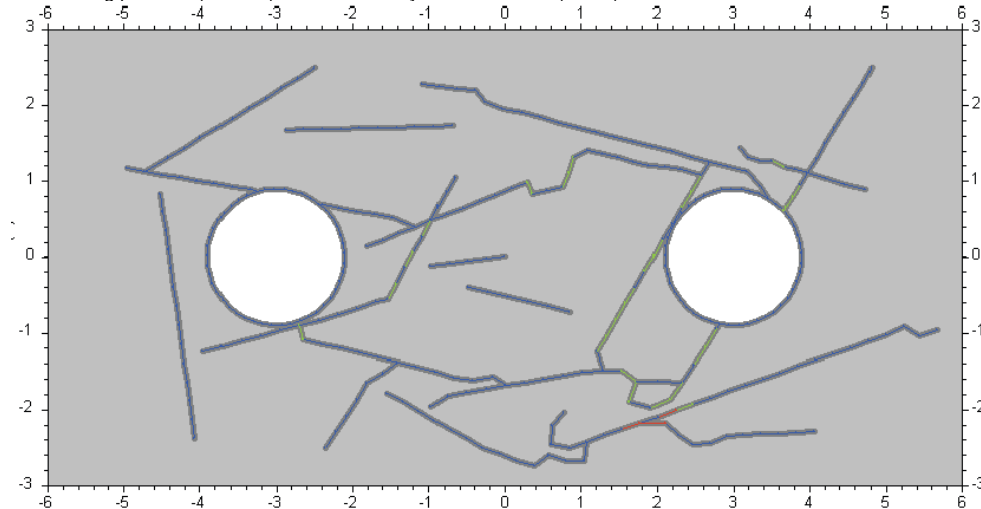


After the closure of the repository the applied stress is increased due to the backfill of the tunnel. This has no significant impact on the DFN.

Figure g. Fracture network evolution (13409b21009083). Stress field according to Ask et al. [2007], DFN I, low swelling pressure, no heating sequence, ice cover and extended ice load fluid pressure. The figures show the fracture network and the type of fracture. Colour code: blue - currently not loaded, green - shear loaded, red - open. Thickening of lines show application of a fluid pressure.

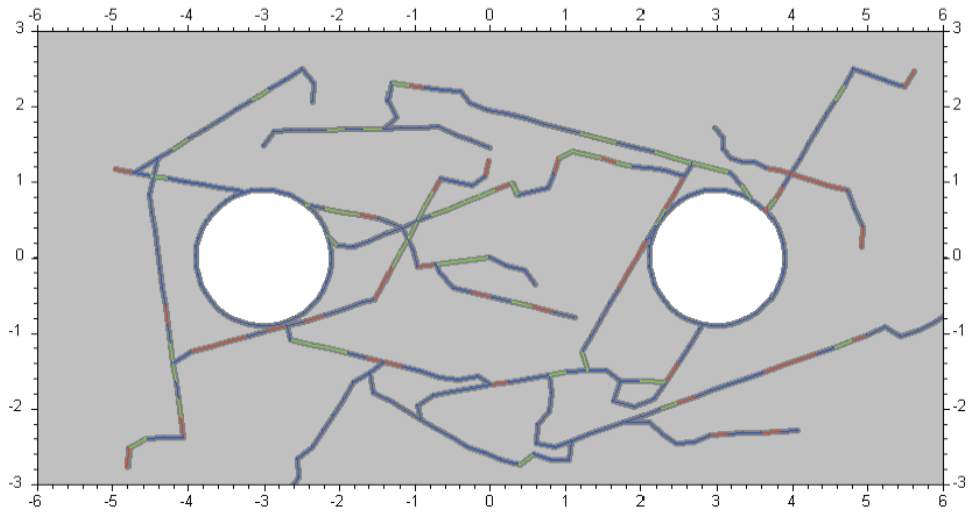


The swelling pressure (5.5MPa) and the recovery of a water head (4MPa) show extension of the DFN.

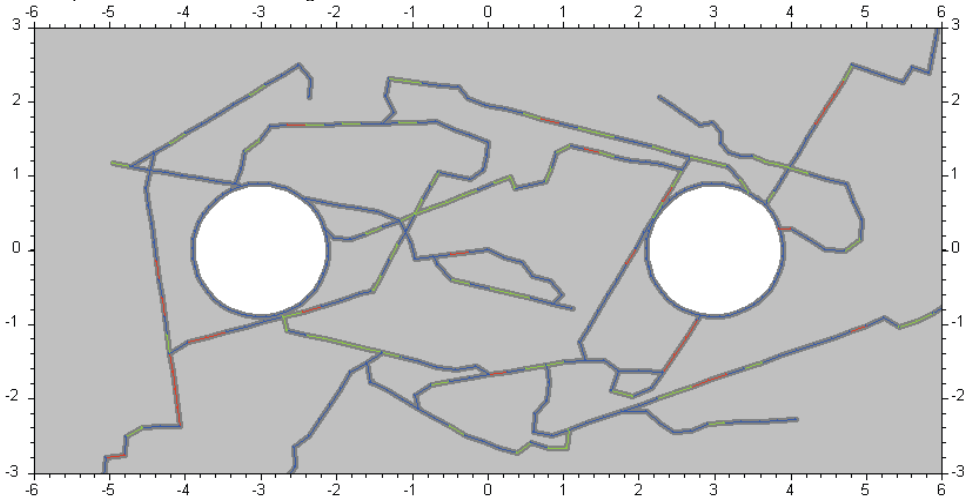


As for simulation of an ice cover of approx. 3km additional load of 24.5MPa ( $S_{yy}$  due to redistribution around backfilled tunnel) is added resulting in no major changes of the DFN.



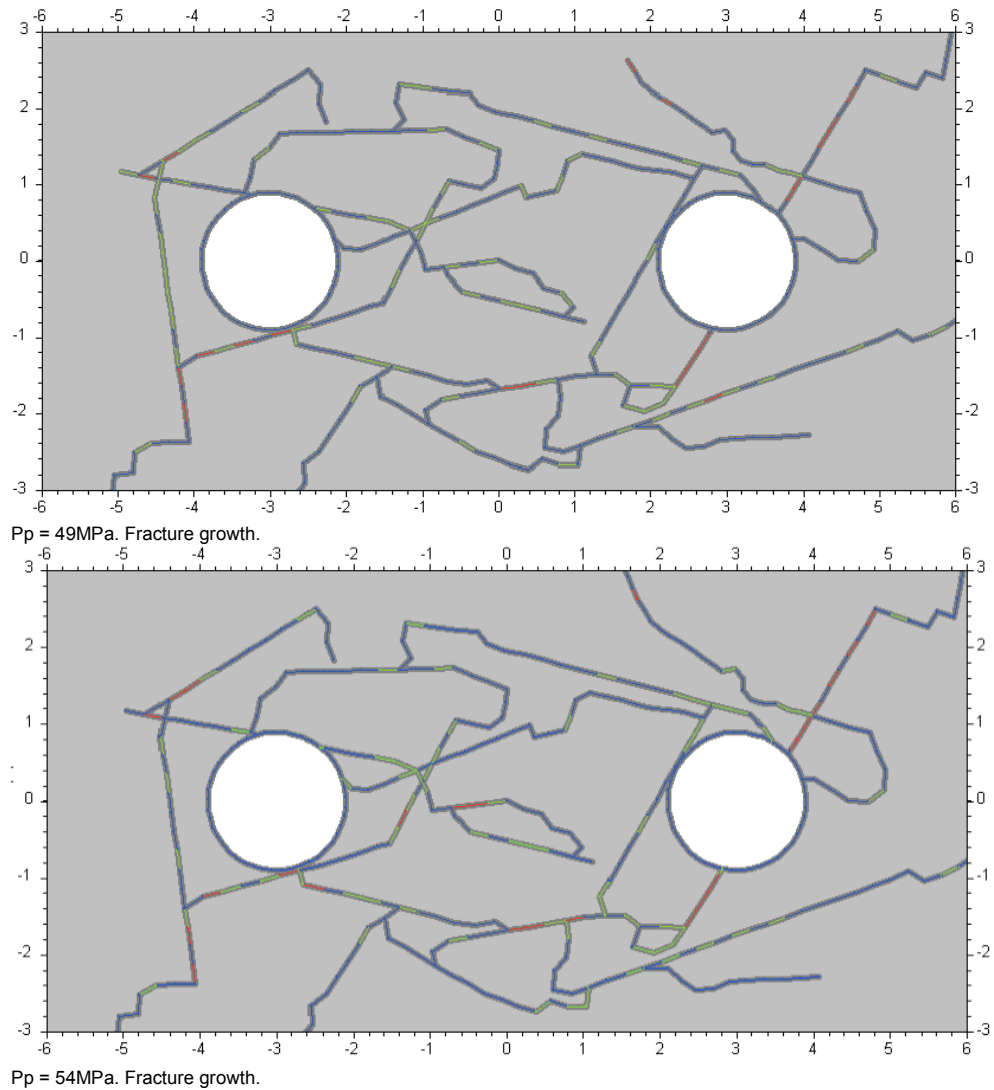


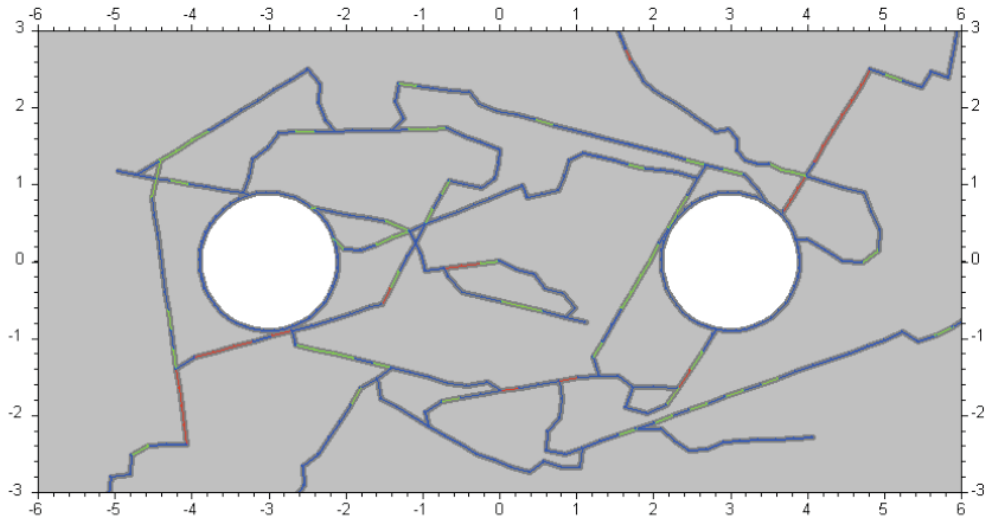
The water pressure acting on the deposition holes and the fractures is increased from  $P_p = 34\text{MPa}$  in steps of  $5\text{MPa}$ .  $P_p = 39\text{MPa}$ . Severe fracturing.



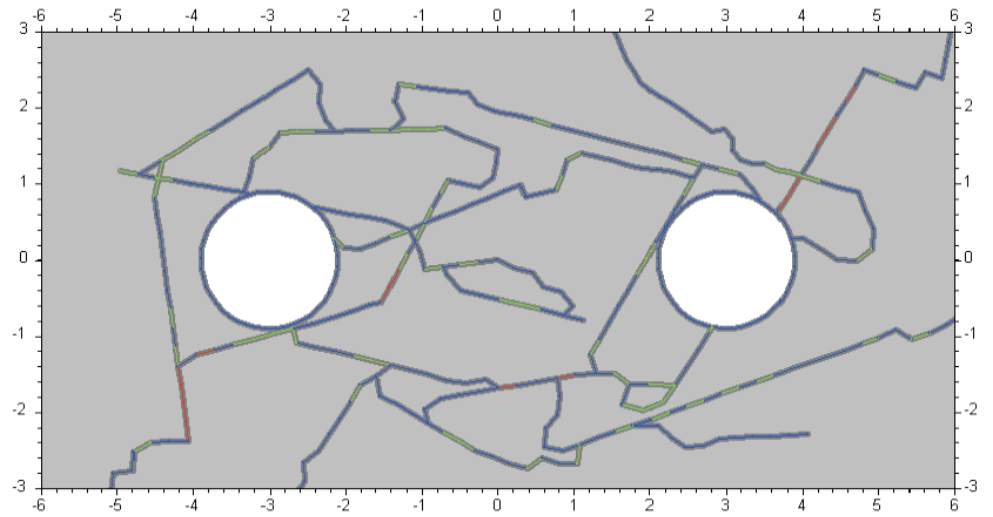
$P_p = 44\text{MPa}$ . Fracture growth.

Figure g. Fracture network evolution (13409b21009083). Stress field according to Ask et al. [2007], DFN I, low swelling pressure, no heating sequence, ice cover and extended ice load fluid pressure. The figures show the fracture network and the type of fracture. Colour code: blue - currently not loaded, green - shear loaded, red - open. Thickening of lines show application of a fluid pressure.



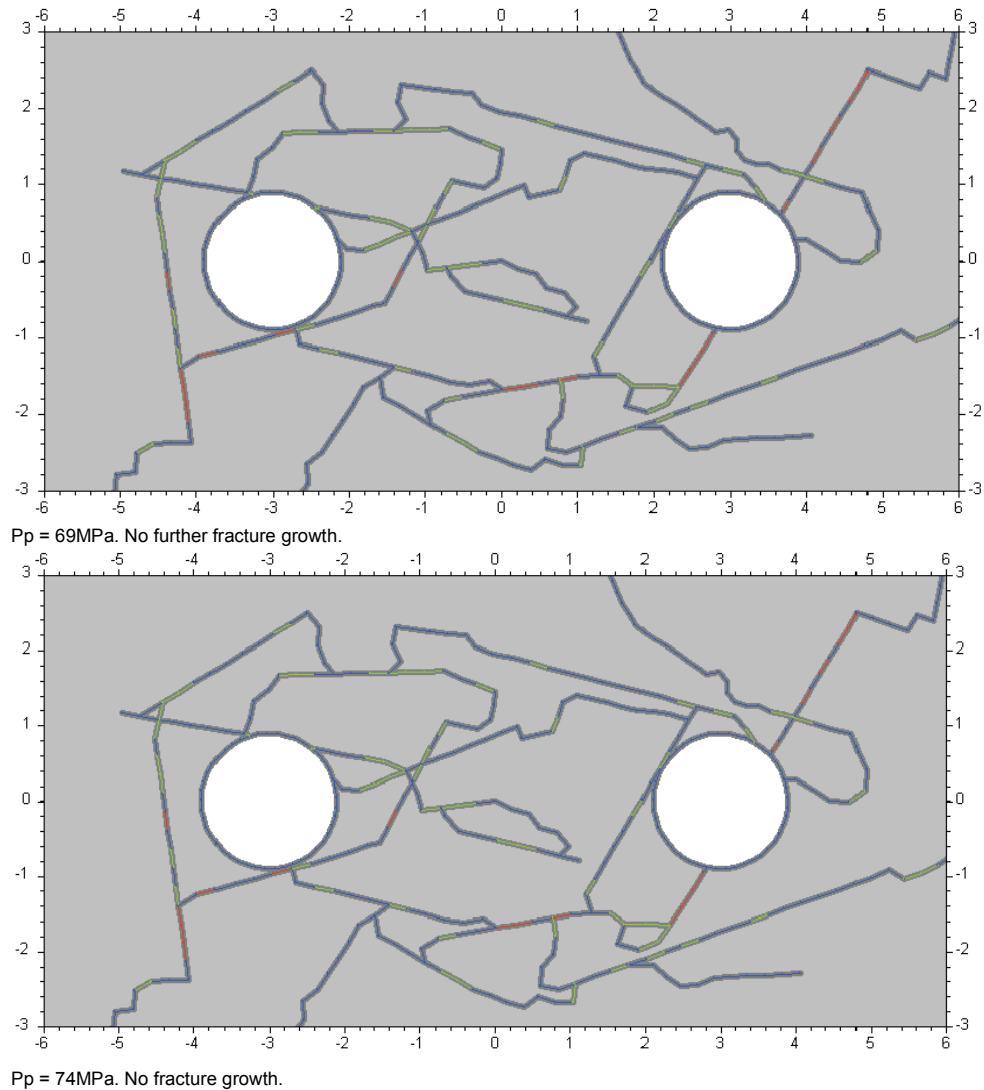


$P_p = 59\text{MPa}$ . Stabilisation.



$P_p = 64\text{MPa}$ . No further fracture growth.

Figure g. Fracture network evolution (13409b21009083). Stress field according to Ask et al. [2007], DFN I, low swelling pressure, no heating sequence, ice cover and extended ice load fluid pressure. The figures show the fracture network and the type of fracture. Colour code: blue - currently not loaded, green - shear loaded, red - open. Thickening of lines show application of a fluid pressure.



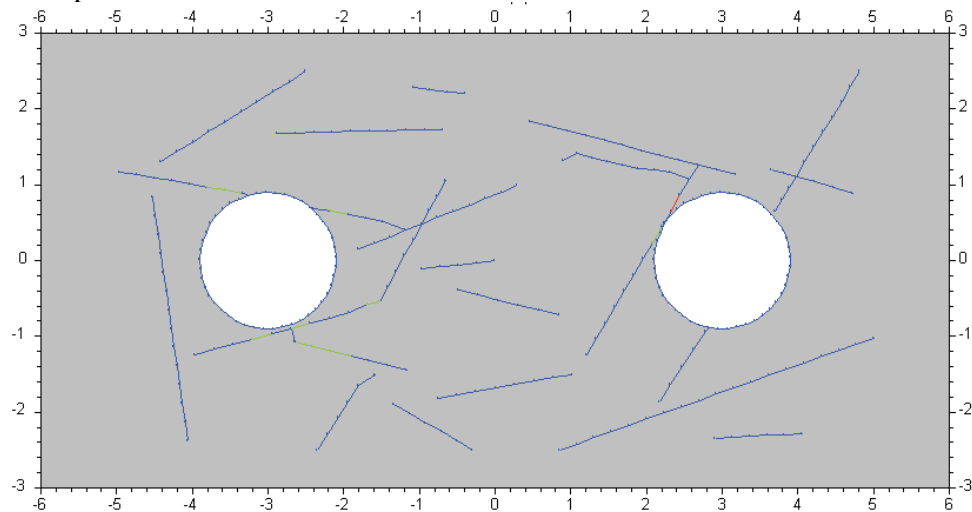
### 11.8. Simulation IA-4

The model in this simulation includes DFN I and is subject to the stress field according to Ask et al. [2007]. It features only a limited loading history including high swelling pressure  $P_s$ , but no heating sequence. As the fluid pressure has shown pronounced effect on the fracture growth, the fluid pressure under ice cover load is stepwise increase.

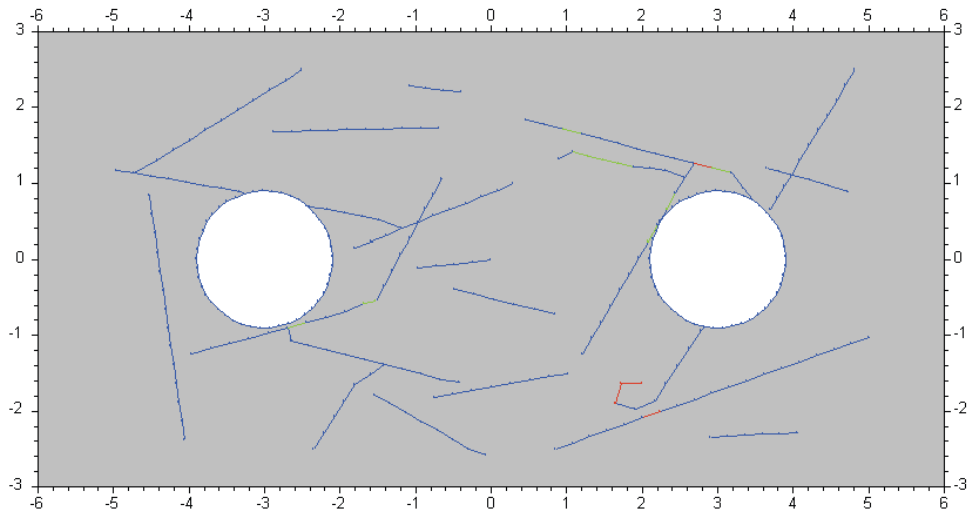
simulation	stress field		DFN	fract.ini	closure			heating	ice cover	
	Sxx	Syy			backfill	Ps	Pp		load	Pp
13409b21009084	19,2	12,2 <sup>2)</sup>	I	x	-3,0	7,2	4,0	x	24,5	34, +5, 60

Only few fractures propagate short distances due to the stress redistribution of the excavations. The increase in Pp due to recovery of water head already introduces significant fracture propagation and DFN development. The increase in load due to the ice cover stabilises the fractures slightly, the increase in fluid pressure due to the ice cover introduces severe fracturing again. At some point almost all fractures have run into an arrester position so that a further increase in Pp does not introduce additional fracture propagation. As the initiation of new fractures is not activated it may be discussed if new fractures would be created; this is beyond the scope of this study, as the applied Pp from the ice cover can already be assumed quite high.

Figure h. Fracture network evolution (13409b21009084). Stress field according to Ask et al. [2007], DFN I, high swelling pressure, no heating sequence, ice cover and extended ice load fluid pressure. The figures show the fracture network and the type of fracture. Colour code: blue - currently not loaded, green - shear loaded, red - open. Thickening of lines show application of a fluid pressure.

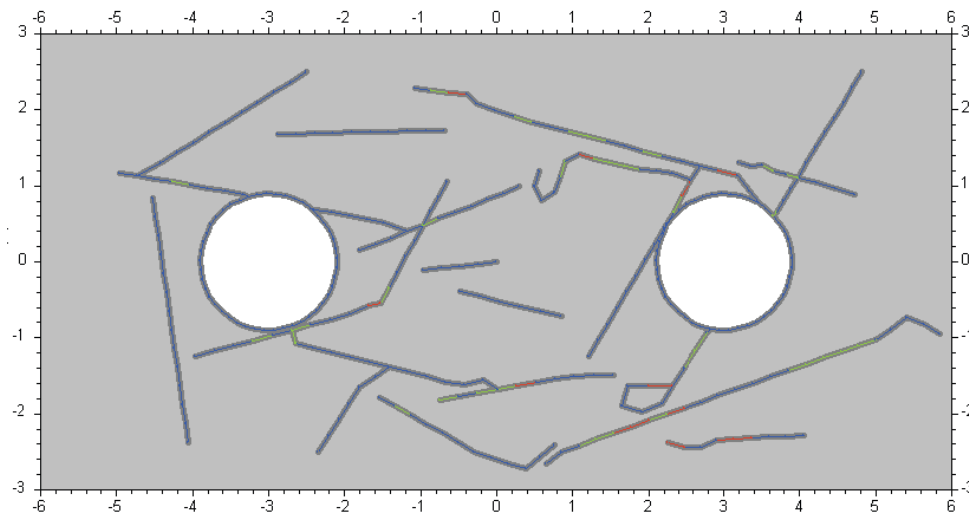


Fracture network after introduction of the excavations. Only few fractures propagated due to the redistribution of the stresses. Stress field according to Ask et al. [2007]; DFN 1.

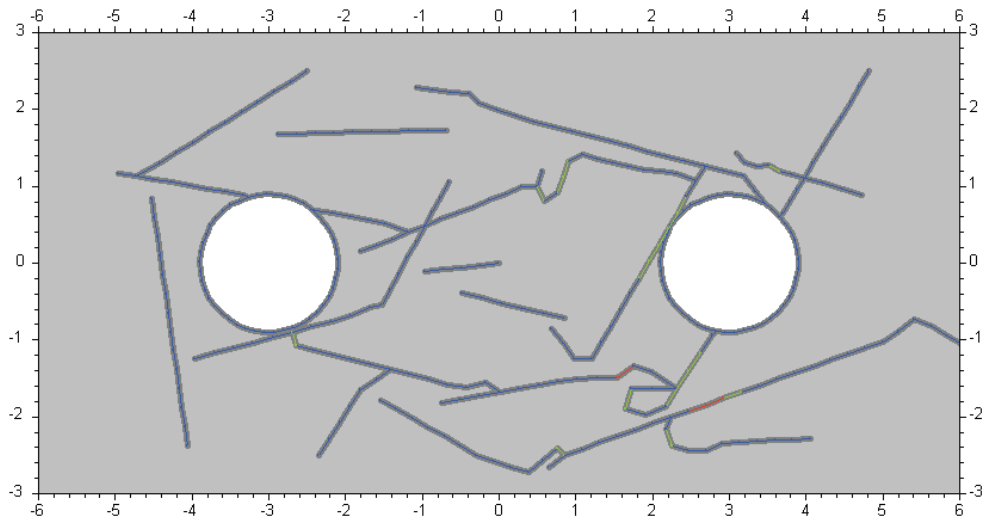


After the closure of the repository the applied stress is increased due to the backfill of the tunnel. This has no significant impact on the DFN.

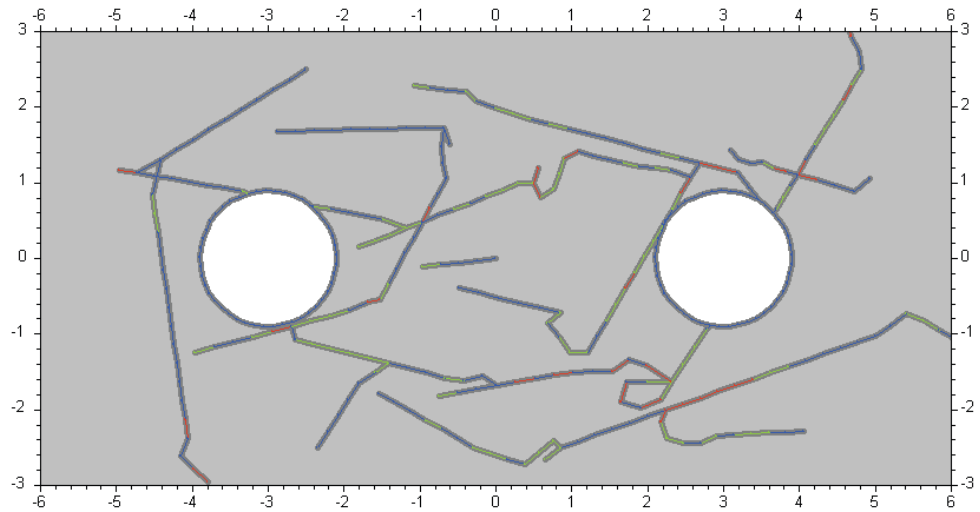
Figure h. Fracture network evolution (13409b21009084). Stress field according to Ask et al. [2007], DFN I, high swelling pressure, no heating sequence, ice cover and extended ice load fluid pressure. The figures show the fracture network and the type of fracture. Colour code: blue - currently not loaded, green - shear loaded, red - open. Thickening of lines show application of a fluid pressure.



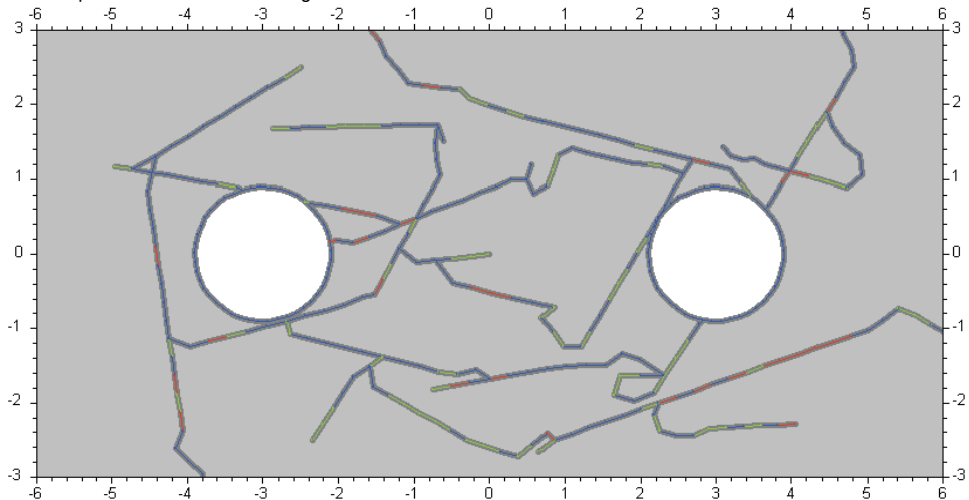
The swelling pressure (7.2MPa) and the recovery of a water head (4MPa) show extension of the DFN.



As for simulation of an ice cover of approx. 3km additional load of 24.5MPa ( $S_{yy}$  due to redistribution around backfilled tunnel) is added resulting in some changes of the DFN.

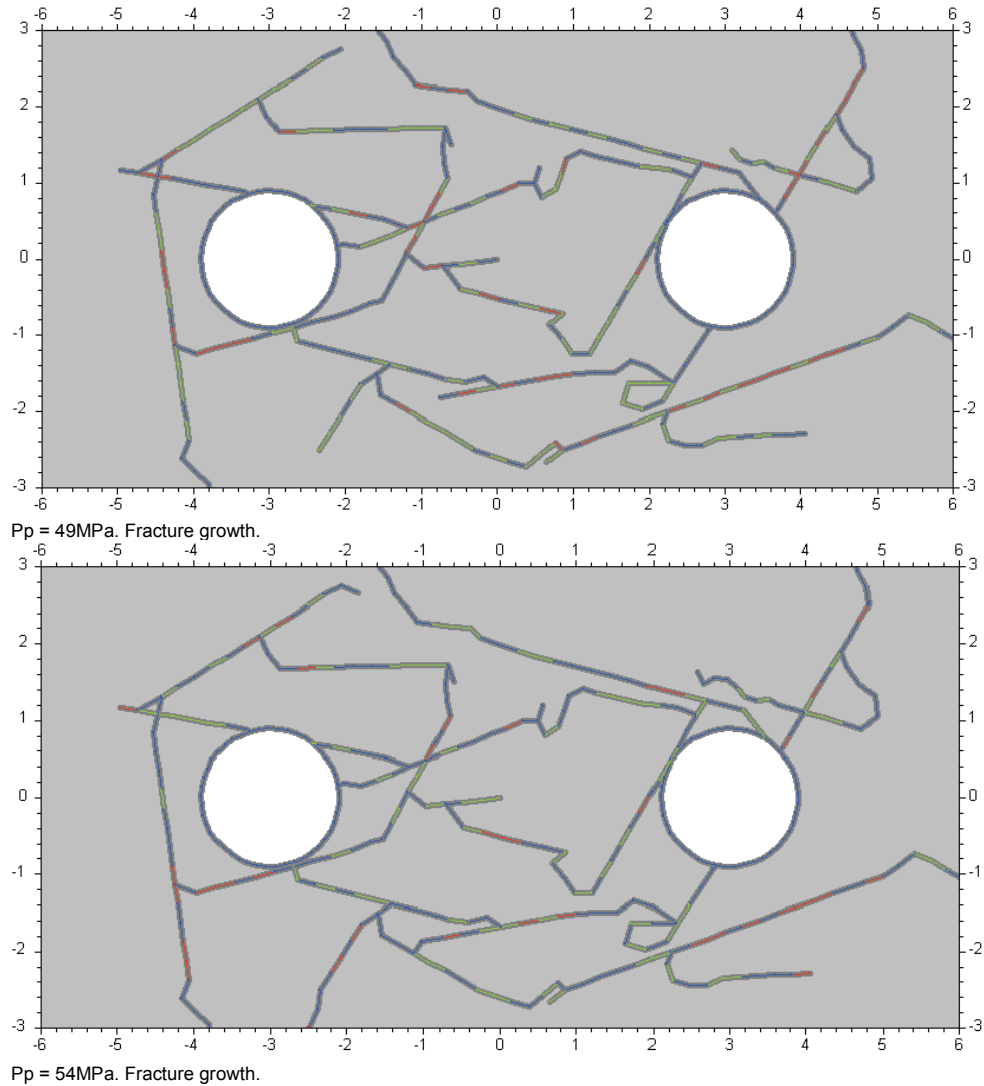


The water pressure acting on the deposition holes and the fractures is increased from  $P_p = 34\text{MPa}$  in steps of 5MPa.  $P_p = 39\text{MPa}$ . Some fracturing.

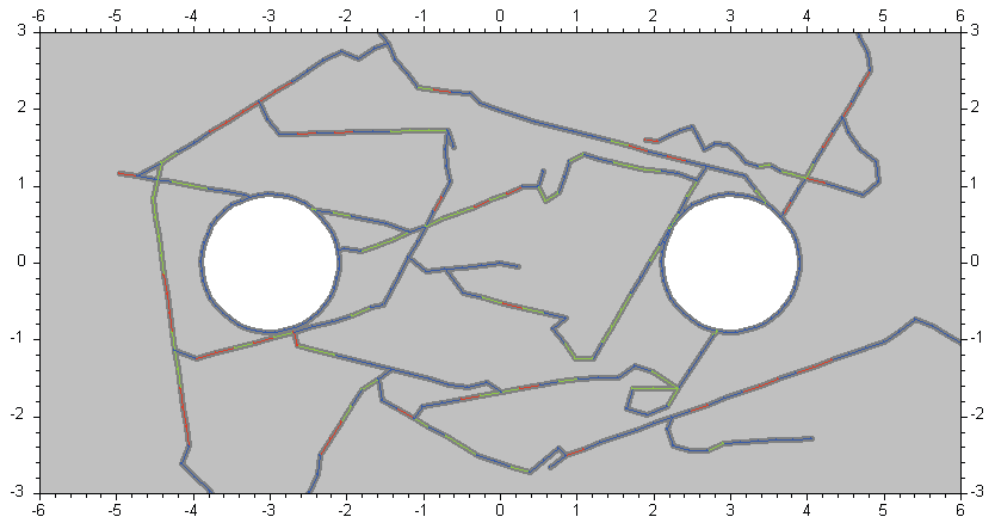


$P_p = 44\text{MPa}$ . Fracture growth.

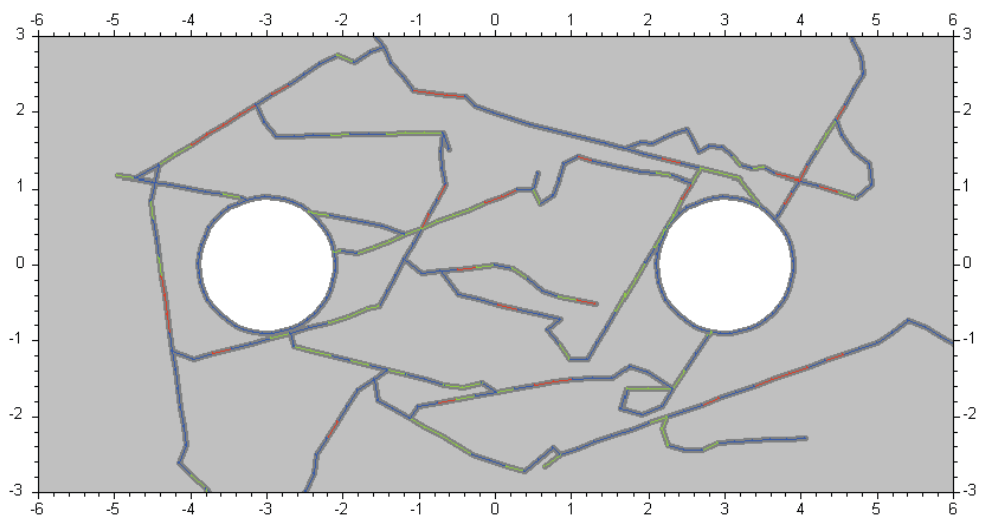
Figure h. Fracture network evolution (13409b21009084). Stress field according to Ask et al. [2007], DFN I, high swelling pressure, no heating sequence, ice cover and extended ice load fluid pressure. The figures show the fracture network and the type of fracture. Colour code: blue - currently not loaded, green - shear loaded, red - open. Thickening of lines show application of a fluid pressure.





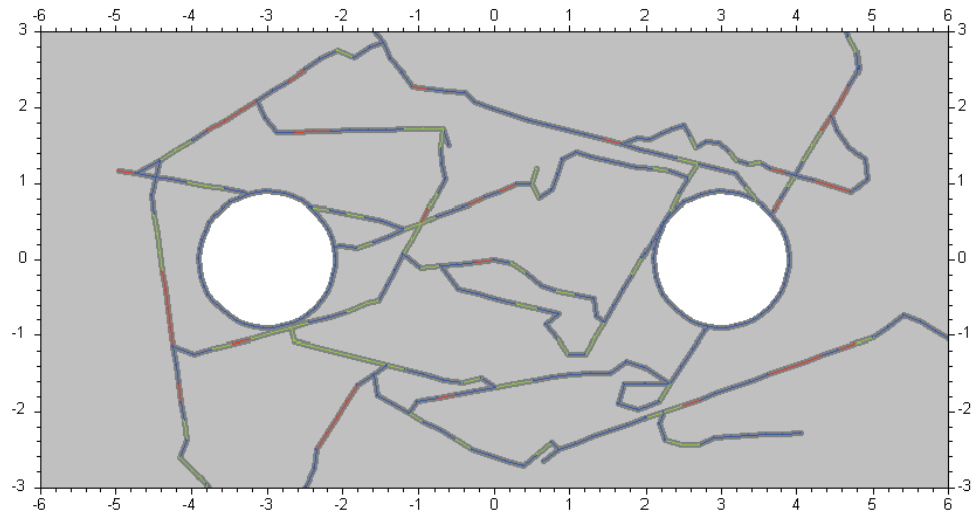


$P_p = 59\text{MPa}$ . Stabilisation.

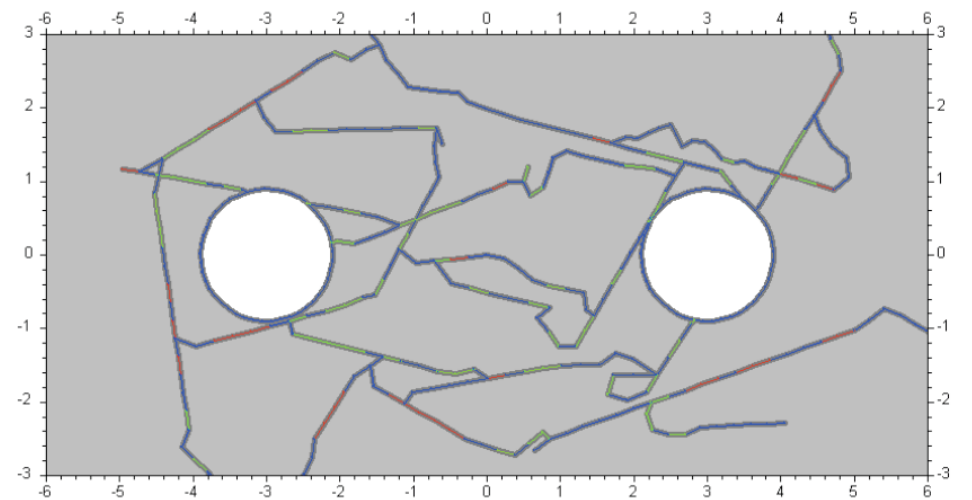


$P_p = 64\text{MPa}$ . No further fracture growth.

Figure h. Fracture network evolution (13409b21009084). Stress field according to Ask et al. [2007], DFN I, high swelling pressure, no heating sequence, ice cover and extended ice load fluid pressure. The figures show the fracture network and the type of fracture. Colour code: blue - currently not loaded, green - shear loaded, red - open. Thickening of lines show application of a fluid pressure.



Pp = 69MPa. No further fracture growth.



Pp = 74MPa. No fracture growth.

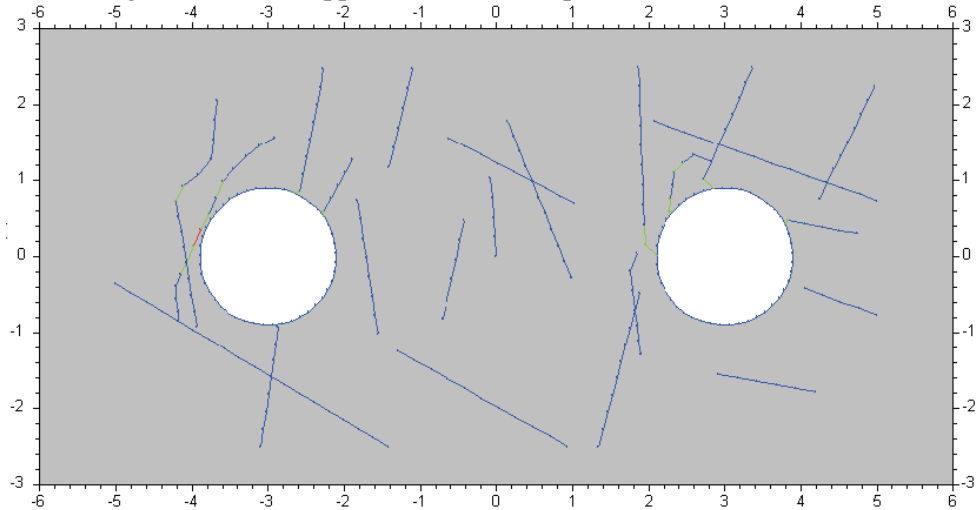
### 11.9. Simulation IIM-1

The model in this simulation includes DFN II and is subject to the stress field according to Martin [2007]. It features the full loading history including low swelling pressure Ps, the heating sequence up to 75°C and the ice cover.

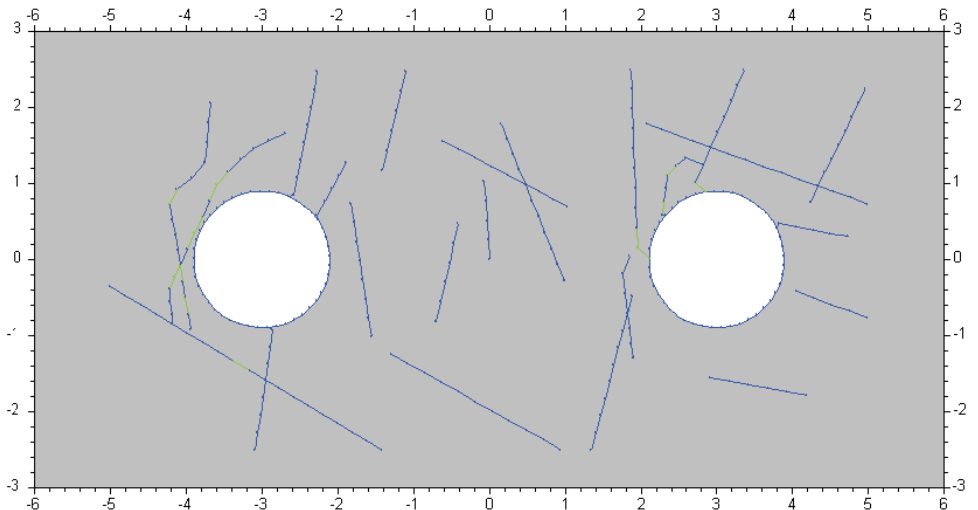
simulation	stress field		DFN	fract.ini	closure			heating	ice cover	
	Sxx	Syy			backfill	Ps	Pp		load	Pp
13409b21009141	38,7	28,2 <sup>1)</sup>	II	x	-3,0	5,5	4,0	✓	24,5	34

Only few fracture propagate short distances due to the stress history until the increased water pressure from the ice cover is applied. The water head from an ice cover might introduce heavy hydraulic fracture growth.

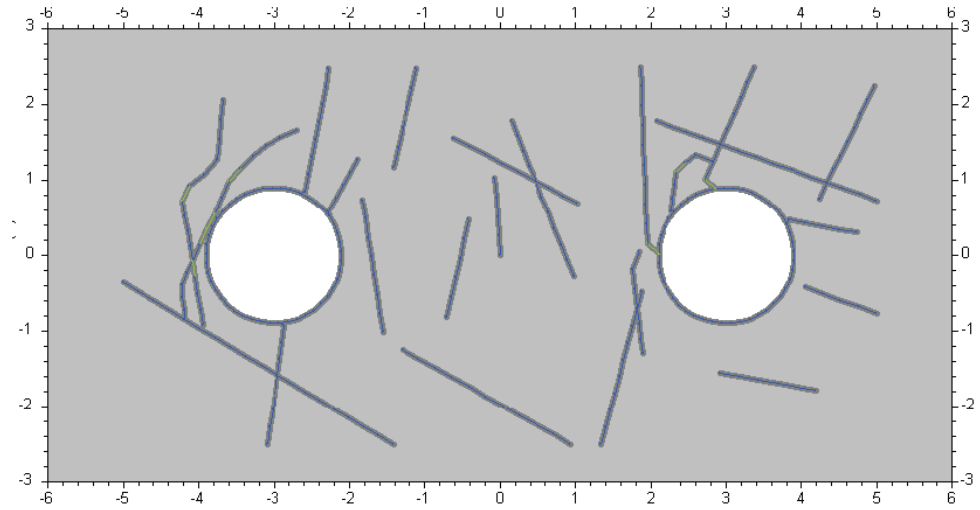
Figure i. Fracture network evolution (13409b21009141). Stress field according to Martin [2007], DFN II, low swelling pressure, heating sequence and ice cover. The figures show the fracture network and the type of fracture. Colour code: blue - currently not loaded, green - shear loaded, red - open. Thickening of lines show application of a fluid pressure.



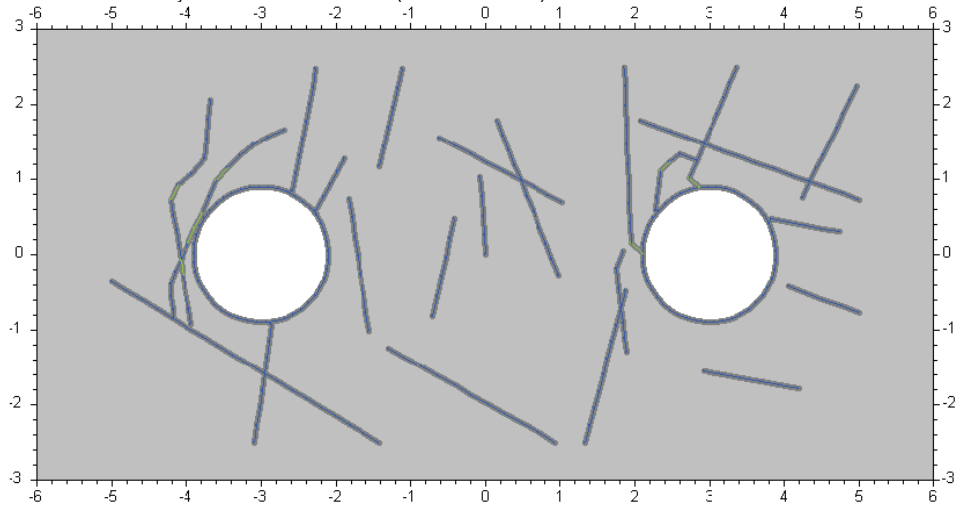
Fracture network after introduction of the excavations. Only few fractures propagated due to the redistribution of the stresses. Stress field according to Martin [2007]; DFN II.



After the closure of the repository the applied stress is increased due to the backfill of the tunnel. This has no significant impact on the DFN.

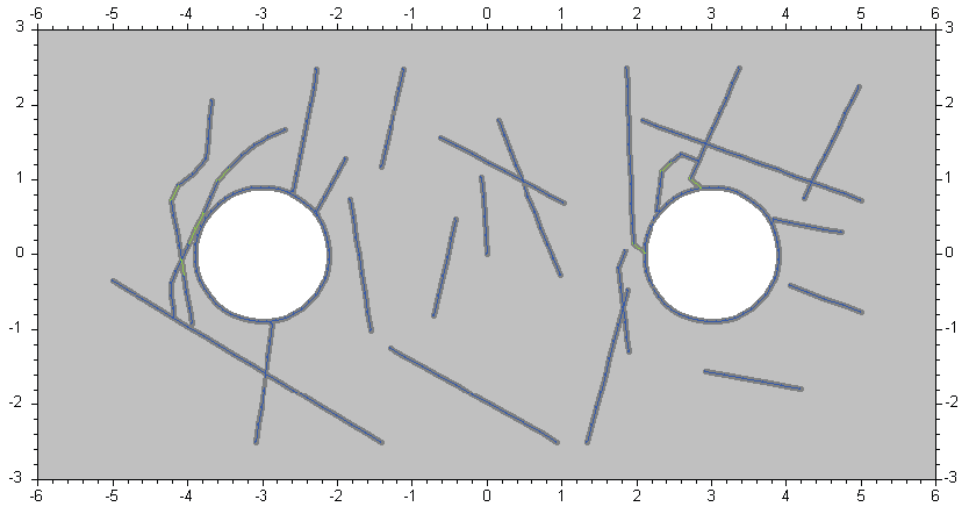


The swelling pressure (5.5MPa) and the recovery of a water head (4MPa) show no impact on the DFN. The fractures are basically tension and traction free (blue colour code)

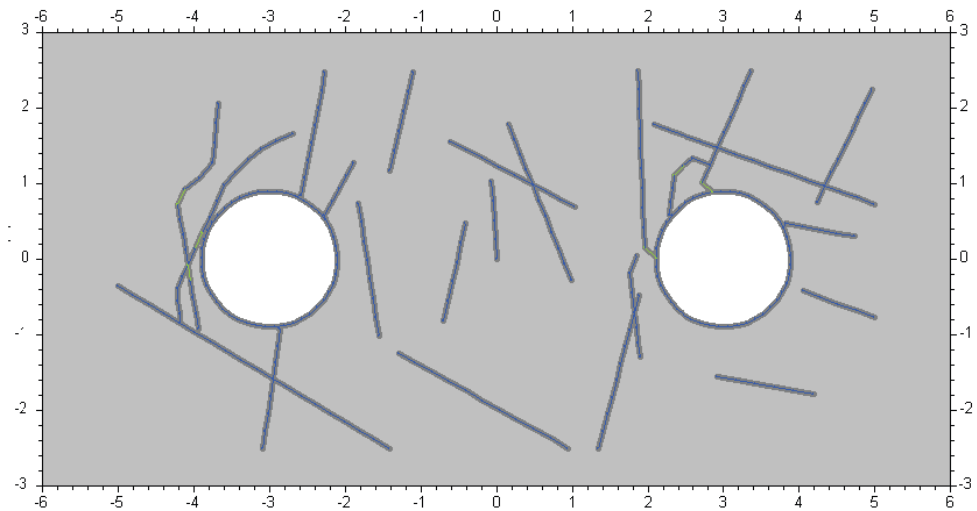


The temperature at the face of the deposition holes is increased from the initial 14.5°C to 25°C. This shows no impact on the DFN.

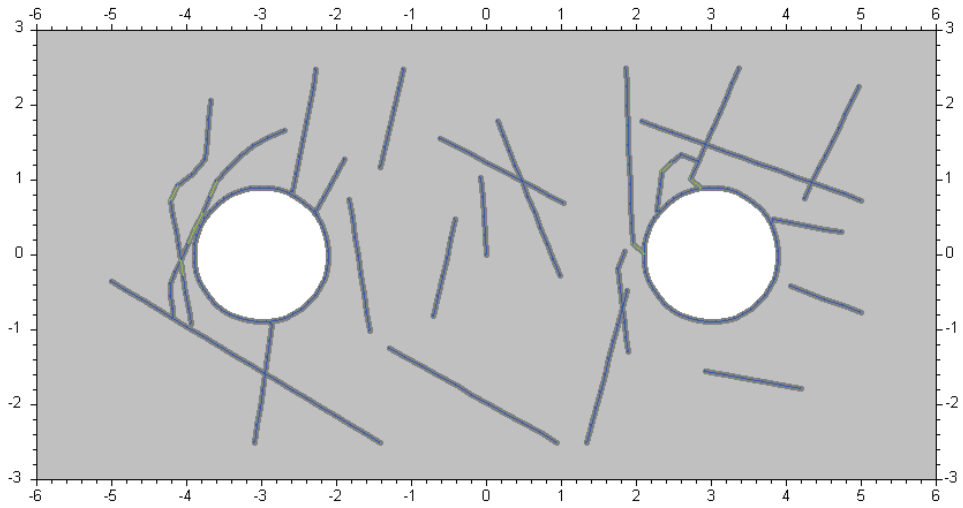
Figure i. Fracture network evolution (13409b21009141). Stress field according to Martin [2007], DFN II, low swelling pressure, heating sequence and ice cover. The figures show the fracture network and the type of fracture. Colour code: blue - currently not loaded, green - shear loaded, red - open. Thickening of lines show application of a fluid pressure.



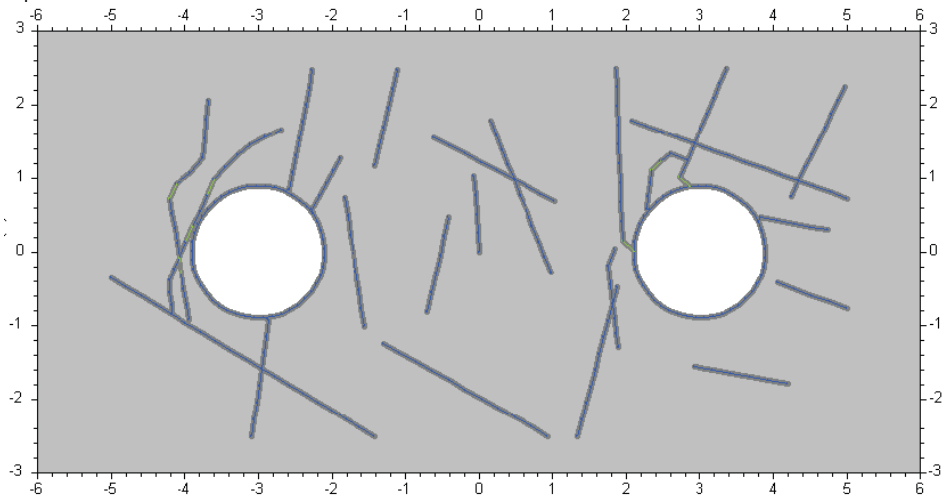
Temperature at the deposition hole face is increased to 50°C. No impact.



Temperature at the deposition hole face is increased to 75°C. No impact.

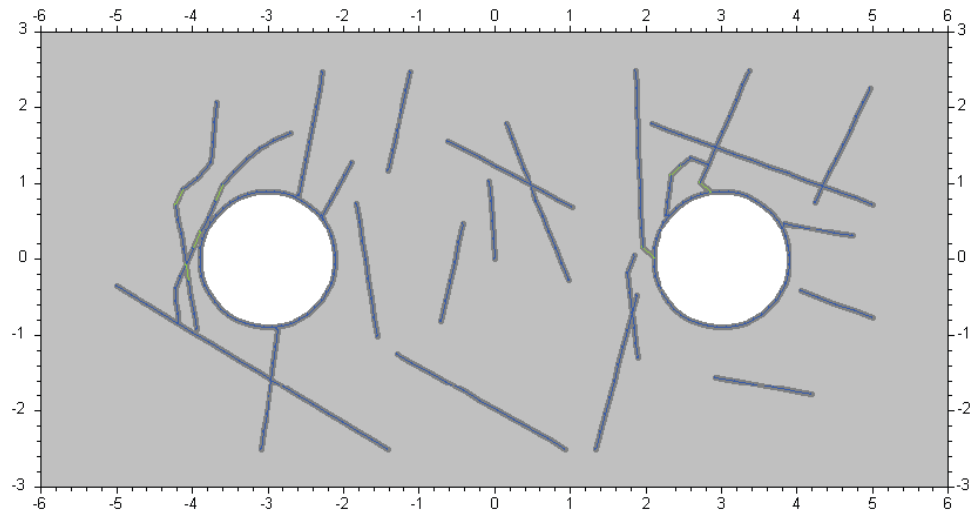


Temperature at the deposition hole face is decreased to 50°C. The aperture of selected fractures reduces. No impact on DFN.

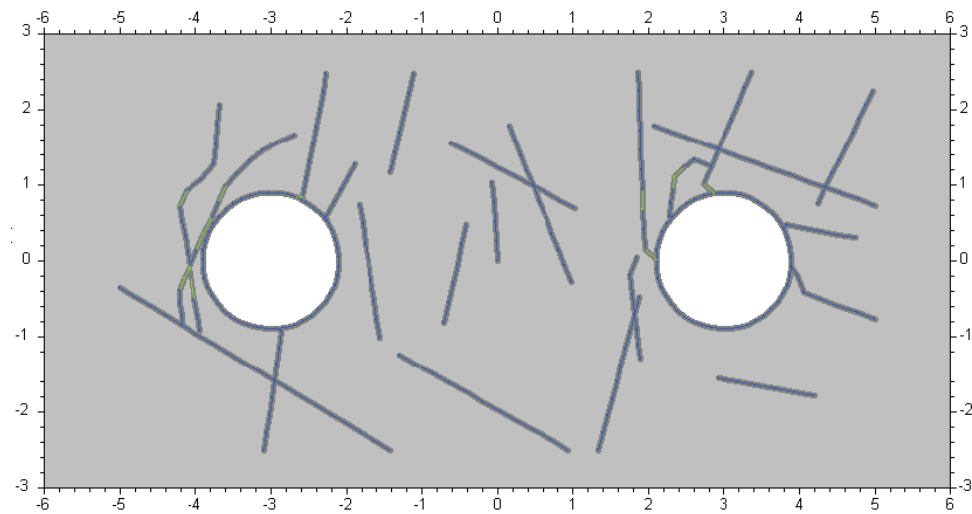


Temperature at the deposition hole face is decreased to 25°C. No impact.

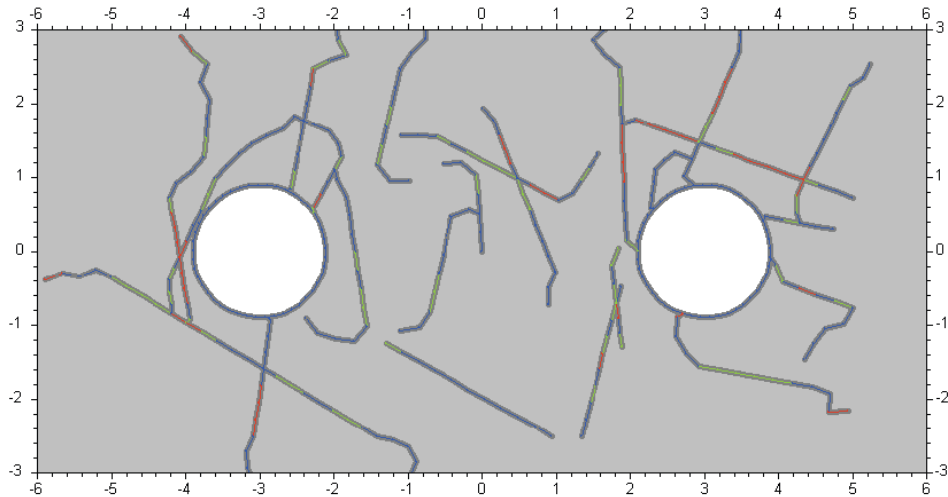
Figure i. Fracture network evolution (13409b21009141). Stress field according to Martin [2007], DFN II, low swelling pressure, heating sequence and ice cover. The figures show the fracture network and the type of fracture. Colour code: blue - currently not loaded, green - shear loaded, red - open. Thickening of lines show application of a fluid pressure.



Temperature at the deposition hole face is decreased to 10°C. The aperture of selected fractures reduces. No impact on DFN.



As for simulation of an ice cover of approx. 3km additional load of 24.5MPa ( $S_{yy}$  due to redistribution around backfilled tunnel) is added resulting in no changes of the DFN.



The water head is increased to 34MPa due to an assumed ice cover fully hydraulically connected to the repository. Additional fracturing is developed and water connection between deposition holes is anticipated.

### 11.10. Simulation IIA-1

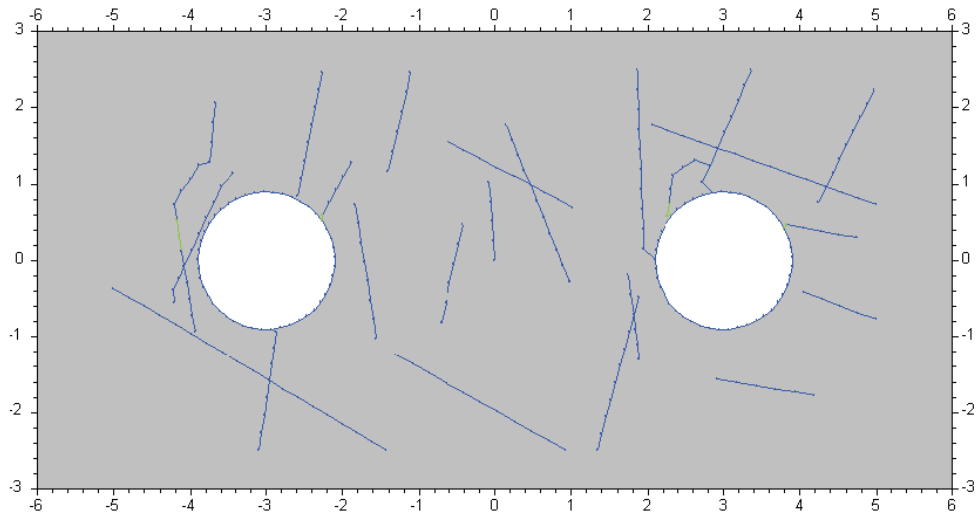
The model in this simulation includes DFN II and is subject to the stress field according to Ask et al. [2007]. It features the full loading history including low swelling pressure  $P_s$ , the heating sequence up to 75°C and the ice cover.

simulation	stress field		DFN	fract.ini	closure			heating	ice cover	
	Sxx	Syy			backfill	$P_s$	$P_p$		load	$P_p$
13409b21009142	19,2	12,2 <sup>2)</sup>	II	x	-3,0	5,5	4,0	✓	24,5	34

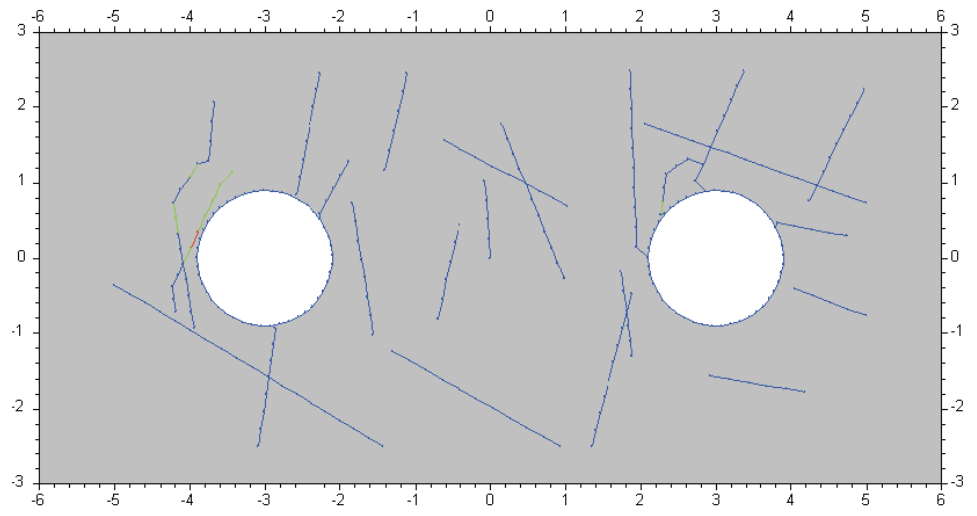
Only few fractures propagate short distances due to the stress history until the ice cover induced increase in  $S_{yy}$ . The isolated  $S_{yy}$  increase resulted in some fracture growth. The additional water head from an ice cover might introduce heavy hydraulic fracture growth. Due to the orientation of the DFN a direct hydraulic connection is not as pronounced as with DFN I.



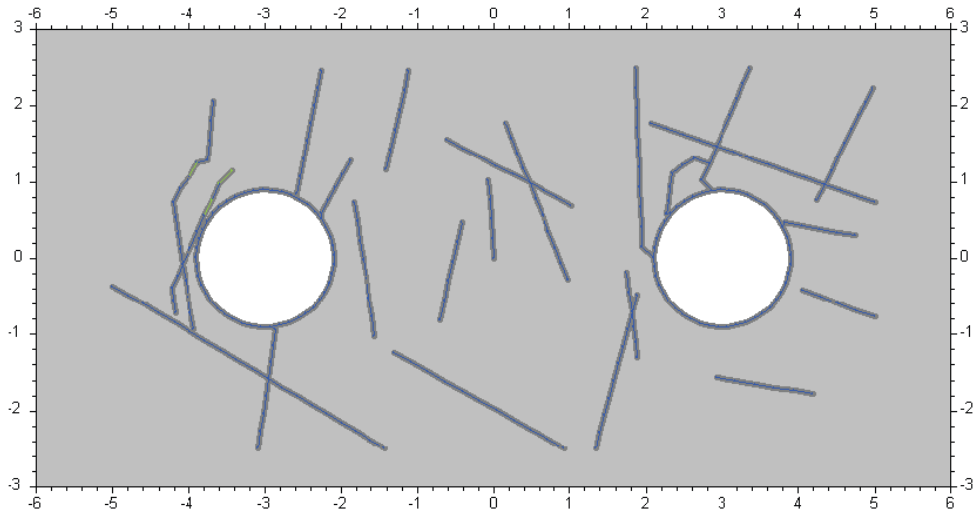
Figure j. Fracture network evolution (13409b21009142). Stress field according to Ask et al. [2007], DFN II, low swelling pressure, heating sequence and ice cover. The figures show the fracture network and the type of fracture. Colour code: blue - currently not loaded, green - shear loaded, red - open. Thickening of lines show application of a fluid pressure.



Fracture network after introduction of the excavations. Only few fractures propagated due to the redistribution of the stresses. Stress field according to Ask et al. [2007]; DFN II.

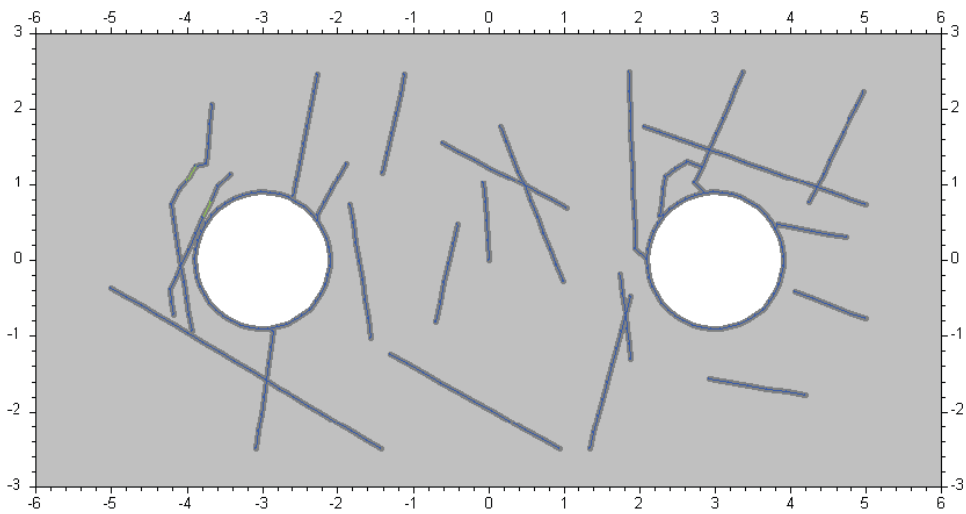


After the closure of the repository the applied stress is increased due to the backfill of the tunnel. This has no significant impact on the DFN.

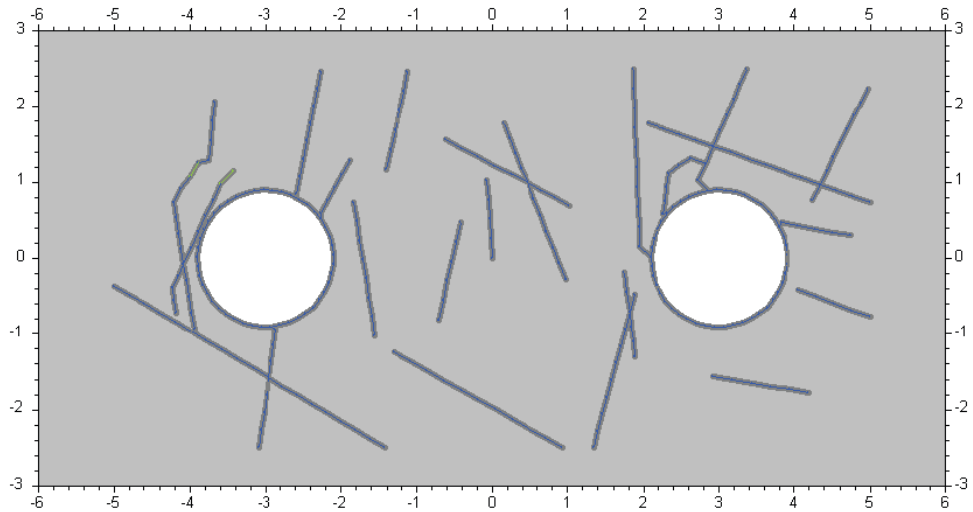


The swelling pressure (5.5MPa) and the recovery of a water head (4MPa) show no impact on the DFN. The fractures are basically tension and traction free (blue colour code).

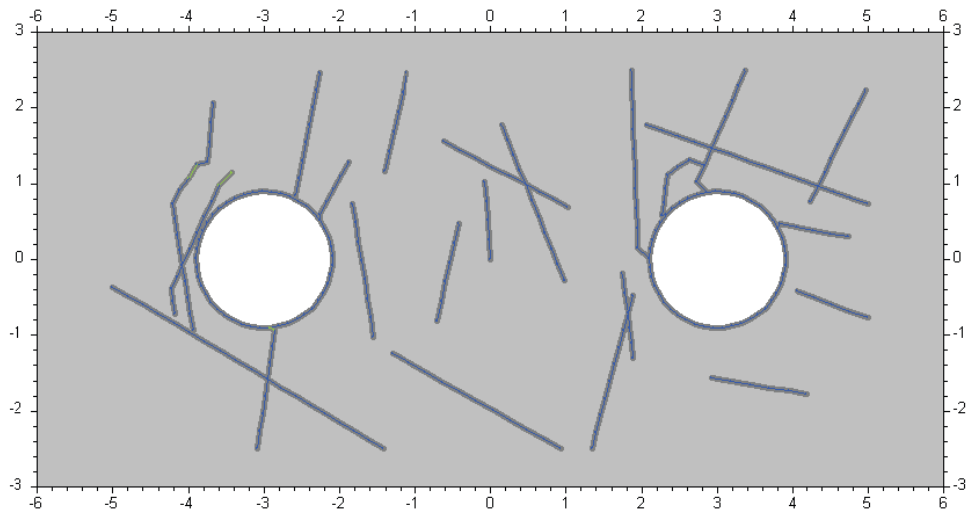
Figure j. Fracture network evolution (13409b21009142). Stress field according to Ask et al. [2007], DFN II, low swelling pressure, heating sequence and ice cover. The figures show the fracture network and the type of fracture. Colour code: blue - currently not loaded, green - shear loaded, red - open. Thickening of lines show application of a fluid pressure.



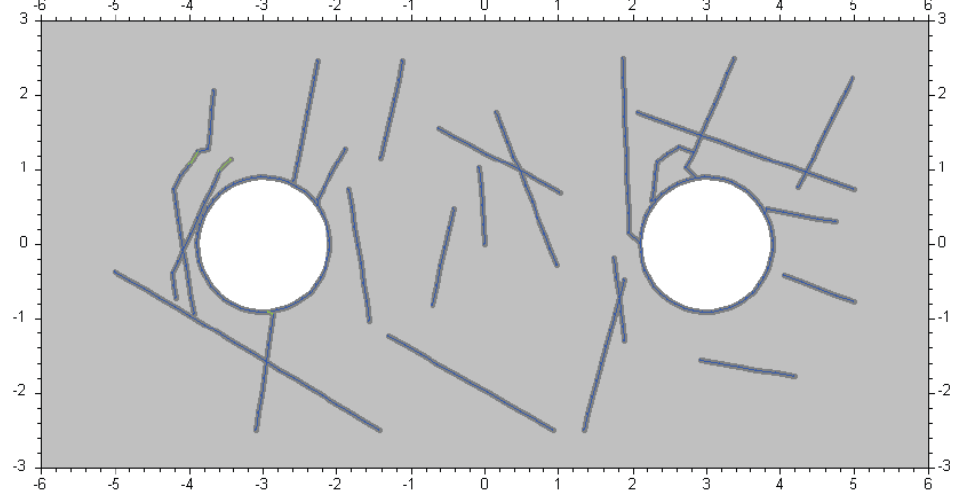
The temperature at the face of the deposition holes is increased from the initial 14.5°C to 25°C. This shows no impact on the DFN.



Temperature at the deposition hole face is increased to 50°C. No impact.

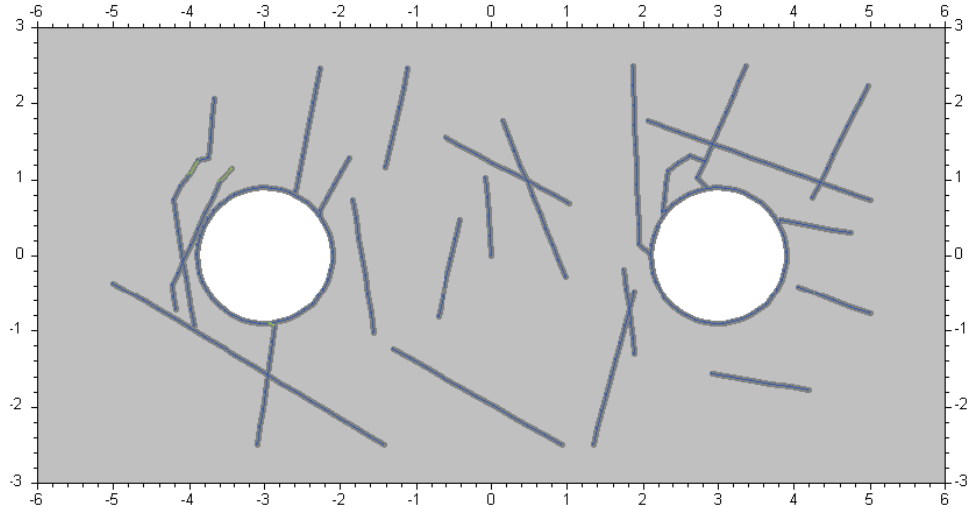


Temperature at the deposition hole face is increased to 75°C. No impact.

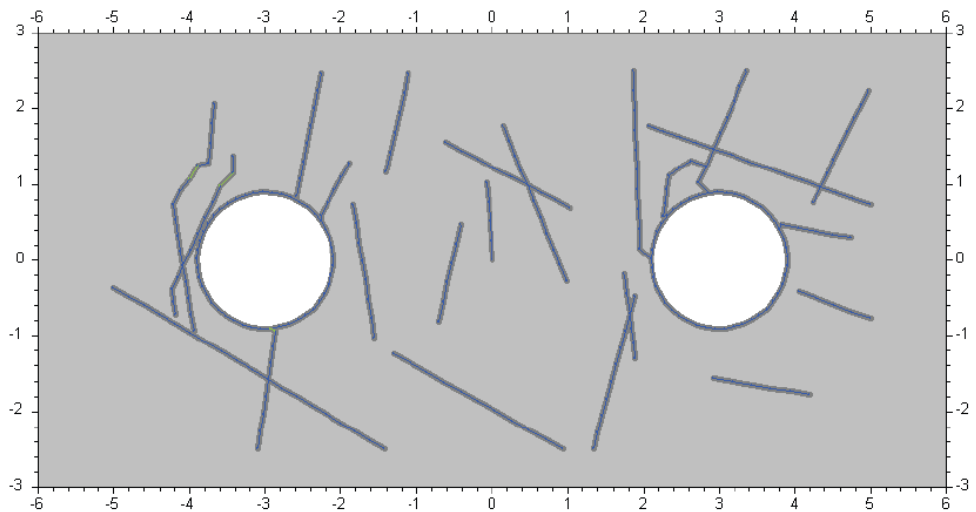


Temperature at the deposition hole face is decreased to 50°C. The aperture of selected fractures reduces. No impact on DFN.

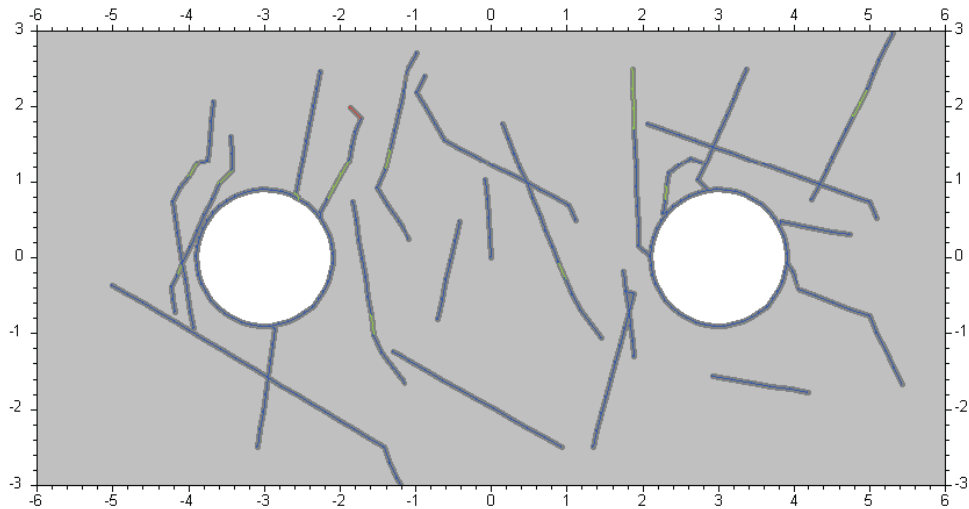
Figure j. Fracture network evolution (13409b21009142). Stress field according to Ask et al. [2007], DFN II, low swelling pressure, heating sequence and ice cover. The figures show the fracture network and the type of fracture. Colour code: blue - currently not loaded, green - shear loaded, red - open. Thickening of lines show application of a fluid pressure.



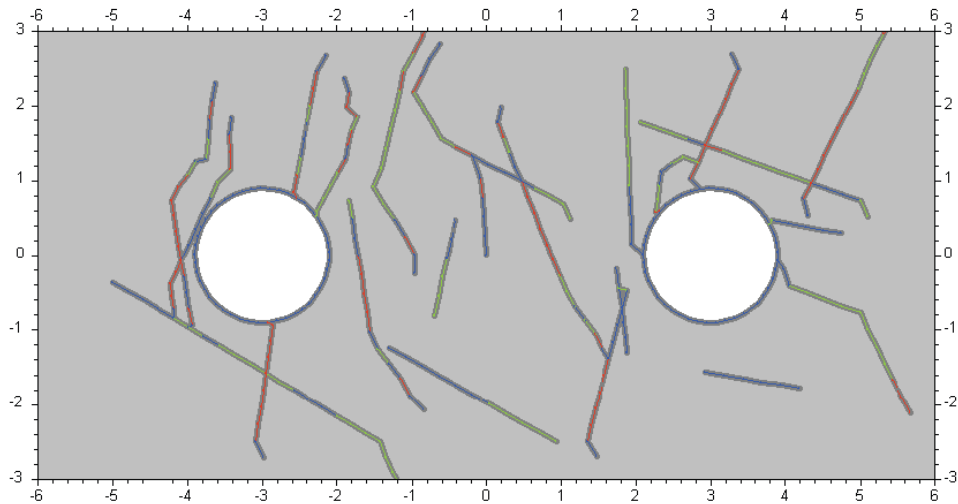
Temperature at the deposition hole face is decreased to 25°C. No impact.



Temperature at the deposition hole face is decreased to 10°C. The aperture of selected fractures reduces. No significant impact on DFN.



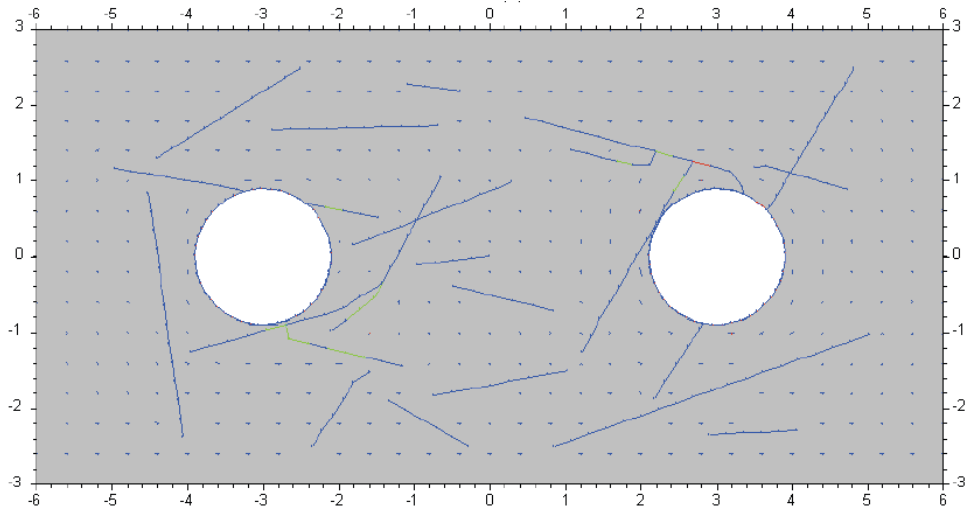
As for simulation of an ice cover of approx. 3km additional load of 24.5MPa ( $S_{yy}$  due to redistribution around backfilled tunnel) is added resulting in pronounced fracture growth.



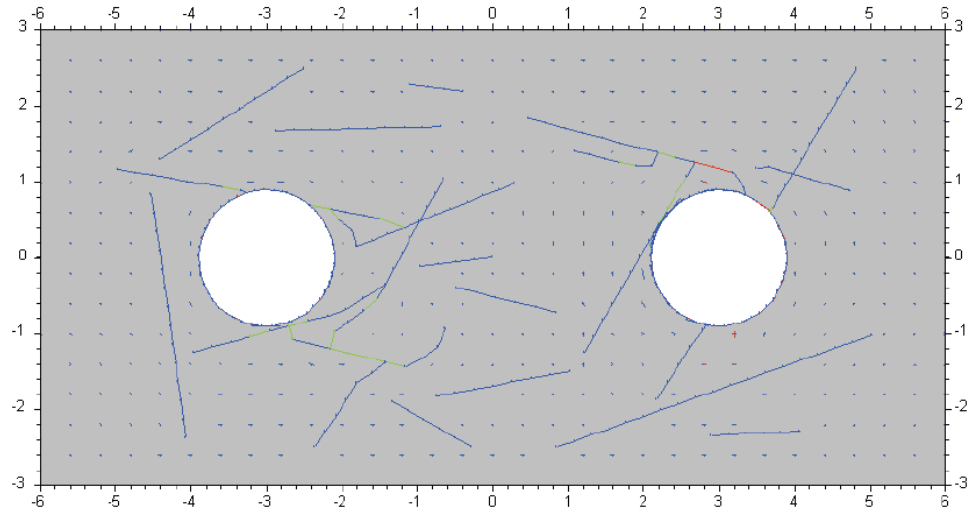
The water head is increased to 34MPa due to an assumed ice cover fully hydraulically connected to the repository. Additional fracturing is developed with potential for short circuit of groundwater between the deposition holes and tunnels.

### 11.11. Simulation IMO-1

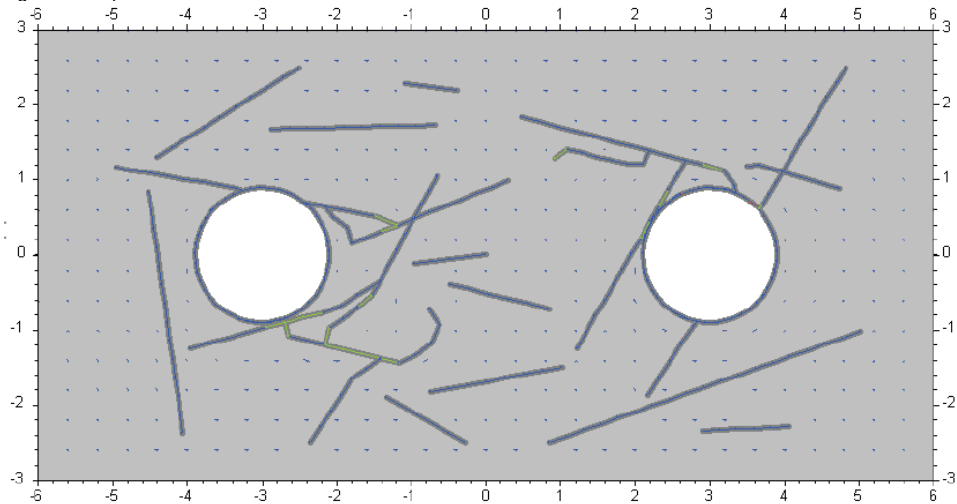
Figure k. Fracture network evolution (13409b21009151). Stress field according to Martin [2007], DFN I, low swelling pressure, no heating sequence, ice cover loading, water head increase and ice cover load decrease. The figures show the fracture network and the type of fracture. Colour code: blue - currently not loaded, green - shear loaded, red - open. Thickening of lines show application of a fluid pressure.



Fracture network after introduction of the excavations. Only few fractures propagated due to the redistribution of the stresses. Stress field according to Martin [2007]; DFN I.

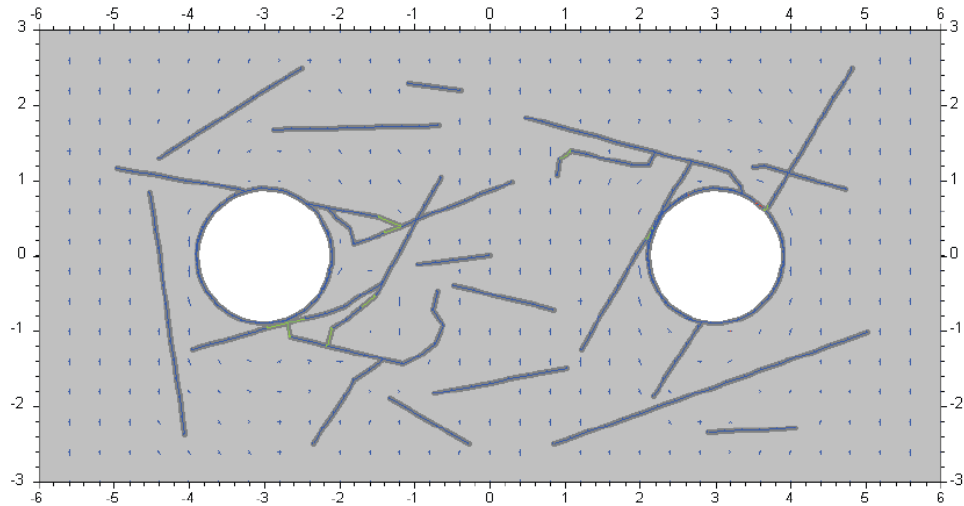


After the closure of the repository the applied stress is increased due to the backfill of the tunnel. This has no significant impact on the DFN.

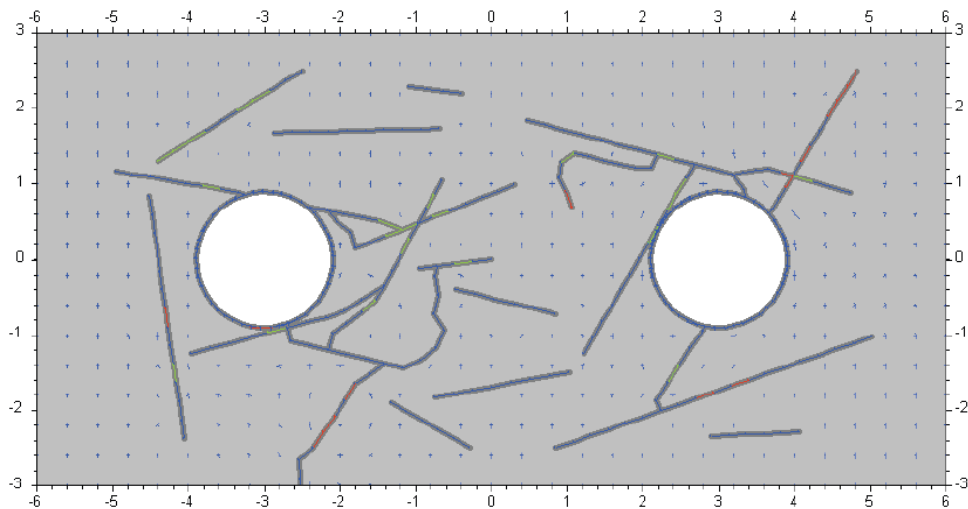


The swelling pressure (5.5MPa) and the recovery of a water head (4MPa) show no impact on the DFN. The fractures are basically tension and traction free (blue colour code). Minor shear failures appear close to one of the deposition holes.

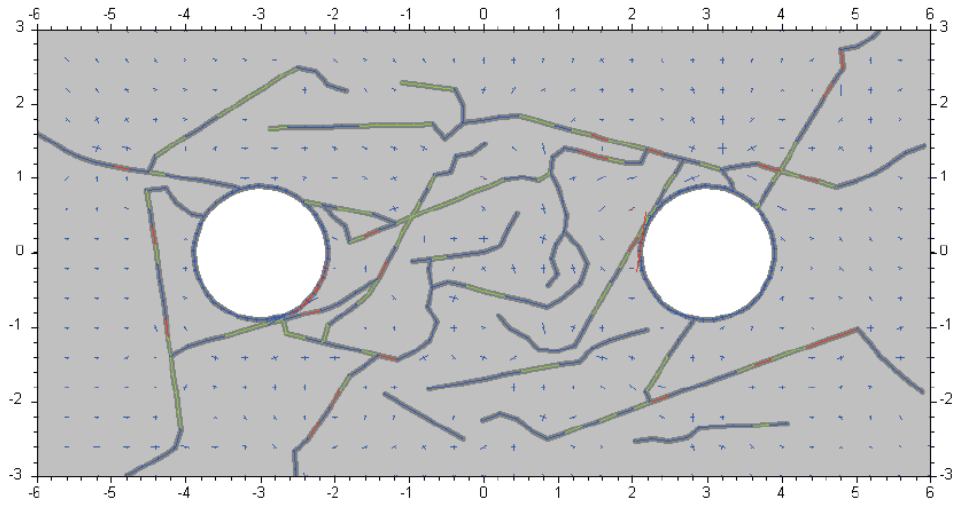
Figure k. Fracture network evolution (13409b21009151). Stress field according to Martin [2007], DFN I, low swelling pressure, no heating sequence, ice cover loading, water head increase and ice cover load decrease. The figures show the fracture network and the type of fracture. Colour code: blue - currently not loaded, green - shear loaded, red - open. Thickening of lines show application of a fluid pressure.



As for simulation of an ice cover of approx. 3km additional load of 24.5MPa ( $S_{yy}$  due to redistribution around backfilled tunnel) is added. No additional fracture growth. The fractures are basically tension and traction free (blue colour code).



The water head is increased to 34MPa due to an assumed ice cover fully hydraulically connected to the repository. Only minor additional fracturing is introduced.



The simulation of the ice cover by adding  $S_{yy}$  is removed, hence the stress field is again as defined by Martin. However, the water pressure  $P_p$  is assumed trapped, introducing severe fracturing and formation of hydraulic connection of the deposition holes.



## 11.12. Code listing examples

### 11.12.1. IM-2

Example of a fracod2d input file with DFN I.

```
TITLE
134.ssm.ls.09b2
<-- geometry -->
SYMM
0 0 0
ARCH
45 -3 0 1.80 3 363 1 0 0 1 0 0
ARCH
45 3 0 1.80 3 363 1 0 0 1 0 0
SWIN
-6 6 -3 3 30 15
IWIN
-5 5 -2 2
<-- starting stresses -->
STRES (stress martin 400m)
-38.7e6 -28.2e6 0
<-- thermal heating -->
TTIME ### define time as operation time before swelling ###
1e6 1
THER ###check density, specific heat###
7.7e-6 3.68 2730 770 10.5 1
TBOU
-6.0 6.0 -2.5 2.5 1
0 0 15
1 1e6 15
<-- elastic and fracture properties -->
MODU <-- intact material -->
0.23 76e+9 1
TOUK <-- intact material -->
2.5e6 4.0e6 1
ROCK <-- intact material -->
60 28e+6 13e+6 1
PROP <-- new fractures -->
1 1.5e+8 3e+7 34 1e6 2 10e-6 1e-6
PROP <-- rock mass fractures -->
2 1.5e+11 3e+11 34 0.6e6 2 1e-6 1e-6
PROP
11 1.5e+8 3e+7 34 1e6 2 10e-6 1e-6
PROP
12 1.5e+8 3e+7 34 1e6 2 10e-6 1e-6
<-- fracture steering commands -->
RAND
0.51 0
```

```

SETF
0.9
ISIZ
0.2
BOUN
INTE
<-- dfn I-->
CYCL 5
<-- filling with bentonite-->
DSTR
3e6 -0e6 0
CYCL 5
<-- swelling pressure as applied after termination of repository plus water-->
DARC
-3 0 0 2 -180 180 0 -5.5e6
DARC
3 0 0 2 -180 180 0 -5.5e6
WATER
RECT -6 6 -3 3 4e6
cycl 5
<-- thermal heating 25°C-->
TTIME
7e6 1
THER ###check density, specific heat###
7.7e-6 3.68 2730 770 10.5 1
TBOU
-6.0 6.0 -2.5 2.5 1
0 0 25
1 7e6 25
cycl 5
<-- thermal heating 50°C-->
TTIME
100e6 1
THER ###check density, specific heat###
7.7e-6 3.68 2730 770 10.5 1
TBOU
-6.0 6.0 -2.5 2.5 1
0 0 50
1 100e6 50
cycl 5
<-- thermal heating 75°C-->
TTIME
700e6 1
THER ###check density, specific heat###
7.7e-6 3.68 2730 770 10.5 1
TBOU
-6.0 6.0 -2.5 2.5 1
0 0 75
1 700e6 75
cycl 5
<-- thermal heating 50°C-->

```

```

TTIME
90000e6 1
THER ###check density, specific heat###
7.7e-6 3.68 2730 770 10.5 1
TBOU
-6.0 6.0 -2.5 2.5 1
0 0 50
1 90000e6 50
cycl 5
<-- thermal heating 25∞C-->
TTIME
90000e6 1
THER ###check density, specific heat###
7.7e-6 3.68 2730 770 10.5 1
TBOU
-6.0 6.0 -2.5 2.5 1
0 0 25
1 90000e6 25
cycl 5
<-- thermal heating 10∞C-->
TTIME
90000e6 1
THER ###check density, specific heat###
7.7e-6 3.68 2730 770 10.5 1
TBOU
-6.0 6.0 -2.5 2.5 1
0 0 10
1 90000e6 10
cycl 5
<-- ice load stress increase -->
DSTR
-0e6 -24.5e6 0
CYCL 5
<--waterload from ice cover-->
WATER
RECT -6 6 -3 3 34e6
CYCL 5
ENDFILE

```

### 11.12.2. IIM-1

Example of a fracod2d input file with DFN II.

```

TITLE
134.ssm.ls.09b2
<-- geometry -->
SYMM
0 0 0
ARCH
45 -3 0 1.80 3 363 1 0 0 1 0 0
ARCH

```

```

45 3 0 1.80 3 363 1 0 0 1 0 0
SWIN
-6 6 -3 3 30 15
IWIN
-5 5 -2 2
<-- starting stresses -->
STRES (stress martin 400m)
-19.2e6 -12.2e6 0
<-- thermal heating -->
TTIME ### define time as operation time before swelling ###
1e6 1
THER ###check density, specific heat###
7.7e-6 3.68 2730 770 10.5 1
TBOU
-6.0 6.0 -2.5 2.5 1
0 0 15
1 1e6 15
<-- elastic and fracture properties -->
MODU <-- intact material -->
0.23 76e+9 1
TOUK <-- intact material -->
2.5e6 4.0e6 1
ROCK <-- intact material -->
60 28e+6 13e+6 1
PROP <-- new fractures -->
1 1.5e+8 3e+7 34 1e6 2 10e-6 1e-6
PROP <-- rock mass fractures -->
2 1.5e+11 3e+11 34 0.6e6 2 1e-6 1e-6
PROP
11 1.5e+8 3e+7 34 1e6 2 10e-6 1e-6
PROP
12 1.5e+8 3e+7 34 1e6 2 10e-6 1e-6
<-- fracture steering commands -->
RAND
0.51 0
SETF
0.9
ISIZ
0.2
*BOUN
*INTE
<-- dfn II-->
FRACTURE 1
3 -3.68 2.06 -3.75 1.28 2 2 1
FRACTURE 2
6 -3.6 0.98 -4.22 -0.38 2 2 1
FRACTURE 3
7 -4.21 0.73 -3.94 -0.93 2 2 1
FRACTURE 4
17 -5 -0.36 -1.42 -2.50 2 2 1
FRACTURE 5

```

6 -2.86 -0.93 -3.09 -2.50 2 2 1  
 FRACTURE 6  
 7 -2.27 2.47 -2.58 0.84 2 2 1  
 FRACTURE 7  
 3 -1.89 1.28 -2.27 0.59 2 2 1  
 FRACTURE 8  
 5 -1.11 2.47 -1.41 1.17 2 2 1  
 FRACTURE 9  
 7 -1.83 0.74 -1.56 -1.02 2 2 1  
 FRACTURE 10  
 5 -0.71 -0.81 -0.41 0.47 2 2 1  
 FRACTURE 11  
 7 -0.61 1.56 1.03 0.69 2 2 1  
 FRACTURE 12  
 9 0.98 -0.28 0.15 1.78 2 2 1  
 FRACTURE 13  
 8 1.88 -0.47 1.34 -2.50 2 2 1  
 FRACTURE 14  
 9 1.95 0.15 1.86 2.50 2 2 1  
 FRACTURE 15  
 5 2.93 -1.56 4.20 -1.78 2 2 1  
 FRACTURE 16  
 4 4.06 -0.42 5.00 -0.77 2 2 1  
 FRACTURE 17  
 12 2.07 1.78 5.00 0.73 2 2 1  
 FRACTURE 18  
 6 2.73 1.02 3.37 2.5 2 2 1  
 FRACTURE 19  
 3 2.34 1.11 2.27 0.58 2 2 1  
 FRACTURE 20  
 7 4.24 0.76 4.97 2.24 2 2 1  
 FRACTURE 21  
 4 -0.07 1.03 0.00 0.00 2 2 1  
 FRACTURE 22  
 10 -1.30 -1.24 0.94 -2.50 2 2 1  
 FRACTURE 23  
 4 1.89 -1.30 1.75 -0.19 2 2 1  
 FRACTURE 24  
 4 4.74 0.30 3.83 0.47 2 2 1  
 CYCL 5  
 <-- filling with bentonite-->  
 DSTR  
 3e6 -0e6 0  
 CYCL 5  
 <-- swelling pressure as applied after termination of repository plus water-->  
 DARC  
 -3 0 0 2 -180 180 0 -5.5e6  
 DARC  
 3 0 0 2 -180 180 0 -5.5e6  
 WATER  
 RECT -6 6 -3 3 4e6

```

cycl 5
<-- thermal heating 25∞C-->
TTIME
7e6 1
THER ###check density, specific heat###
7.7e-6 3.68 2730 770 10.5 1
TBOU
-6.0 6.0 -2.5 2.5 1
0 0 25
1 7e6 25
cycl 5
<-- thermal heating 50∞C-->
TTIME
100e6 1
THER ###check density, specific heat###
7.7e-6 3.68 2730 770 10.5 1
TBOU
-6.0 6.0 -2.5 2.5 1
0 0 50
1 100e6 50
cycl 5
<-- thermal heating 75∞C-->
TTIME
700e6 1
THER ###check density, specific heat###
7.7e-6 3.68 2730 770 10.5 1
TBOU
-6.0 6.0 -2.5 2.5 1
0 0 75
1 700e6 75
cycl 5
<-- thermal heating 50∞C-->
TTIME
90000e6 1
THER ###check density, specific heat###
7.7e-6 3.68 2730 770 10.5 1
TBOU
-6.0 6.0 -2.5 2.5 1
0 0 50
1 90000e6 50
cycl 5
<-- thermal heating 25∞C-->
TTIME
90000e6 1
THER ###check density, specific heat###
7.7e-6 3.68 2730 770 10.5 1
TBOU
-6.0 6.0 -2.5 2.5 1
0 0 25
1 90000e6 25
cycl 5

```

```
<-- thermal heating 10°C-->
TTIME
90000e6 1
THER ###check density, specific heat###
7.7e-6 3.68 2730 770 10.5 1
TBOU
-6.0 6.0 -2.5 2.5 1
0 0 10
1 90000e6 10
cycl 5
<-- ice load stress increase -->
DSTR
-0e6 -24.5e6 0
CYCL 5
<--waterload from ice cover-->
WATER
RECT -6 6 -3 3 34e6
CYCL 5
ENDFILE
```







2011:26

The Swedish Radiation Safety Authority has a comprehensive responsibility to ensure that society is safe from the effects of radiation. The Authority works to achieve radiation safety in a number of areas: nuclear power, medical care as well as commercial products and services. The Authority also works to achieve protection from natural radiation and to increase the level of radiation safety internationally.

The Swedish Radiation Safety Authority works proactively and preventively to protect people and the environment from the harmful effects of radiation, now and in the future. The Authority issues regulations and supervises compliance, while also supporting research, providing training and information, and issuing advice. Often, activities involving radiation require licences issued by the Authority. The Swedish Radiation Safety Authority maintains emergency preparedness around the clock with the aim of limiting the aftermath of radiation accidents and the unintentional spreading of radioactive substances. The Authority participates in international co-operation in order to promote radiation safety and finances projects aiming to raise the level of radiation safety in certain Eastern European countries.

The Authority reports to the Ministry of the Environment and has around 270 employees with competencies in the fields of engineering, natural and behavioural sciences, law, economics and communications. We have received quality, environmental and working environment certification.

**Strålsäkerhetsmyndigheten**  
**Swedish Radiation Safety Authority**

SE-171 16 Stockholm  
Solna strandväg 96

**Tel:** +46 8 799 40 00  
**Fax:** +46 8 799 40 10

**E-mail:** [registrator@ssm.se](mailto:registrator@ssm.se)  
**Web:** [stralsakerhetsmyndigheten.se](http://stralsakerhetsmyndigheten.se)